Identification of the regulators of the immune checkpoint B7-H4 in a triple-negative breast cancer cell line

Irina Perlitch

Division of Experimental Medicine

Department of Medicine

McGill University, Montreal

April, 2019

A thesis submitted to McGill University in partial fulfillment of the requirements of the degree of Master of Science.

Table of contents

Acknowledgements

This work was supported by an RI-MUHC and an FRQS studentship.

I would like to first and foremost thank my supervisor, Dr. Morag Park, for supporting my research and passion for all things immunology. I am thankful for the opportunity I received to take an observation and mold it into a research project I could be passionate about. I thank Tina Gruosso, for her mentorship, patience, kindness and unwavering confidence in my capabilities as a scientist. I am grateful for her friendship and support through difficult times, and honesty in the face of obstacles. She has taught me survival skills in the world of academic research. I also want to thank Danielle de Verteuil, though we spent a short time working together, you are a wonderful teacher and made learning Western blots almost fun.

I want to thank all Park lab members for their companionship and camaraderie during my time with them, and for sharing in the joys and sorrows of graduate school. I thank all the current post-docs in the Park lab, Anne-Marie, Hellen, Geneviève and Elena, for their help and guidance. Thank you, Gabe Brewer, for hours upon hours of enriching conversation, chip dates, uncontrollable laughter over anything and everything, and being my crutch during hard times, I am most thankful to have met you. Thank you, Paula Coelho, for always making yourself available for my million questions (mostly about Western blots and all things RNA). Thank you, Tunde Golenar, for endless cat discussions. Thank you Virginie Pilon, for allowing me to share my compassion for our mice and all animals, and back and forth sending of cat videos. Thank you, Vanessa Sung, for valuable tips regarding life and love, and enriching conversations about Harry Potter. Thank you, Bruce Huang, for delicious snacks and talks about everything from aliens to headless chickens.

Thank you, Constanza Martinez, for helping me anchor my 100-or-so tubes in the bacterial shaker at midnight when I was about to give up. Thank you, Yaakov Stern, for conversations on late evenings in the lab, and teaching me all the things I should know about Judaism. And finally thank you Veena Sangwan, Valentina Muñoz Ramos, Monica Naujokas and Nancy Laterreur, for organizing the Park lab and helping us all accomplish our work.

I want to thank the laboratory of Dr. Sidong Huang for their help with this project, especially Geneviève Morin, and the FACS facility at the GCRC for their expertise.

I want to thank my most valuable and wonderful friends Sabrina, Samantha, Claudia and Lukas, that supported me every step of the way and were available to hear both my good stories and my bad stories. Thank you for your strong and unconditional friendship.

I thank my family, my sisters, my brothers, my beloved parents, for seeing all the best and worst of me, and still loving me just as much, I am thankful for your presence in my life most of all.

Finally, I dedicate this thesis to my grandmother Galina, you are my motivation for this path in life, and I hope one day to help treat and cure those who are suffering from the disease that took you from us too soon.

I, Irina Perlitch, have read, understood and abided by all norms and regulations of academic integrity of McGill University.

ABSTRACT

Breast cancer, which affects 1 in 9 Canadian women, consists of multiple subtypes associated with different prognosis and standard of care. The triple-negative subtype (TNBC) consists of ~15% of cases, is negative for common biomarkers, lacks a targeted therapeutic approach, and has the worst outcome. Several cancer immunotherapy approaches target regulatory interactions required to negatively balance the level of the immune response, referred to as “immune checkpoints”. Uncoupling these checkpoints boosts host anti-tumour response and the cytotoxic activity of $CD8^+$ T cells. We have identified distinct TNBC tumour microenvironments, where tumours with an immune-cold microenvironment display restriction of $CD8^+$ T cells to tumour margins, elevated expression of the PD-L1 family member B7-H4, and poor outcome. I hypothesize that B7-H4, when expressed in tumour epithelia, enhances immunosuppression and is a potential therapeutic target for a subset of TNBC, but little is known about its regulation. I have developed a high throughput, functional genetic screen using a genome-wide CRISPR/Cas9 library to identify regulators of B7-H4. My results have shown that genes that modulate the glycosylation pathway are important negative regulators of B7-H4 location to the cell surface, and these were subsequently chosen for individual validation by shRNA editing. My data showed a variable impact indicating a complexity of phenotypes. Extended validation strategies will be required to pursue both glycosylation-related targets discovered in the screen, but also additional positive regulators of B7H4. The characterization of novel regulators of B7-H4 are expected to lead to potential clinically relevant targets and companion diagnostics in several cancers.

RÉSUMÉ

Le cancer du sein, touchant une femme sur neuf au Canada, comprend plusieurs sous-types associés à différents pronostics et standards de soins. Les traitements disponibles ciblent les cancers avec une expression élevée de marqueurs hormonaux, sans cibler les cancers négatifs pour ceux-ci, dénommées ‘triple-négatifs’ (TNBC). Une branche de l'immunothérapie, qui se base sur les défenses immunitaires, cible les ‘points de contrôle immunitaires’, dont l’inhibition peut stimuler la réponse anti-tumorale de l'hôte. Des niveaux élevés de lymphocytes T $CD8^+$ dans les tumeurs TNBC corrèlent avec une réponse améliorée à la chimiothérapie. Par conséquent, les stratégies visant à augmenter ces cellules ont été proposées. Nous avons identifié des microenvironnements tumoraux distincts chez des patientes TNBC, où les tumeurs pauvres en cellules immunitaires ont une expression élevée du point de contrôle immunitaire B7-H4 et un mauvais pronostic. J’hypothèse que l’expression tumorale de B7-H4, favorise l'immunosuppression et constitue une cible thérapeutique pour ces patientes, mais peu est connu sur sa régulation. À cette fin, j'ai développé une analyse CRISPR pour identifier des régulateurs de B7-H4. Les résultats montrent que des gènes liés à la modulation de la glycosylation de protéines sont aussi des régulateurs négatifs de l’expression tumorale de B7-H4; ces gènes ont subséquemment été sélectionnés pour validation par shRNA. Le processus de validation présentait des résultats variables, indiquant la complexité du rôle de ces gènes liés à la glycosylation. Des stratégies de validation plus élaborées sont nécessaires pour poursuivre l’étude des gènes liés à la glycosylation et des régulateurs positifs de B7-H4 qui ont aussi été identifiés. Ces études s’attendent à identifier des cibles thérapeutiques ainsi que des outils de diagnostic améliorés pour les patientes atteintes de TNBC.

Contribution of authors

In collaboration with Dr. Tina Gruosso and Dr. Morag Park, I was responsible for the experimental design, execution, data analysis and writing of this thesis. Dr. Tina Gruosso, a formal post-doctoral researcher in the laboratory of Dr. Park, and myself, initiated the founding basis of this project and contributed to the experimental design, execution and data analysis of the clinical patient data relating to this project, including the immunofluorescence staining of immune checkpoints on patient tumor samples, and the correlation of genes from patient samples and genes identified within the genome-wide CRISPR screen. These findings were published in March 2019 in The Journal of Clinical Investigation (Gruosso et al. 2018). I was responsible for the experimental design, execution and data analysis of the genome-wide CRISPR screen presented in this thesis, and all associated analyses.

Publications arising from this work:

1. Gruosso, T., Gigoux, M., Manem, V. S. K., Bertos, N., Zuo, D., Perlitch, I., . . . Park, M. (2019). Spatially distinct tumor immune microenvironments stratify triple-negative breast cancers. J Clin Invest, 129(4), 1785-1800. Retrieved from: https://www.ncbi.nlm.nih.gov/pubmed/30753167. doi:10.1172/JCI96313

Introduction

1. The immune system and its effector cells

1.1. The four tasks of the immune system

Over the course of an individual's life, one will be confronted by a multitude of pathogens and infectious agents that may, for one purpose or another, inflict damage upon the vessels they invade (1). To protect themselves against these, our bodies are equipped with an immune system, which is composed of a variety of effector cells, molecules and compounds (1). In order to serve as an effective defense, our immune system must complete four tasks (1). The first is immunological recognition, or the ability to identify the presence of an infection (1). This task is mainly carried out by the white blood cells of the innate immune system, such as neutrophils or macrophages, in the form of a quick and immediate but non-specific response, but also supported by the B and T lymphocytes of the adaptive immune system (1). The aim of the second task is to contain and/or eliminate the infection by involving other immune effector functions such as the complement system, antibodies and the cytotoxic capacities of lymphocytes and other white blood cells (1). Whilst eliminating the infection, it is important for the immune response to be kept under control so that it does not cause damage to the body (1). The ability of the immune system to limit itself is an important feature and is defined as the third task (1). An impairment to this mechanism often results in conditions such as allergy and autoimmune disease (1). The fourth and final task is the reinforced defense of the body upon re-exposure to the same pathogen (1). This ability is based on immunological memory, or the ability of the immune system to preserve a memory of previously encountered antigens, the component of a pathogen recognized by our immune systems,

so that upon re-exposure, the immune system can mount a quicker, more potent, and specific response to the same pathogen (1).

1.2. Cells of the adaptive immune system

There are two major types of lymphocytes in the vertebrate immune system, B lymphocytes, or B-cells and T-lymphocytes, or T-cells (1). Each type has a distinct role and different antigen receptors (1). Lymphocytes that have not yet encountered their corresponding antigen are known as naïve lymphocytes (1). Upon recognition of their antigen, lymphocytes become activated and have to differentiate further into fully functional lymphocytes; at this stage they are known as effector lymphocytes (1).

B and T-cells are distinguished by their antigen receptor (1). The B-cell antigen receptor, or B-cell receptor (BCR) is formed by the same genes that encode antibodies, a class of proteins known as immunoglobulins (Ig) (1). The T-cell antigen receptor, or T-cell receptor (TCR) is also related to immunoglobulins but is distinct in its structure and recognition properties (1). Once they encounter their corresponding antigen, B and T-cells mature into different types of effector lymphocytes (1). After antigen-binding to the BCR, the B-cell with proliferate and differentiate into a plasma cell, the effector cell form of B lymphocytes, which then secretes antibodies that have the same antigen specificity as the plasma cell's B-cell receptor (1). On the other hand, when a T-cell first encounters the antigen specific to its TCR, it proliferates and differentiates into one of several different functional types of effector T lymphocytes (1). Effector T-cells can manifest three broad classes of activity (1). Cytotoxic T-cells ($CD8^+$ T-cells) directly kill target cells that are infected with viruses or other intracellular pathogens that bear the antigen (1). Helper T cells ($CD4^+$ T-cells, which can be of different subclasses, such as Th1, Th2, Th17 and

others) provide signals, often in the form of specific cytokines that activate the function of other cells, such as production of antibody by B-cells and macrophage killing of engulfed pathogen (1). For example, Th1 cells are responsible for activating macrophages to help control certain types of bacteria, while Th2 cells specialize in promoting responses at mucosal surfaces, particularly in response to parasitic infections (1). The main functions of Th17 cells in adaptive immunity focus on enhancing neutrophil response and promoting barrier integrity (i.e skin, intestine, etc.) (1). Regulatory T-cells (T_{regs}) suppress the activity of other lymphocytes and help to limit the possible damage of immune responses (1). A certain number of effector B and T-cells activated by antigen will differentiate into memory lymphocytes, which will be retained for long-lasting immunity (1).

1.3. T-cell activation

T-cells circulate throughout the body after leaving the thymus, where they are generated, in search of their corresponding antigen on the surface of antigen-presenting cells (APCs) (1-3). The antigen is held in place on the APC surface by the MHC complex, which has the ability to bind the TCR on T-cells (1-3). Once binding occurs, it triggers an initial activation state within the cells, known as the first signal of T-cell activation (Figure 1, left panel) (1-3). To create a stable interaction, T-cells must recognize the foreign antigen strongly and specifically, thus mounting an effective immune response (1-3). The second signal is delivered by co-stimulatory molecules, which are located on both T-cells and APCs (Figure 1, left panel) (1-3). The interaction of a co-stimulatory molecule with its corresponding ligand results in further stimulation of the T-cell (1-3). If the first signal is not followed by the second signal, this response will not lead to a productive activation or further differentiation of the T-cell (1-3). Various co-stimulatory molecules exist, in the

case of $CD4^+$ helper T cells the most common are B7.1 (CD80) and B7.2 (CD86), present on APCs, which bind to CD28 on T-cells (Figure 1, left panel) (1-3). In order to contain this response, and as a negative feedback mechanism, stimulation of CD28 by B7.1 or B7.2 induces the production of CTLA-4 (CD152), an inhibitory molecule which competes for B7 binding sites with CD28, and in consequence reduces activation signals to the T-cell, winding down the immune response (Figure 1, right panel) (1-3). Collectively, these co-stimulatory and co-inhibitory molecules are known as immune checkpoints (1-3). The third and final signal comes as additional instructions from cytokines secreted by the APC, which will determine into which type of effector cell the T-c ell will further differentiate into (Figure 1, left panel) (1-3).

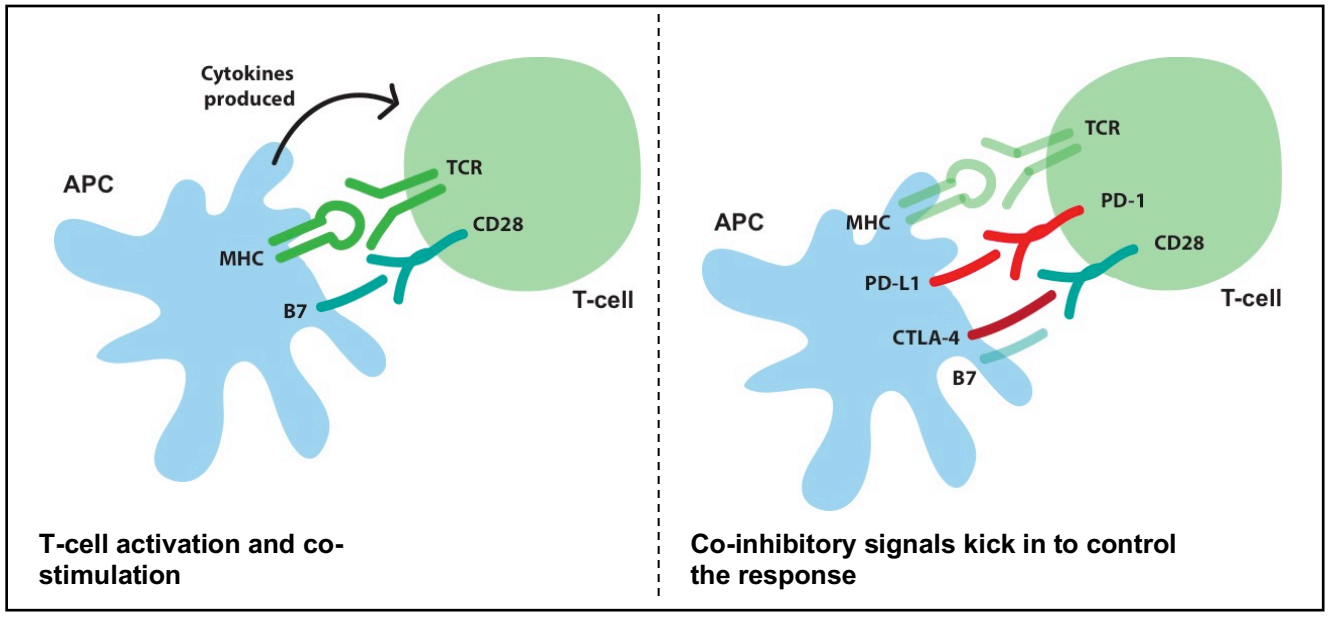

Figure 1) T-cell activation and regulation (adapted from Sharma et al. 2011 (3)). Left panel represents initial state of T-cell activation and further co-stimulation. Right panel represents the negative feedback mechanisms that are triggered in turn, to control the immune response.

2. Immunity in the cancer field

2.1. History

For over a century, scientists have attempted to harness the power of the immune system to fight malignancies (1, 4). There is growing awareness to the fact that the success of chemotherapy and radiotherapy, where a patient's disease can be stabilized well beyond discontinuation of treatment, and occasionally cured, also relies on the induction of a durable anti-cancer immune response that could discriminate between tumorigenic and normal cells within our bodies (1, 5-6). Cancer immunotherapy, which aims to enhance immunity to reject tumors or prevent tumor recurrence, relies on this concept that patients can generate immune lymphocytes capable of responding specifically to tumor-associated antigens (1, 5-6). Several strategies building on this concept have been devised, including cytokine treatments, vaccines, adoptive cell therapies, oncolytic viruses and immune checkpoint inhibitors, the latter of which we will be discussing here in detail (1, 5-6).

Early studies in the 1940s to 1960s on transplantable tumors in mice first revealed that the host immune system could recognize and eliminate cancer cells (1, 7). After initial tumor resection, subsequent inoculation with the same tumor cells did not result in growth. Moreover, immunization with irradiated cancer cells also afforded protection against tumor growth on subsequent inoculation (7, 8). These observations indicate that tumors can express antigens that trigger a tumor-specific T-cell response to protect the host from tumor growth (1). To demonstrate the contribution of T-lymphocytes to this response, adoptive transfers of T-cells from mice capable of rejecting the tumors could prevent

tumor growth in naïve, irradiated mice (8, 9). However, similar experiments performed on mice with spontaneous tumors, as opposed to chemical carcinogens or oncolytic viruses, failed to show any signs of tumor control by the host's immune response (10). In the 1970s, cancer immunogenicity was further elucidated when experiments showed that certain cancer cell clones derived from a mutated carcinoma cell line were rejected when injected into syngeneic mice, despite the undeterred growth of the original parental cells (7, 11-14). Moreover, these mice were protected upon subsequent challenge with the original parental cells (7, 12-14). The conclusions from these studies pointed to the fact that T-cell responses triggered by highly immunogenic antigens also triggered a response against poorly immunogenic antigens found on the original parental cells, that could not initially trigger an immune response on their own (4). These observations show that poorly immunogenic tumors, such as those that are spontaneously-derived, may express tumor antigens that are incapable of inducing a significant T-cell response (4). As such, efforts in immunotherapy have focused on developing methods to trigger and reinforce immune responses against these antigens (4).

2.2. Immune checkpoints

In the mid 1990's, the complexity of T-cell activation and regulation was becoming clearer to researchers (15). In addition to initiation, proliferation and functional differentiation, T-cell activation could also induce an inhibitory pathway through immune checkpoints, that could eventually attenuate and terminate an immune response (15). The advent of checkpoint blockade, a strategy that aims to inhibit immune checkpoints, has significantly advanced the field of cancer immunotherapy within the last decade (1, 15). Immune checkpoints, as previously described, are molecules in charge of boosting or dampening

the activation level of a particular lymphocyte (1, 15). Immunotherapy strategies focus largely on negative regulatory immune checkpoints, as their inhibition has the potential to unleash the anti-tumorigenic potential of an immune response. To date, checkpoint blockade has produced dramatic results in a subset of malignancies and is currently one of the most exciting developments in cancer immunotherapy (1, 15).

2.2.1. PD-1 and CTLA-4, two immune checkpoints harnessed for cancer immunotherapy

As previously described, expression of CTLA-4, a gene with very high homology to CD28, is initiated by T-cell activation. Though CTLA-4 shares a ligand with CD28 (the B7 molecules) it can bind them much more effectively than CD28 can (15). At the time, two laboratories had independently showed that CTLA-4 could oppose CD28 co-stimulation and thus down-regulate T-cell responses (15-17). With this knowledge, CTLA-4 function was translated into the cancer immunotherapy field by proposing that blocking its interaction with B7 molecules could allow T-cell responses to persist sufficiently to result in tumor eradication (15). Several studies were done in mice (18-22) to test this hypothesis and show that by releasing endogenous immune responses, perhaps even without the specificity of antigenic targets, one could trigger the immune response to kill tumor cells, and if combined with agents that can directly kill tumor cells and release antigens for presentation by APCs, could further improve antitumor responses (15). The data generated lead to the development of ipilimumab, an antibody against human CTLA-4 for clinical testing. Its use in clinic led to considerable improvement in overall survival for metastatic melanoma patients (23-24), with FDA approval being obtained in 2011. The success of anti-CTLA-4 opened up the field of immune checkpoint therapy and additional

checkpoints were and still are being studied as therapeutic targets (15, 25). In 2000, programmed cell death-1 (PD-1) was shown to be another immune checkpoint that limits the responses of activated T-cells (26). PD-1, like CTLA-4, has two ligands, PD-L1 and PD-L2 (for PD-1 ligand 1 or 2), which are expressed on many cell types (15). The function of PD-1, however, is distinct from CTLA-4, in the sense that it does not interfere with co-stimulation, but rather with the subsequent signaling mediated by the T-cell antigen receptor (27). Therefore, it was hypothesized that rather than functioning early in T-cell activation, the PD-1/PD-L1 pathway acts downstream to protect target cells (those expressing the antigen specific to the T-cell's TCR and a PD-1 ligand) from attack (15, 27). Its ligand, PD-L1 (B7-H1), has been documented to be expressed on various cells types, including T-cells themselves, epithelial cells, endothelial cells and tumor cells after exposure to the cytokine interferon-γ (IFN-γ), which is produced by activated T-cells (28).

2.2.2. Success of immune checkpoints in the clinic

Ipilimumab, the antibody to human CTLA-4, began being tested in clinical trials in the later 1990s and early 2000s (15). Tumor regression was observed in patients with various tumor types, including melanoma (29), renal cell carcinoma (30), prostate cancer (31), urothelial carcinoma (32) and ovarian cancer (33) in Phase I/II clinical trials. Phase III clinical trials were conducted in patients with advanced melanoma and demonstrated improved overall survival for patients (23-24). About 20% of patients lived for more than four years after treatment, with a recent analysis indicating survival of 10 years or more for a subset of patients (34).

Antibodies against the PD-1/PD-L1 axis also show clinical responses in multiple tumor types, including melanoma, renal cell carcinoma, non-small cell lung cancer (35) and

bladder cancer (36). A large phase I clinical trial for the anti-PD-1 antibody Pembrolizumab was shown to lead to response rates nearing 40% in patients with advanced melanoma (37), with a subsequent study reporting an overall response rate to of 26% in patients who showed progressive disease following ipilimumab treatment (38). Pembrolizumab was FDA-approved in September 2014 (15). A phase III trial of a different anti-PD-1 antibody (Nivolumab) also showed clinical benefit in patients with metastatic melanoma, with an objective response rate of 40% and overall survival rate of 72.9%, as compared to an objective response rate of 13.9% and overall survival rate of 42.1% for patients treated with dacarbazine chemotherapy (39). Nivolumab received FDA approval in December 2014 as a treatment for patients with metastatic melanoma (15, 39). Given the success of these two targets, there has been a rising interest in harnessing other immune checkpoints within the immunotherapy field, with several other candidates currently being studied in the field (15). Moreover, existing immune checkpoints therapies are currently being translated to more cancer types, such as triple-negative breast cancer, a breast cancer subtype that displays a higher relative infiltration of cytotoxic $CD8^+$ T-cells, and thus proves an interesting candidate for available immunotherapies (40-42).

3. Triple-negative breast cancer

3.1. Breast cancer overview and statistics

Breast cancer is the most common cancer, if excluding non-melanoma skin cancers, and the second-leading cause of death from cancer in Canadian women (43). In their lifetime, 1 in 8 women are expected to develop breast cancer, and as many as 1 in 31 will die from it. Breast cancer accounted for 25% of all new cancer cases in 2017, and 13% of all

cancer-related deaths in Canadian women (43). While the incidence of breast cancer has remained unchanged since the 1980's, mortality rates have decreased by 44% due to increased screening and therapeutic advancements (43). As such, the current 5-year survival rate for women diagnosed with breast cancer in Canada is 87% (43). Though the statistics are encouraging, breast cancer remains a highly heterogeneous disease comprised of multiple subtypes with varying molecular and histological characteristics, resulting in different therapeutic approaches and prognoses (44).

Upon diagnosis, treatment decisions are made by assessing breast tumors by several established clinical parameters, which are also used to predict the prognosis of a patient's disease (44-45). A tumor is staged according to its size and the extent to which it has spread locally or to the rest of the body (44-45). Higher stage cancers are associated with worse patient outcome (44, 46-47). The level of differentiation exhibited by the tumor cells is referred to as the tumor grade. Differentiation is defined by how morphologically similar they are to normal, non-cancerous breast epithelial cells. High grade and poorly differentiated tumors are indicative of aggressive disease and are often associated with a poor prognosis (44, 49).

3.2. Breast cancer subtypes

3.2.1. Histopathological subtypes

Breast cancer subtype stratification is based on immunohistochemical detection of the estrogen receptor (ER), progesterone receptor (PR), and human epidermal growth factor receptor 2 (HER2) (44). The majority of all breast cancers diagnosed (70%), are ER+/PR+/HER2- tumors, and tend to be low grade, with low metastatic burden and rate of recurrence (49). These tumors, termed hormone receptor-positive, are considered

hormone-dependent and have the best clinical outcome due to targeted therapeutic strategies. HER2+ tumors represent 20% of all breast cancers diagnosed and are characterized by overexpression and amplification of the HER2 protein (50). Though associated with poor prognosis, the development of therapies directed against HER2 have shown significant benefit in the clinic (50-52). Breast tumors that are negative for all these markers (i.e ER-/PR-/HER2-) are collectively termed triple-negative breast cancers (TNBC) and represent around 15% of all breast tumors (53). The TNBC subtype has the worst overall outcome and occurs most frequently in young women (53-54). It is a highly heterogeneous group of diseases, as it is classified based on the exclusion of hormonal markers and has been challenging due to the absence of well-defined molecular targets (55). Although TNBC patients show higher rates of clinical response to neoadjuvant chemotherapy, they present with a higher rate of recurrence compared to other subtypes. Less than 30% of women with metastatic TNBC survive past 5 years and almost all die as a direct cause of the disease despite chemotherapy, the current standard of care (55). Recent gene expression profiling of breast cancers has further highlighted this heterogeneity within the subtype (55-56).

3.2.2. Molecular ‘intrinsic’ subtypes

To provide insight into breast cancer heterogeneity, global gene expression was performed using a 496-gene ‘intrinsic’ gene set to divide the cancers based on their gene expression profiles (44). The determined profiles were termed luminal-like, HER2-enriched, basal-like and normal-like subtypes (57). Subsequent studies further subdivided luminal-like into luminal A and B and identified an additional subtype termed claudin-low (58). These molecular subtypes have distinct clinical outcomes, with the

luminal-like subtype showing the best prognosis, and the basal-like subtype presenting with the worst (59-60). The original gene ‘intrinsic’ gene set was curated down to 50 genes, termed the prediction analysis of microarrays (PAM) 50 (61). These are routinely used in clinical research to classify breast cancers and predict response to treatment and patient outcome.

When compared to the previously defined histopathological subtypes, the molecular subtypes showed striking, though incomplete, overlap, with most ER+ tumors falling into the luminal A and B subtypes, HER2+ tumors into the HER2-enriched subtype and the basal-like and claudin-low subtypes making up approximately 50% to 30% of triple-negative breast cancers, respectively (57, 62). Basal-like breast cancers are named so due to their expression of markers of breast basal/myoepithelial cells, such as CK5/6, 14 and 17, EGFR and vimentin (63). With a highly proliferative and genomically unstable phenotype, these tumors are often associated with poor prognosis (63). The claudin-low subtype is characterized by tumors with low expression of tight junction and cell adhesion proteins, such as Claudin 3, 4, 6 and E-Cadherin, and enrichment in the expression of stem and mesenchymal gene signatures (64-65).

Moreover, more recent studies further subdivided TNBC into 6 subtypes based on gene expression. Initially, the six subtypes included basal-like 1 (BL1), basal-like 2 (BL2), immunomodulatory (IM), mesenchymal (M), mesenchymal stem-like (MSL) and luminal androgen receptor (LAR) (55). However, after further refinement by removal of stromal and immune cell contamination, which was blurring the epithelial cell signal, these were refined down to BL1, BL2, M and LAR, with each subtype showing characteristic patterns of treatment response and clinical outcome (56), highlighting the heterogeneity within this

subtype. Ongoing efforts continue to generate additional tumor stratification schemes to resolve the complicated heterogeneity observed in both histopathological and 'intrinsic' TNBC subtypes recorded in the clinic (44). The goal is to help determine an appropriate therapeutic strategy by establishing accurate patient stratification according to their disease's specific traits (44).

4. Immune checkpoints in triple-negative breast cancer

It was predicted that immune therapies would be an effective strategy to treat TNBC, based on the observation that high levels of $CD8^+$ T cells within TNBC tumours correlate with good clinical response to standard-of-care chemotherapy (66-68). This interaction between the immune system with tumor cells in breast cancer is mostly associated with TNBC and HER2-positive breast cancer, as they are thought to be more immunogenic than luminal A carcinomas (40). As a consequence, strategies to increase the number and cytotoxic potential of $CD8^+$ T cells through immune checkpoint therapy have been proposed as a therapeutic option for TNBC patients (69). Moreover, TNBC, show a higher number of tumor-infiltration lymphocytes (TILs) and a higher PD-L1 protein or mRNA expression compared with other breast cancer subtypes (70).

However, in phase I clinical trials of a PD-L1 and PD-1 inhibitor, only ~20% of TNBC patients responded (71-73). This low response rate stressed the need to identify those patients that are most likely to respond to immune checkpoint therapy and suggested that there were other factors influencing this response. A recent study of ~3,500 ER-negative breast cancer patients concluded that only patients with $CD8^+$ T cells interspersed between tumour cells were associated with better outcome; high numbers of stromal

$CD8^+$ T cells lacking contact with tumour cells were even associated with poor outcome (66). On this basis, we have identified distinct tumour microenvironments associated with $CD8^+$ T cell localization patterns and outcome in TNBC using laser-capture microdissection (LCM) on isolated tumour and stroma from a cohort of 38 TNBC patient tumours (invasive ductal carcinomas prior to therapy) (74). To address correlations between $CD8^+$ T cell localization and outcome, the location of $CD8^+$ T cells in TNBC FFPE tumour sections was identified by immunohistochemistry (IHC) directed against $CD8^+$ and quantified in an unbiased manner using software algorithms (Aperio Image Analysis) (74). This identified distinct patient subsets defined by differences in $CD8^+$ T cell localization.

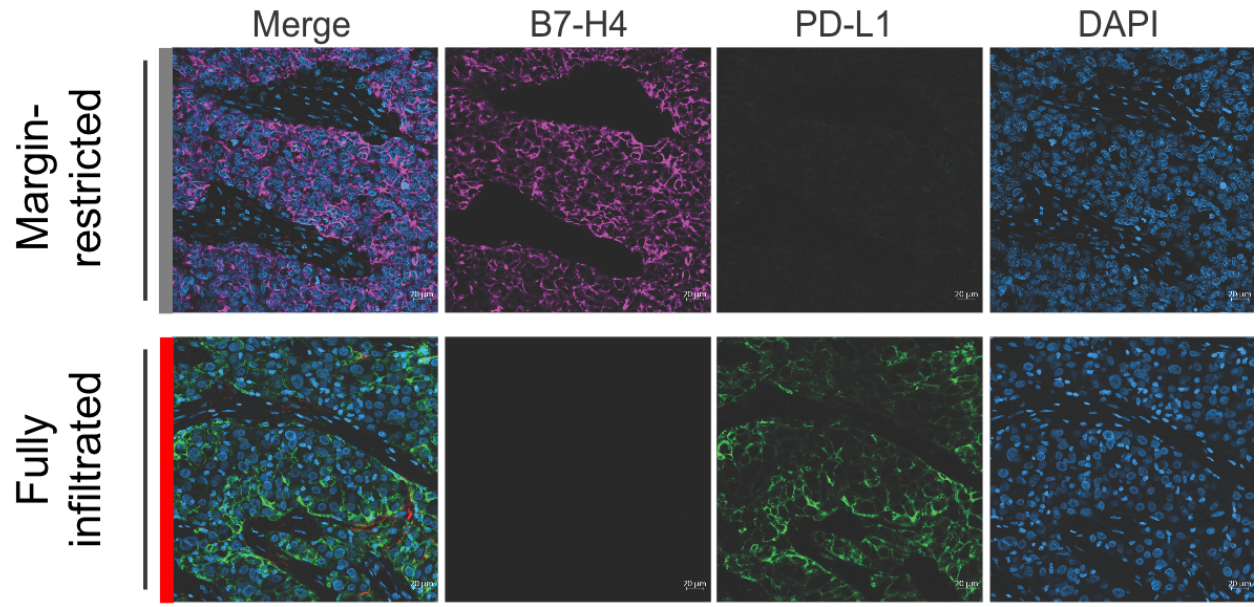

Figure 2) The margin-restricted subset of TNBC patients demonstrates high expression of the PD-L1 family member, B7-H4, within the tumor epithelia. Representative staining showing high expression of the immune checkpoint, B7-H4, in the tumor epithelia of a TNBC tumor with margin restriction of $CD8^+$ T-cells, when compared to a fully infiltrated tumor with high PD-L1 expression with the tumor epithelia. DAPI represents the cell nuclei.

One of these subsets showed an immunoreactive microenvironment, defined by the presence of granzyme-B, $CD8^+$ T cell infiltration, tumour expression of PD-L1 and good outcome (74).

These tumours are thought to be those that would mostly benefit from anti-PD-1/PD-L1 immunotherapy (74). In contrast, an immune-cold microenvironment displayed restriction of $CD8^+$ T-cells to tumour margins, elevated tumour expression of another immune checkpoint, the PD-L1 family member B7-H4, and poor outcome (Figure 2) (74).

These findings raised the question of whether B7-H4 expression on the tumor epithelium could be responsible for the exclusion of $CD8^+$ T-cells from the tumor core.

5. B7-H4, a PD-L1 family member

5.1. B7 family of immune checkpoints

As previously discussed, under normal physiological conditions, immune checkpoints prevent autoimmunity and protect surrounding tissues from the immune response, they also down-regulate an immune response once the pathogen is cleared (25). In the context of cancer, immune checkpoints are hijacked and dysregulated by the tumor. By up-regulating negative immune checkpoints, which aim to decrease an immune response, the tumor prevents attack by immune cells (25). With the recent interest in co-inhibitory molecules as an immunotherapy strategy, characterization of various B7 immune checkpoint family members was done (75). 10 members were characterized so far: B7-1 (CD80), B7-2 (CD86), PD-L1 (B7-H1, CD279), PD-L2 (B7-DC, CD273), B7-H2 (ICOSL, CD275), B7-H3 (CD276), B7-H4, B7-H5 (VISTA), B7-H6, and B7-H7 (HHLA2), all of which are transmembrane proteins with extracellular immunoglobulin-like domains and a

subset of which have characterized receptors (75). They can be expressed on various cell types, though initially thought to be only on haematopoietic cells such as APCs and T-cells, they were also identified on tumor cells (76).

5.2. B7-H4

B7-H4, also known as B7x, B7s1, Dd-0110 and Vtcn1, was first identified in 2003 by sequence similarity with other B7 family members (77-79). Its sequence encodes a glycosylphosphatidylinositol (GPI)-linked protein that is heavily glycosylated and by current consensus, is defined as a protein having an inhibitory role on T-cell function by limiting proliferation, cytokine production and cytotoxicity (76-79). Characterization of the protein over the years has shown that it doesn't share binding partners with any other B7 family members, and although BTLA was once proposed to be the B7-H4 ligand, specific and stable interaction between the two could not be demonstrated (77-78, 80-81). To this day, the ligand for B7-H4 has not been identified (76).

5.2.1. Expression and function

Though the presence of B7-H4 transcripts has been documented across a wide variety of tissues, B7-H4 surface expression is limited in most normal tissues (77, 82-83), but has been observed in thymus, spleen, kidney, placenta (85, 85), female genital tract, lung, and pancreas (85).

The immunosuppressive role of B7-H4 has been widely observed in various *in vivo* models, especially in the context of diabetes. In another setting, overexpression of the protein in transplanted islets prolonged transplant survival and reduced proinflammatory infiltrates (86). In addition, host deficiency in B7-H4 conferred resistance to a lethal pulmonary infection with *Streptococcus pneumoniae*, as disease improvement correlated

with an increase in immune cell presence, specifically with regards to infiltrating $CD4^+$ helper and $CD8^+$ cytotoxic T-cells (87). Collectively, studies on B7-H4 function reveal an immunosuppressive and tissue-protective role in multiple mouse and disease models (76).

5.2.2. Expression in innate immunity

B7-H4 expression on a highly immunosuppressive subset of tumor-infiltrating macrophages was identified in ovarian cancer, whose expression could be induced by stimulation with IL-10 and IL-6 (88). Immunosuppressive $B7\text{-}H4^+$ tumor-associated macrophages have also been observed in glioma patients (89). In another study, *ex-vivo* stimulation of mouse macrophages with IL-10 and TGF-b increased B7-H4 expression (90). Several other studies showed that B7-H4 expression was STAT3-dependent (89), and blockage of both IL-10 and IL-6 (89-90) or stimulation with granulocyte macrophage colony-stimulating factor (GM-CSF) and IL-4 (88) reduced B7-H4 expression. Overall, these data show that a number of stimuli can affect B7-H4 expression on cells of the innate system (76).

5.2.3. Expression in adaptive immunity

To date, expression of B7-H4 itself on T-cells is uncertain, but the expression pattern of its receptor is better documented due to studies using B7-H4 fusion proteins, detecting its expression on T-cells (76). Naïve T-cells do not express the B7-H4 receptor, but it has been shown that it can be induced with concanavalin-A (77) or anti-CD3 (79) stimulation. Ligation of B7-H4 to its receptor inhibits T-cells proliferation and activation, partly through a reduction in JunB expression, a component of the AP-1 family that binds the IL-2 promoter, resulting in T-cell proliferation (77). Interestingly, a study showed that strong

TCR stimulation or co-stimulation was able to overcome B7-H4 inhibition, suggesting that the suppressive effects of B7-H4 were more relevant in the context of low-affinity antigens, such as those associated with an anti-tumor response (76, 77).

B7-H4 knockout did not show impairment in normal lymphocyte development with normal numbers, proportions or level of activation in naïve mice (91). However, an impairment was documented in T-cell polarization where T-cells from B7-H4 knockout mice showed an increased production of IFN-γ, a prototypic Th1 cytokine (Th1 being a subtype of $CD4^+$ helper T cell, favorable in a cancer setting), in response to infection with *Leishmania major* (91). Since Th1 responses improve the development of cytotoxic T-cell responses, a key population currently studied in promoting tumor regression, this finding brought about the concept of blocking B7-H4 function may prove beneficial in improving antitumor immunity (92).

5.2.4. B7-H4 in tumor cell biology

Though most normal tissues do not express B7-H4 at their cell surface, the same cannot be said for human tumors, including ovarian carcinoma (82, 84-85, 93), breast cancer (84-85), endometrial adenocarcinoma (94), bladder cancer (95), esophageal and oral squamous cell carcinoma (96-97), glioma (89), prostate cancer (90), pancreatic cancer (98), cervical cancer (99), melanoma (100), lung cancer (82, 101-102), gastric cancer (103-104) and renal cell carcinoma (105-106). *In vitro* assays with a colorectal carcinoma cell line (HCT-116) show B7-H4 protein upregulation after culture with TGFβ-1 through an increase in the microexon miR-155, in turn leading to a decrease in the B7-H4-inhibitory microexon, miR-143 (107). B7-H4 protein can be membrane-bound but has also been documented in intracellular form, though the mechanisms of B7-H4 subcellular

localization remain unclear (94, 105). In one paper, a decrease in the level of membrane-bound B7-H4 of APCs from diabetic mice and patients coincided with an increase in serum levels of soluble B7-H4 after cleavage with nardilysin, a metaloendopeptidase (108). Liberation by cleavage was also proposed as the mechanism resulting in increased levels of soluble B7-H4 in the serum of patients with more advanced ovarian cancer (109). In another instance, human B7-H4 was documented to have a nuclear localization sequence (NLS) that allows it to shuttle between the cytoplasm and the nucleus, as blocking nuclear export with an inhibitor caused an increase of B7-H4 nuclear localization (105). Point mutation of the NLS suppressed the inhibitor-induced nuclear localization of B7-H4 (105). Mechanisms of B7-H4 shuttling from the nucleus to the cytoplasm and vice-versa were not elucidated however (105).

In tumor cell lines, B7-H4 has been documented to have an intrinsic role in augmenting proliferation and decreasing susceptibility to apoptosis (101, 105, 110). Knock-down of the protein in A549 cells, a lung adenocarcinoma cell line, inhibited cell proliferation, invasion and migration (101). Additionally, knockdown cells had lower expression of anti-apoptotic protein Bcl-2 and higher expression of pro-apoptotic protein Bax, as well as caspase-3 and 8 (101). B7-H4 overexpression in renal cell carcinoma cell lines increased survival in response to doxorubicin or docetaxel treatment (105). In esophageal squamous cell carcinoma cell lines, B7-H4 knock-down reduced proliferation and increased apoptosis, possibly though augmentation of IL-6 production with the JAK2/STAT3 pathway (110).

5.2.5. B7-H4 in disease

B7-H4's role in disease has mostly been studied in the context of autoimmunity and cancer. There have been reports of high B7-H4 expression correlating with increased lymphocytic infiltration (106), reduced levels of tumor invasion (107), and improved survival for patients with breast cancer (10). However, B7-H4 is most commonly reported to correlate with lower survival rates, advanced clinical stage, increased lymph node involvement, decreased T-cell infiltration, and increased macrophage infiltration (76). The consensus being that B7-H4 expression contributes to, or is associated with, pro-tumorigenic factors (76). Given that B7-H4 can be expressed by many different cell types and can shuttle between the cytoplasmic and nuclear compartments in humans, it is possible that it has many roles depending on its subcellular location (76). Moreover, levels of soluble B7-H4 vary with ovarian cancer subtype (112) and are increased in patient with advanced stage tumors (109). Its presence in the serum is also a negative prognostic indicator for multiple diseases including glioma (89), renal cell carcinoma (113), type 1 diabetes (108), and rheumatoid arthritis (114). Notably, B7-H4 expression was also recently identified as a biomarker for poor outcome immune cold non-small cell lung cancers (73).

5.2.6. B7-H4 as a novel therapeutic target

With the previously outlined findings for the role of B7-H4 in inhibiting T-cell proliferation and effector function (77-79), research groups have strived to develop antibodies to block B7-H4-mediated T-cell inhibition (115). Moreover, the observed up-regulation of B7-H4 with disease progression and its retention on metastases of certain cancers, make it an attractive target for treating late-stage, refractory malignancies (85, 100). In tumor

immunity, studies support an inhibitory role for B7-H4 (76). B7-H4 knockout mice developed fewer metastatic lung nodules after intravenous infusion of 4T1 breast cancers, a murine mammary tumor cell lines, when compared with control mice (76). Knockout mice also had higher survival rates, with resistance to tumor re-challenge and an immune infiltrate characteristic of an improved anti-tumor response (76). Similarly, transplantation of a 4T1 breast tumor cell line (12B), a derivative of the line that elicits a strong $CD8^+$ T-cell response, showed reduced tumor growth in a B7-H4 deficient host as a result of increased antitumor T-cell activity (116). High levels of B7-H4 expression are often associated with lower levels of T-cell infiltration, consistent with the idea that blocking B7-H4 interactions may promote T-cell infiltration and enhance immunotherapy (86, 94, 98, 103). With the recent clinical success of immune inhibitory molecules such as CTLA-4 and PD-1/PD-L1, it is important to continue evaluating the potential for B7-H4 blockade in enhancing antitumor responses (76, 117).

5.2.7. Antibody treatments for B7-H4

In studies using mice where treatment with monoclonal antibodies against B7-H4 was administered, blocking the interaction of B7-H4 with its ligand, primary tumor growth was significantly suppressed, metastatic nodules were reduced, survival was prolonged, T and natural killer (NK)-cell infiltration was increased and myeloid-derived suppressor cells (MDSCs), an immunosuppressive cell type, were reduced (76, 116). Half of the mice that received a B7-H4-blocking antibody survived tumor challenge (with a colon carcinoma line: CT26), whereas none of the mice receiving the isotype control survived (116). Moreover, mice that did survive were subsequently protected against re-challenge with CT26 cells (116). Moreover, *in vitro* evaluation of 1H3 activity, an immunoglobulin G1 or

IgG1 monoclonal antibody developed against B7-H4, revealed that it promoted cell death through antibody-dependent cell cytotoxicity and blocked B7-H4-mediated co-inhibition of T-cells (116). Similarly, another study by Dangaj and colleagues found that an anti-B7-H4 single chain antibody could restore antigen-specific T-cell activation *in vitro* and delay the growth of established tumors *in vivo* (93).

Accumulating evidence supports B7-H4 as an attractive negative regulatory target for intervention, however, it is important to note the previous finding that B7-H4 knock-out mice did not reveal a drastic phenotype (91, 118), unlike its counterparts CTLA-4 and PD-1. Both CTLA-4 and PD-1 show profound (119-120) and moderate (121-122) autoimmune phenotypes in their respective knock-out mice models (76). Though one could interpret this as B7-H4 blockade having less severe autoimmune consequences, it could also mean that it may not prove as efficacious as CTLA-4 or PD-1 (76).

One important characteristic of B7-H4 remains its high expression on tumor cells when compared to normal cells, suggesting that it may confer an advantage to tumor cells (76). This has also highlighted that elevated expression of B7-H4 may be used as a target for various therapies, such as antibodies or chimeric antigen receptor T-cells (CAR) (76).

There remain many outstanding questions related to B7-H4 biology, first and foremost, more research is needed to identify its ligands to facilitate the study of its role in our bodies, and in cancer (76). There are many properties that make B7-H4 an attractive target for antibody-based therapies (76). Studies suggesting that blockade of B7-H4 should results in increased tumor-specific T-cell responses (77-79, 83, 88-89, 116, 123) and promising preclinical results show efficacy of B7-H4 antagonistic antibodies in reducing tumor growth and augmenting antitumor immunity (93, 116). In addition, B7-H4

upregulation on tumor tissues can and has been selectively used to target drugs (124) and CAR T-cells (125) to tumor tissues in preclinical mouse models. However, it is important to consider lethal on-target off-tumor activity of CAR T-cells or antibodies (76). The current momentum in the field of immunotherapy for cancer treatment will no doubt encourage the research required to develop B7-H4 into another successful therapeutic target (76).

6. Immune checkpoint glycosylation in cancer

6.1. PD-L1 glycosylation and B7-H4 glycosylation

A recent study by Li et al. investigated the role of protein glycosylation for PD-L1, and how it could contribute to immunosuppression (126). The role of tumor glycosylation in immune evasion has until recently, mostly been overlooked, despite the fact that aberrant tumor glycosylation alters how the immune system perceives the tumor and can also induce immunosuppressive signaling through glycan-binding receptors (127).

The key finding by Li et al. is the identification of a glycosylation event on PD-L1 that is essential for its interaction with PD-1 and subsequent suppression of T-cell activities. Their research found that epidermal growth factor (EGF) induces PD-L1 interaction with PD-1, and that this interaction requires β-1,3-N-acetulglucosaminyl transferase (B3GNT3) expression in triple-negative breast cancer (126). Downregulation of B3GNT3 enhanced cytotoxic T-cell-mediated anti-tumor immunity, and a monoclonal antibody targeting specifically glycosylated PD-L1 blocked PD-L1/PD-1 interaction whilst promoting PD-L1 internalization and degradation (126). In addition, drug conjugated antibody against glycosylated PD-L1 induced a potent cell-killing effect as well as a

bystander-killing effect on adjacent cancer cells lacking PD-L1 expression without detectable toxicity when tested in a mouse model (126). Their work proposed targeting protein glycosylation as a potential strategy to enhance immune checkpoint therapy (126).

A heavily glycosylated molecule, B7-H4 has been documented to have seven potential N-linked glycosylation sites (78). This is a common feature for many checkpoint targets, as was documented in the work by Li et al (126). Moreover, their work verified whether glycosylation of immune receptor/ligands was critical for binding to their corresponding receptor (126). By using an *in vitro* receptor-ligand binding assay to investigate the interaction between receptors and glycosylated vs. non-glycosylated ligands (126). PD-L1 and PD-L2 binding to PD-1 was abrogated and showed the most striking result compared to other immune checkpoints, such as CTLA-4, which only showed moderate loss of binding to its ligands, B7.1/B7.2 (126). Moreover, co-inhibitory but not co-stimulatory ligand/receptor pairs exhibited significant loss of binding upon loss off glycosylation (126). This experiment did not prove fruitful in the case of B7-H4, as its ligand is not known, and therefore could not be assessed as for the other inhibitory checkpoints (126). However, the evidence for the importance of glycosylation to PD-L1 function by Li et al. supports its involvement in co-inhibitory signaling interactions, suggesting that the status of membrane receptor glycosylation in other immune checkpoints should be considered to improve the efficacy of cancer immunotherapy (126). Moreover, as one of the major concerns regarding antibody-drug-conjugates (ADC) is its clinical toxicity, targeting the glycosylated form of PD-L1 could improve treatment specificity and reduce toxicity, as shown in the mice experiments by Li. et al (126).

6.2. Mechanisms of glycosylation

Most plasma-membrane and secretory proteins undergo addition of carbohydrate moieties that are subsequently trimmed and modified (128). This type of protein modification is known as glycosylation and is categorized by N-linked and O-linked glycosylation (128). O-linked glycosylation entails the addition of an oligosaccharide to a hydroxyl group of a serine or threonine (128). In N-linked glycosylation, the oligosaccharide is linked to the amide nitrogen of asparagine (128). As we will be focusing on N-linked glycosylation of B7-H4, I will orient this introduction as such.

6.2.1. N-linked glycosylation

N-linked glycosylation occurs in all eukaryotes, in some Archaea and bacteria. Its assembly is a complex sequence that spans the ER and Golgi apparatus (128). N-glycans have a plethora of roles for protein function, including maturation and intracellular trafficking of glycoproteins, as well as forming epitopes involved in protein-protein interactions in the extracellular space (128). The addition of carbohydrates also contributes to maintaining protein integrity (129). Biosynthesis of all N-linked oligosaccharides begins with the addition of a pre-formed oligosaccharide precursor in the rough ER (128). The transfer of the entire oligosaccharide from a carrier to an asparagine residue on a nascent polypeptide (as soon as it enters the luminal side of the ER) is catalyzed by the oligosaccharide-protein transferase or OST complex (128). Select asparagine residues must be part of the tripeptide sequences Asn-X-Ser or Asn-X-Thr (where X is any amino acid but proline) to qualify as substrates for this transferase (128). The human OST complex is formed of seven different polypeptide chains, the sequences of which are highly conserved among mammalian species, I will summarize here a few

key subunits of interest (128, 130). There are two isoforms of the catalytic subunit of the complex, STT3A and STT3B, which differ in their acceptor substrate selectivity (130). There are also two ribophorin subunits, RPN1 and RPN2, which interact with ribosomes and participate in co-translocational glycosylation of entering polypeptides in the ER (130). Another subunit, DAD1, initially discovered in the search for genes involved in apoptosis, was also observed to be tightly associated with the active OST complex (130). It is hypothesized that DAD1 provides structural and functional integrity for the OST complex, and a deficiency was shown to cause a time-dependent defect on OST activity (130, 131). Finally, the DDOST subunit, also known as OST48, is poorly characterized in its function, with only findings in the yeast analog, Wbp1, showing that it could be responsible for binding of the lipid linked-oligosaccharide donor substrate (130, 132), however, further research supporting this notion was not generated. It is important to keep in mind that the OST complex is a key player in transferring the glycan onto selected glycosylation sequences present in a multitude of different protein substrates (130). Therefore, studies characterizing its subunits have proven difficult given that the output of the N-glycosylation process is a large number of different N-glycoproteins, therefore knock-out studies make it difficult to pinpoint particular phenotypes and limiting off-target effects (130).

Following the OST translocation, nascent proteins that have undergone N-linked glycosylation in the ER enter the Golgi complex bearing one or more $Man_8(GlcNAc)_2$ oligosaccharide chains (128). The cis, medial and trans cisternae of the Golgi all contain different sets of enzymes that add or remove specific sugar residues as a protein moves through the Golgi complex to the cell's exterior, called glycosyltransferases (128). Added

sugars are transferred directly to the oligosaccharide, one at a time, from sugar nucleotide precursors (which are imported from the cytosol) by a variety of specific glycosyltransferase enzymes (128). Differences in oligosaccharide processing within the ER and Golgi generate variations in the structures of N-linked oligosaccharides (128).

7. Genome editing with CRISPR/Cas9 technology

Genome editing tools present a valuable approach to elucidate which genes and pathways are involved in various cellular processes, especially if these processes can later be targeted therapeutically (133). Several genome engineering approaches are available, among which the CRISPR/Cas9 system, or Clustered Regularly Interspaced Short Palindromic Repeats/CRISPR-associated protein 9 system, has proven to be the least expensive and time-consuming, as well as more precise and scalable and overall incredibly valuable for genome engineering (134). Moreover, last year, two publications were released almost simultaneously, with the discovery of novel regulators of PD-L1 function, demonstrating the utility of genomic editing tools in immune checkpoint research (135, 136)

7.1. Genetic modification tools

Two types of gene dysregulations are commonly used, knocking-down a gene product or knocking-out a gene itself (137).

7.1.1. siRNA vs shRNA

The first works at the RNA level, by generating gene downregulation using single short hairpins (shRNAs) or interference (siRNA) (138). siRNAs are 21–23 nucleotides-long, double-stranded RNAs with two nucleotide overhangs on their 3′ ends that are capable

of being incorporated into an RNA-induced silencing complex (138). shRNAs are composed of RNA folded into stem-loop structures, which require processing by the cell's DICER complex before incorporation into an RNA-induced silencing complex (138). Both siRNA and shRNA are reported to be able to achieve target-specific silencing, though they are mechanistically different (138). However, varying levels of effectiveness are expected based on considerations of both silencing efficiency and off-target effects (138). As both methods are only limited to transcribed elements of a particular gene, they do not always provide a genuine phenotypical effect and the knock-down may be short-lived (137-138, 140).

7.1.2. Common genome editing methods

The second method works at the DNA level, by knocking-out a gene, generating a complete loss-of-function phenotype (137). Multiple methods exist to generate a gene knock-out, including but not limited to zinc finger nucleases (ZFNs), transcription activator-like effector nuclease (TALENs) and the CRISPR/Cas9 system (141-142). ZFNS and TALEN are two methods commonly used in the past that are based on transcription factors coupled to nuclease domains, that are designed to target a specific sequence by matching different modules together, resulting in a double-strand break in the helix (141-142). In either strategy, after the break occurs, the cell seeks to repair it, which can be done in two ways, either through homology-directed repair (HDR) or non-homologous end-joining (NHEJ) (134, 141-142). NHEJ is the simplest method, as the cell 'polishes' off the two ends of the broken DNA and seals them back together, often producing a frame-shift mutation (134, 141-142). HDR, on the other hand, occurs when the cell tries to fix the break using an alternate copy of the sequence as a back-up

template, the unbroken chromosome for example (134, 141-143). By providing a template to the system during the gene editing process, one can force the system to insert a sequence of interest instead (134, 141-142).

7.1.3. CRISPR/Cas9 system

The most recent comer to the family of genome-editing strategy is the CRISPR/Cas system, a DNA-targeted form of RNA interference (134, 143).

CRISPR/Cas, or Clustered Regularly Interspaced Short Palindromic Repeats/CRISPR associated protein, is an important component of the bacterial immune system which allows it to build memory for and destroy bacteriophages through recognition of their RNA (134). CRISPR sequences were first discovered in the *E. Coli* genome in 1987, but their function as a protective mechanism against viral invaders wasn't understood until 2007 (134, 137). CRISPR-associated proteins or 'Cas' are composed of polymerases, nucleases and helicases, and were discovered while studying the *S. thermophilus* bacterium (134, 137). It was hypothesized that bacteria had developed an adaptive immune system using various Cas genes to store a record of invading phages and destroy them upon re-exposure (134, 137). Specific Cas proteins snip foreign DNA into small fragments (~30bp in length) which are inserted into the CRISPR sequence (134). Separate Cas proteins express and process the CRISPR loci to generate CRISPR RNAs (crRNAs) (134). These then guide (through sequence homology) the Cas nuclease to the exogenous sequence, which is located next to a species-specific protospacer-adjacent motif (a specific 3-nucleotide sequence downstream of the target sequence) or PAM (134). The CRISPR/Cas complex then binds to the foreign DNA and cleaves it, destroying the phage (134). For genome engineering purposes, the Cas9 endonuclease, or

CRISPR-associated protein 9, is targeted by a single guide RNA (sgRNA), reminiscent of the above described crRNA, with sequence homology to a particular locus, where it will induce a double-stranded break and knock-out expression of that gene (134). Whereas the native CRISPR/Cas systems have various enzymes responsible for processing foreign DNA, the optimized CRISPR/Cas9 system used in research only requires the Cas9 endonuclease and sgRNA for the gene of interest (134).

The Cas9 has the necessary components to do the following (illustrated in Figure 3):

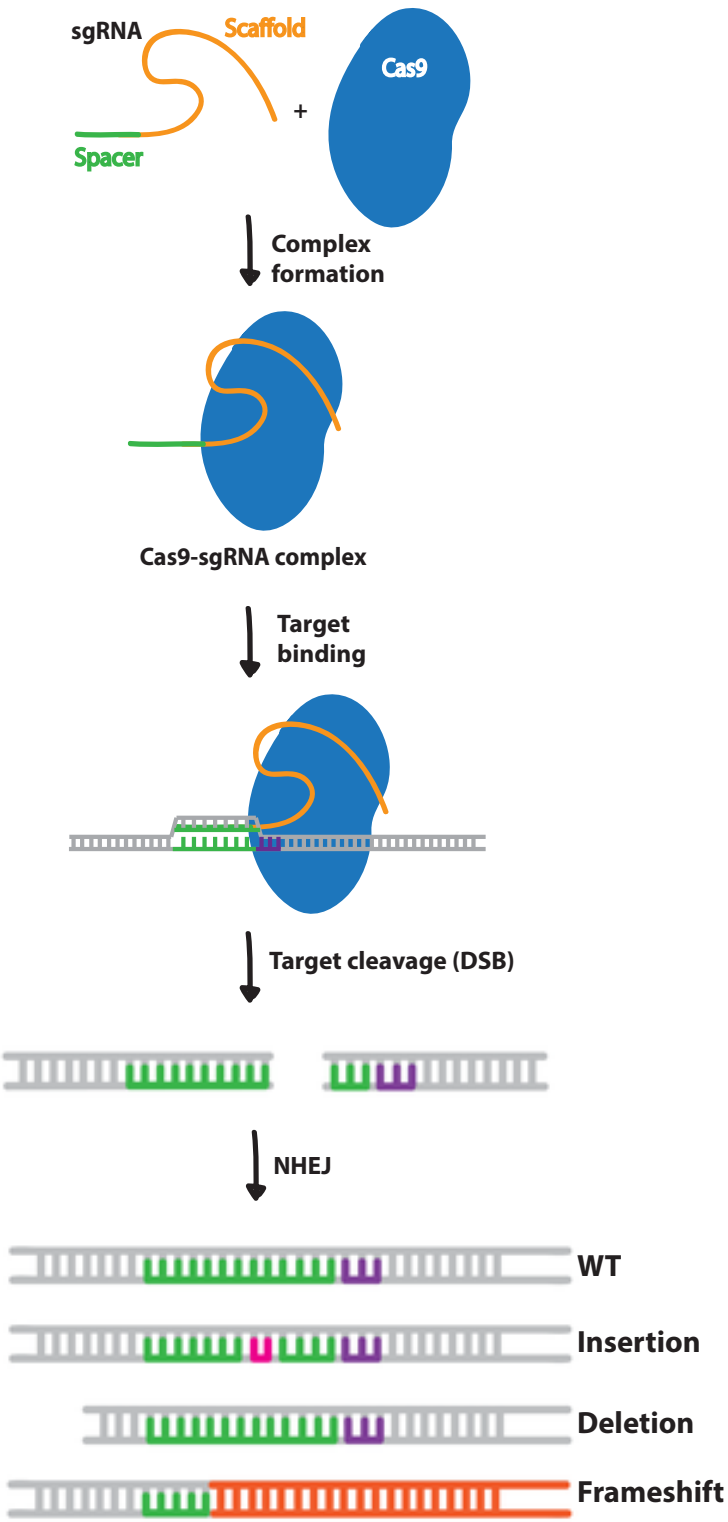

Figure 3) CRISPR-mediated gene knock-out schematic adapted from Addgene (134).

1. *Bind to an sgRNA*

The sgRNA enables Cas9 to cut a specific genomic locus of many possible loci, without it, the Cas9 cannot cut (134). The sgRNA contains both the 20-nucleotide long target or spacer sequence to direct Cas9 to a specific genomic locus and the scaffolding sequence that is necessary for Cas9 binding (134). It is important to note that the sgRNA is designed to be a genomic target that is unique compared to the rest of the genome, to ensure specificity of the knock-out and to minimize off-target effects (134).

2. *Bind to target DNA in the presence of an sgRNA provided that the target is upstream of a protospacer adjacent motif (PAM)*

Cas9 endonuclease binding to the target genomic locus is mediated by the target sequence encoded within the sgRNA, but also a 3-base pair sequence known as the protospacer adjacent motif or PAM, the protospacer being the target sequence complementary to the sgRNA sequence (134, 144). In order for a dsRNA strand to be cut by Cas9, it must contain a PAM sequence immediately downstream of the site targeted by the guide RNA, not within the sgRNA sequence itself (144). The most commonly used Cas9, derived from *S. pyogenes*, recognizes a PAM sequence of NGG, found directly downstream of the target sequence in the genomic DNA, on the non-target strand (144). Recognition of the PAM sequence is hypothesized to destabilize the adjacent sequence, allowing interrogation of the sequence by the sgRNA, resulting in RNA-DNA pairing with the matching sequence to the sgRNA (144).

3. *Cleave target DNA resulting in a double-strand break (DSB*)

Cas9 possesses two different endonuclease domains, upon target binding, it undergoes a conformational change that positions the nuclease domains to cleave opposite strands

of the target DNA (134). Thus, the end result is a DSB within the target DNA, 3~4 nucleotides upstream of the PAM sequence (134). As previously described, non-homologous end-joining (NHEJ) or homology-directed repair (HDR) can also be used to generate the desired CRISPR edits (134).

7.2. Large scale CRISPR/Cas9 applications

When studying a disease for which the underlying genetic cause is not always entirely known, identifying which genes could be important for a particular phenotype can lead to a wealth of additional leads to elucidate the mechanisms and cellular pathways at play (134). While CRISPR/Cas9 technology is not the first technique established to carry out large genetic screening experiments, it has proven to be the most robust due to its simplicity and versatility (134). Large scale uses of CRISPR technology bred genome-wide technology, where every gene in the human genome could be cleaved in a large cell population (134). The purpose of a genome-wide screen is to identify genes all across the genome that are involved in a phenotype of interest (134). In this case, variations in the expression levels of a gene of interest (134). CRISPR/Cas9 can be readily scaled up for genome-wide screening due to the broad range of potential target sequences and the ease of generating sgRNA-containing plasmids, commonly using lentivirus to deliver a pooled population of sgRNAs to Cas9-expressing cells (134). Moreover, pooled lentiviral CRISPR libraries consist of a heterogeneous population of sgRNA-containing lentiviral transfer vectors, each targeting a specific gene within the genome (134). Individual sgRNAs can also be designed using publicly available sgRNA design software and then synthesized (134). They are then pooled and cloned into a lentiviral transfer vector, resulting in a custom CRISPR library (134). Several CRISPR libraries are currently

commercially available, with some encoding the Cas9 within the lentiviral vector backbone, bypassing the requirement for Cas9-expressing cells (134).

7.2.1. Analysis of genome-wide CRISPR screen

There are several existing algorithms for the analysis of sgRNA abundance in the population of interest isolated in a CRISPR-screening experiment (145). For example, edgeR, DESeq, baySEQ and NBPSeq are all commonly used algorithms in the case of differential RNA-Seq expression analysis (145). These algorithms have the ability to evaluate the statistical significance of hits in CRISPR/Cas9 knockout screens, though only at the sgRNA level (145). Recently, a CRISPR/Cas9-specific statistical approach was developed, termed Model-based Analysis of Genome-wide CRISPR/Cas9 Knockout or MAGeCK, to identify essential sgRNAs, genes and pathways derived from CRISPR/Cas9 knockout screens (145). MAGeCK was shown to outperform existing computational methods in its control of the false discovery rate (FDR) and its high sensitivity (145). Moreover, results generated from this algorithm are robust across different sequencing depths and numbers of sgRNAs per gene (145). Validation against publicly available CRISPR/Cas9 knockout screening datasets showed that MAGeCK is able to perform both positive and negative selection screens simultaneously and identify biologically meaningful and cell type-specific essential genes and pathways (145).

8. Concluding summary

As a poorly characterized potential immune checkpoint, B7-H4 proves difficult to study, especially when it is expressed in tumor epithelial cells, on which existing studies are even more limited compared to haematopoietically-expressed B7-H4. Given our previous

finding of strong B7-H4 expression in the tumor epithelia of TNBC patients with poor immune infiltration and poor prognosis, I chose to identify the regulators of surface-expressed B7-H4 in a TNBC cell line, in order to elucidate the mechanisms responsible for its expression in TNBC. To do so, I performed a genome-wide CRISPR screen, a strategy proven useful for other immune checkpoints such as PD-L1, to identify a wide selection of potential regulators (direct or indirect) of B7-H4 cell surface levels. This screen identified many proteins involved in the glycosylation pathway. Given the recent findings by Li et al. for PD-L1 regulators (126), also identifying specific proteins within the glycosylation pathway (i.e OST complex, B3GNT3 glycosyltransferase and others), several of which I also identified in my screen, I chose to focus my downstream validation process on these select glycosylation-associated proteins: RPN1, RPN2, DDOST, DAD1, STT3B, MGAT1 and B3GNT2, which will be detailed in the results section of this thesis.

Materials and methods

Cell culture

Cell lines: BT20, HCC1143, HCC70, MDA468, HCC1569, MDA231, HCC38, SKBR3 and T47D were cultured according to ATCC recommendations. All cells were grown at 37˚C and 5% CO_2.

Flow cytometry

Single cells were stained with fluorophore-conjugated antibodies for a viability marker (BD Horizon™ Viability stain 510 FVS 510 for all experiments leading to genome-wide CRISPR screen and BioLegend Zombie Aqua™ for shRNA validation steps post genome-wide CRISPR screen) in 100μL of PBS for 15 minutes protected from light. Single cells were then washed at 1500rpm for 5 minutes in PBS with 2% FBS. CD16/32 antibodies (eBioscience™) were used to block non-specific binding and were incubated for 15 minutes on ice in 100μL pf PBS with 2% FBS. Single cells were then stained with fluorophore-conjugated antibodies for B7-H4 (BioLegend PE anti-human B7-H4 antibody) in 100μL pf PBS with 2% FBS for 30 minutes on ice protected from light. Multi-colour cell sorting was performed on a FACS Fortessa (BD Biosciences) and data analysis was performed using FlowJo (Tree Star Inc.). Antibodies used are detailed below.

Immunoblotting

Tumour-derived cell lines were lysed in RIPA buffer (5mL 1M Tris-Cl, pH 8.0, 3mL 5M NaCl, 10mL of 10% NP-40, 5mL of 10% Na-deoxycholate, 1mL of 10% SDS, made up to 100mL with double distilled H_2O) containing protease and phosphatase inhibitors. Whole cell lysates were resolved by SDS/PAGE and transferred to nitrocellulose membranes. Membranes were blocked with Li-COR Blocking Buffer (Li-COR Biosciences) and proved

with primary antibodies overnight at 4˚C. After TBST washes, membranes were incubated with infrared-conjugated (Li-COR Biosciences) for 1 hour at room temperature for signal detection by Odyssey IR Imaging System (Li-COR Biosciences). Antibodies detailed below.

Knock-out by CRISPR/Cas9 editing

B7-H4 KO lines were generated using the lentiCRISPRv2 system. Briefly, B7-H4 specific guide RNAs (designed with the MIT CRISPR design and analysis tool and ordered from IDT) were cloned into the lentiCRISPRv2 using BsmBI restriction sites. Lentiviral particles were produced by Lipofectamine 2000 transfection of 293T cells with B7-H4 sgRNA, psPAX2 and pMD2.G vectors. Filtered supernatant was the used to infect MDA468 cells for 8 hours, and 30 hours post-infection the cells were selected in puromycin for 2 days.

Genome-wide CRISPR screen for regulators of B7-H4

Infection of cell line with genome-wide CRISPR library

The Brunello genome-wide CRISPR library was obtained through Dr. Sidong Huang's library from Addgene. The library is described as such: "ready-to-use lentiviral pooled library for CRISPR screening in human cells. This backbone contains SpCas9 and unique gRNAs and can be used to make edits across 19,114 genes in the human genome". The library MOI was calculated through titration with puromycin. MDA468 cells were plated on four 100mm dishes at ~60% confluence. The first dish was to be used as a control with only MDA468 cells and no antibiotic selection, the second dish would receive puromycin at a concentration of 0.5μg/mL, the third dish would receive 50uL of the virus library preparation and puromycin and the fourth dish would receive 250uL of the virus library preparation and puromycin. The cells were allowed to settle for at least 16 hours before

infection. The media in each dish was changed 8 hours post-infection to fresh media. 30 hours post-infection, each dish was passed into a fresh 100mm dish with the addition of puromycin to the media at a concentration of 0.5μg/mL. 48 hours post-selection, the surviving cells were counted to determine the MOI of the viral library.

MDA468 cells to be infected were prepared 16 hours in advance in the number of 32 150mm dishes, plated with $8x10^6$ cells each. As the Brunello library contains a total of 76,000 sgRNAs (4 sgRNAs per gene), and we wish to achieve a MOI of 0.3 and a 1000X representation of cells to sgRNAs to ensure a low MOI, requiring a total of about $250x10^6$ cells, with $8x10^6$ cells per 150mm dish, this requires 32 dishes in total. One additional control dish was prepared as an antibiotic control, which would not be infected with virus and then selected with puromycin. 20mL of corresponding media, 10% DMEM with 5% FBS, was added to each dish, cultured at 37˚C in 5% CO_2. The following day, a stock of media with virus (volume of virus library to add to stock was determined by previous MOI titration) was prepared, including polybrene (8μg/ml polybrene). The media was removed from dishes plated the previous day and replaced with 10mL of the stock of media, virus and polybrene. Media was changed 8 hours post-infection to 20mL of fresh, pre-warmed media. 30 hours post-infection, cells were trypsinized and re-plated into new 150mm dishes with 20mL of pre-warmed media with puromycin at 0.5μg/mL, including the control plate to be used as a selection control. 48 hours later, cells were washed with pre-warmed PBS and media was replaced (again with puromycin). Once all the cells in the control dish (with no virus infection, only puromycin selection) were killed, all cells were trypsinized, pooled together in 50mL Falcon tubes and plated in thirty 150mm dishes with $4x10^6$ cells were dish. Remainder of cells were pelleted at 300g for 15 minutes, and frozen

as pellets in 10 Eppendorf tubes with $36x10^6$ cells were tube. Remainder of cells following this step were frozen in DMEM with 10%-DMSO into cryotubes at $8x10^6$ cells per tube. After a total of 7 days post-infection, cells were prepared for FACS sorting. Preparation of cells was done in three batches of 10 plates per batch. Cells were trypsinized, collected in a 50mL Falcon tube and spun down at 800g for 5 minutes. Pellet was re-suspended in 1.5mL of PBS-1% FBS and transferred to a 2mL Eppendorf tube for FACS sorting.

FACS sorting

Three compensation controls were prepared in Eppendorf tubes for FACS sorting with 20uL of the cell re-suspension obtained from library-infected MDA468 cells: unstained control, 7AAD control and PE control, delineating the staining procedure of each sample. The main tube was stained with 75uL of PE antibody against B7-H4 (1/20 dilution, Cell Signaling). The PE compensation control was stained with 1uL of B7-H4 PE. The tube was placed on a shaker for 30 minutes, at 4˚C, protected from light. Main tube was then re-suspended in 12mL of PBS-1%FBS in a 15mL Falcon tube and spun down at 1500rpm for 5 minutes, at 4˚C. Compensation tube for PE was spun down at 300g for 5 minutes at 4˚C. Supernatant was removed from main tube and re-suspended in 2.5mL of PBS-1%FBS. All compensation tubes were re-suspended in 500μL of PBS-1%FBS in 15mL Falcon tubes. Main tube was then stained with 25μL of 7AAD antibody, and the corresponding 7AAD compensation tube was stained with 5uL of 7AAD antibody. 5uL of EDTA was added to main tube to prevent clumping. All tubes were placed on ice and protected from light and brought to the FACS sorting facility within the Goodman Cancer Research Center. Once sorted cells (top 10% B7-H4-expressing cells and bottom 10% B7-H4-expressing cells) were obtained, they were spun down at 1500rpm for 5 minutes

and re-suspended in 1mL of PBS and spun again at 300xg for 5 minutes. Media was carefully aspirated, and pellet was frozen down at -80˚C. The pellets from various batches were handed over to Dr. Sidong Huang's lab for sequencing and MAGeCK analysis.

Sequencing of DNA isolated from FACS-sorted cells of genome-wide CRISPR screen

Sequencing of the DNA isolated from the top and bottom 10% B7-H4 expressing cells from the CRISPR screen was pelleted and frozen at -80˚C. Tubes were handed over to Dr. Sidong Huang's laboratory, and processed at the TCAG SickKids Facility for DNA Sequencing/Synthesis on an Illumina HiSeq 2500.

MAGeCK analysis

The MAGeCK algorithm was run on the sequencing results obtained by Dr. Geneviève Morin from Dr. Sidong Huang's laboratory. Briefly, read counts obtained from different samples are first median-normalized to adjust for the effect of library sizes and read count distributions. A negative binomial model is then used to test whether sgRNA abundance differs significantly between treatment conditions and controls. sgRNAs are ranked based on P-values calculated from this binomial model, and a robust ranking aggregation algorithm or α-RRA is used to identify positively or negatively selected genes in the population. Put more simply, the α-RRA algorithm assumes that if a gene has no effect on selection (does not increase or decrease the expression of the read-out gene), sgRNAs targeting this gene should be uniformly distributed across the ranked list of all the sgRNAs. Therefore, α-RRA ranks genes by comparing the skew in the rankings to the uniform null model. It then prioritizes genes whose sgRNA rankings are consistently higher than what is expected. In its output, the MAGeCK algorithm (145) delivers a well-organized spreadsheet representing all the targeted genes in a particular library. Each

gene is assigned a rank based on the algorithm, and information such as the individual hit's P-value, FDR value and log fold-change are also provided. For my screen, I utilized the rank assigned by MAGeCK to the identified regulators, their log fold-change and FDR.

Quantitative RT-PCR

RNA was isolated using the RNAeasy Mini Kit (Qiagen) according to the manufacturer's instructions. One step RT-PCR was performed with the isolated RNA using the QuantiTect® SYBR® Green RT-PCR kit. qPCR reactions were performed on a LightCycler 480 (Roche). Primer sequences from IDT (Integrated DNA Technologies) were used as follows. Data were normalized to the TBP gene.

Name	**Primer**	**Sequence**
B7-H4	Forward	GGCAGATCCTCTTCTGGAGCATAA
	Reverse	CCATCCTCCCCAATGTTCCC
MGAT1	Forward	AGCCATGGACTTTGGACCTG
	Reverse	CCATGCACCTGGACAGAGTAA
DDOST	Forward	GATGGGGTACTTCCGGTGTG
	Reverse	CGCATGTGGATACTGGGTGAT
DAD1	Forward	CCTAGCGGTTTGCCTGAGAA
	Reverse	AATCAGCAAAGGCTCGCTCT
B3GNT2	Forward	ATGGGACAGCCAGAGAGATATGA
	Reverse	CCGATGAGGTCCAGCATTGT
STT3B	Forward	CGGAGTCAGAGGTTGCTTGAG
	Reverse	CCTGGGTAAACAGTACCACCTAC
RPN1	Forward	CGACAGAGTGAGCGAAATGC
	Reverse	AAACGGCAAACTCACACTGC

RPN2	Forward	AGCAGGCAGTCAAGAGAACA
	Reverse	TCTGCTGTGTGTTGGGGAAA
TBP	Forward	TCAGGAAGACGACGTAATGG
	Reverse	TTACAGAAGGGCATCACCTG

Knockdown by shRNA

Knockdown of RPN1, RPN2, DDOST, STT3B, B3GNT2, MGAT1, DAD1 and B7-H4 in MDA468 cells were carried out using shRNAs cloned into pLKO.1 lentiviral vectors (Sigma-Aldrich). I obtained the shRNAs (Sigma Aldrich) from the RNAi Consortium (TRC) collection from the Broad Institute, available and distributed by Dr. Sidong Huang's laboratory. The following clones were used.

Symbol	Gene ID	TRC Clone ID
RPN1	6184	TRCN0000072588
		TRCN0000072589
		TRCN0000072591
RPN2	6185	TRCN0000159835
		TRCN0000159361
		TRCN0000166805
MGAT1	4245	TRCN0000035195
		TRCN0000035196
		TRCN0000035198
DDOST	1650	TRCN0000035384
		TRCN0000035387
		TRCN0000035388

B3GNT2	10678	TRCN0000035874
		TRCN0000035877
		TRCN0000035876
DAD1	1603	TRCN0000083038
		TRCN0000083039
		TRCN0000083042
STT3B	201595	TRCN0000141176
		TRCN0000142062
		TRCN0000145241

HEK293T cells were transfected using Lipofectamine2000 (brand) to produce lentivirus. Packaging vectors used were pMD2.G and psPAX2. Medical containing viral particles was collected and passed through a 0.45μM filter. MDA468 cells were treated with virus in media containing polybrene (8μg/ml polybrene). Infected MDA468 cells with stable knockdown were selected under puromycin (0.5μg/mL).

Analysis of genome-wide CRISPR hits by Gene Set Enrichment Analysis (GSEA)

Pathways analysis on genes identified as positive or negative regulators of B7-H4 was run through Gene Set Enrichment Analysis (GSEA) through their 'Molecular Signatures Database – Investigate Gene Sets' function. Briefly, a list of genes previously delineated by significance (below 10% or 25% FDR) and plugged in to the Gene Identifiers box. Selected MSigDb were: C5 – GO gene sets, C6 – Oncogenic signatures, C7 – Immunologic signatures and H – Hallmark gene sets. FDR q-value was extracted for identified pathways and plotted as -logFDR in GraphPad.

Results

Little is known about the regulation of the immune checkpoint B7-H4, identified as a strongly expressed marker within our cohort of 38 TNBC patients with poor immune infiltration within the tumour core. I decided to perform a genome-wide CRISPR screen to identify tumor intrinsic regulators of B7-H4 cell surface expression in a basal breast cancer cell line and shed light the mechanisms involved in the expression on this immune receptor in the context of a breast cancer cell line.

1. Selection of candidate cell line for genome-wide CRISPR screen

To conduct a CRISPR-based genome wide knock-out screen, I first identified a candidate cell line. An ideal cell line would have the following characteristics: ease of handling, rapid doubling time, intermediate surface expression level of the gene to be used as a read-out, in this case, B7-H4, in order to allow for an appropriate range that could display an increase or decrease in expression level and susceptibility to knock-out with the use of B7-H4-targeted sgRNA guides. To select a candidate cell line, I followed the steps outlined below.

1.1. Identifying an array of cell lines to assay initially for B7-H4 expression

The candidate cell line was selected from an array of basal breast cancer cell lines, as basal breast cancer tumors reflect the majority of TNBC tumors. The basal A subtype consists of 50% of TNBC whereas the basal B subtype is less prevalent and includes claudin-low characteristics, a feature that is less prevalent among TNBC patients (62, 146). RNA expression Z-scores obtained from the Cancer Cell Line Encyclopedia (CCLE) for basal breast cancer cell lines demonstrated that basal A cell lines had a significantly higher expression score for *VTCN1* (B7-H4) when compared to basal B cell lines (Figure

4). I decided to proceed with further validation of all Basal A cell lines for which I obtained a score, that showed an intermediate to high score of B7-H4 expression, and a few Basal B cell lines as controls for low B7-H4 expression, precisely MDA231 and HCC38. Notably, HCC38 showed an intermediate RNA expression score for *VTCN1*. Cell lines HCC1187, HCC2157 and HCC1599 proved difficult to maintain in culture, with low adherence to plastic dishes and poor survival upon passage. They were not further examined as candidates.

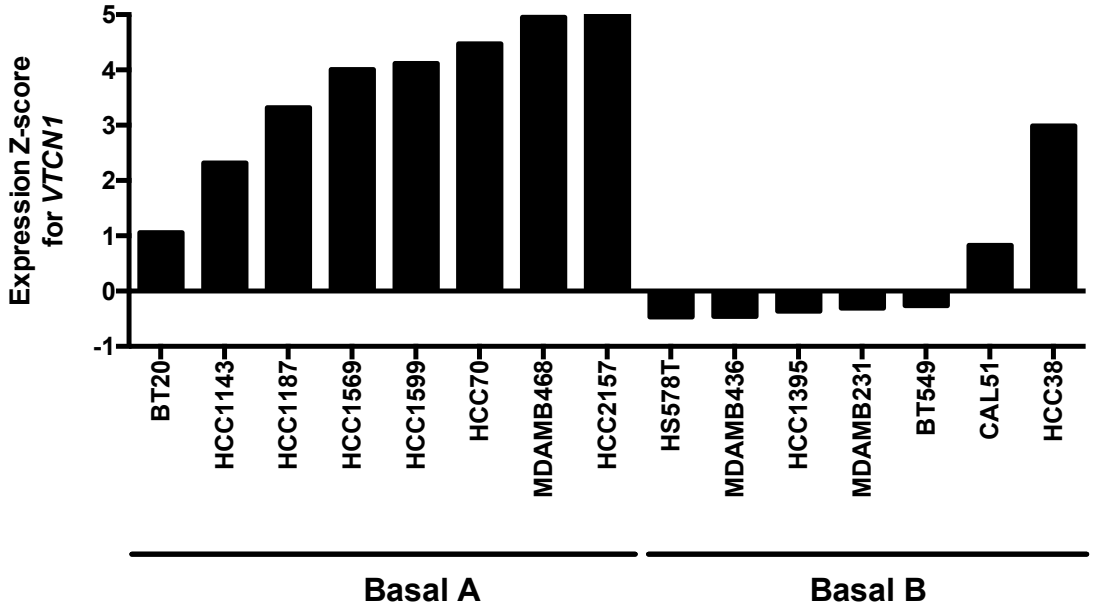

Figure 4: Gene expression Z-scores for *VTCN1* (B7-H4) in basal breast cancer cell lines. Gene expression scores were generated from the Cancer Cell Line Encyclopedia (CCLE) for basal A and B cell lines and plotted on GraphPad for visualization.

1.2. Evaluating B7-H4 cell surface expression by flow cytometry in select cell lines

To validate the expression scores extracted from CCLE, chosen cell lines were selected to undergo flow cytometry to assess cell surface protein levels of B7-H4 (Figure 5). Results indicated that the highest B7-H4 surface-expressing cell lines were HCC70,

MDA468 and HCC1569. Intermediate protein expression of B7-H4 was preferable for the candidate cell line, with a uniform expression pattern across the entire cell population. For this reason, HCC70 did not prove as a suitable candidate, as it presented with a strikingly divided population of B7-H4 expressing cells by flow cytometry, with two peaks showing low and intermediate levels of expression of B7-H4. Moreover, of the Basal B cell lines, none showed significant expression of B7-H4 at the cell surface, including HCC38, which had shown an intermediate gene expression from CCLE data. MDA468 and HCC1569 remained as potential candidates for the CRISPR screen.

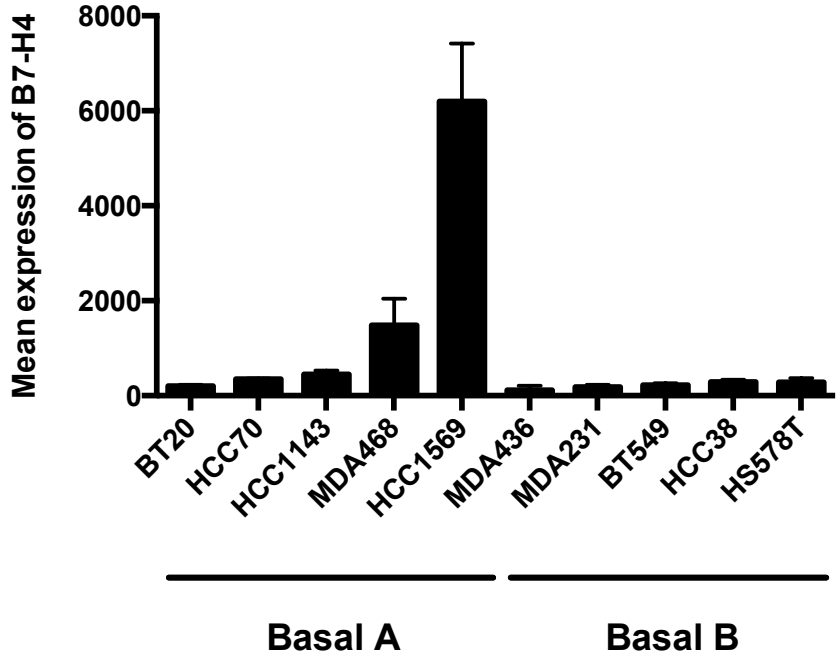

Figure 5: Cell surface expression levels of B7-H4 in basal breast cancer cell lines by flow cytometry. Cell lines selected for further validation from Figure 4 were grown in culture according to ATCC regulations and stained for flow cytometry to measure cell surface expression levels of B7-H4 (n=3).

1.3. CRISPR-generated knock-out of B7-H4 in select cell lines

To confirm whether the expression of B7-H4 could be knocked-out with the use of CRISPR/Cas9 tools, three individual sgRNAs were designed to target B7-H4. Cell lines MDA468 and HCC1569 were each infected with the virus and tested by flow cytometry and immunoblotting (Figures 6 and 7). HCC1569 did not show a significant knock-out with any of the three guides, whereas two of three guides showed efficient knock-out at both the total protein and cell surface protein levels in MDA468. The third guide showed comparable knock-down at the cell surface, but incomplete knock-down at the total protein level, indicating that the though the protein has been removed from the cell's surface, it has not yet fully been eliminated within the cytoplasm. This can be explained by the fact that both guides 1 and 2 targeted regions present in the shortest and longest isoforms of the B7-H4 gene, whereas the third guide only targeted the first and longest isoform, therefore there could be leftover protein produced from the third isoform of the gene that is not being targeted by the guide.

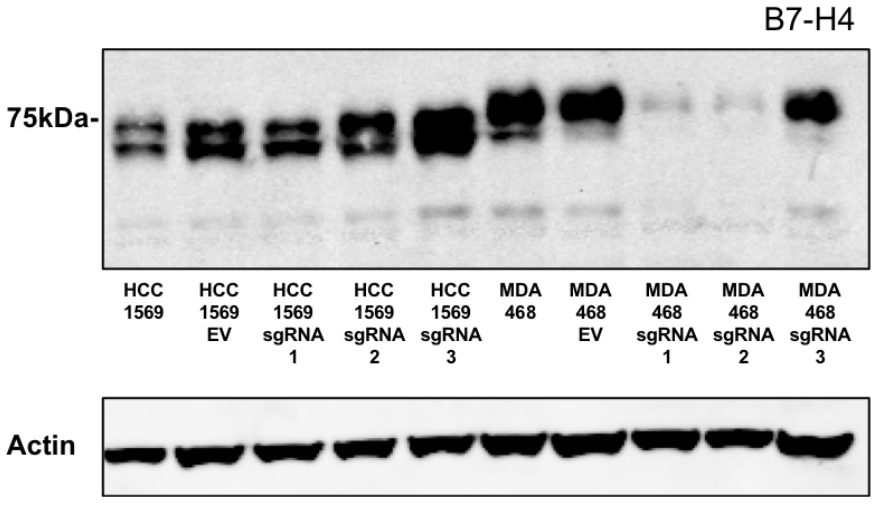

Figure 6: Cell lines HCC1569 and MDA468 were infected with viral vectors to knock-out B7-H4 expression by CRISPR. Immunoblotting for B7-H4. Cell lines that showed highest B7-H4 expression and ease of handling were infected with three

CRISPR vectors targeting B7-H4 and an empty vector as a control. Cells were lysed and run on an SDS-PAGE gels.

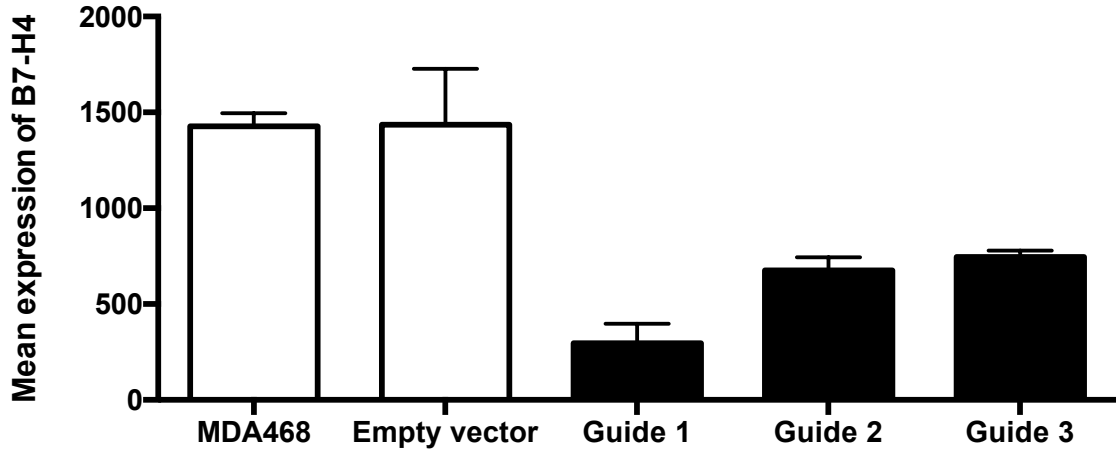

Figure 7: Cell surface levels of B7-H4 shown in MDA468 cells infected with viral vectors to knock-out B7-H4 expression by CRISPR. Cell lines that showed highest B7-H4 expression and ease of handling were infected with three CRISPR vectors targeting B7-H4 and an empty vector as a control. Cells were stained for flow cytometry to assess cell surface expression levels of B7-H4 (n=3).

Given the requirements outlined previously, MDA468 was chosen as the candidate cell line: it showed an intermediate cell surface expression of B7-H4, with a relatively uniform expression across the cell population, showed great ease of handling with a doubling time of 41 hours and its B7-H4 expression could be efficiently knocked-out with CRISPR technology.

2. Genome-wide CRISPR screen for regulators of B7-H4 cell surface expression

A flow chart depicting the broad steps of the genome-wide CRISPR screen are outlined in Figure 8, which will be explained in detail below.

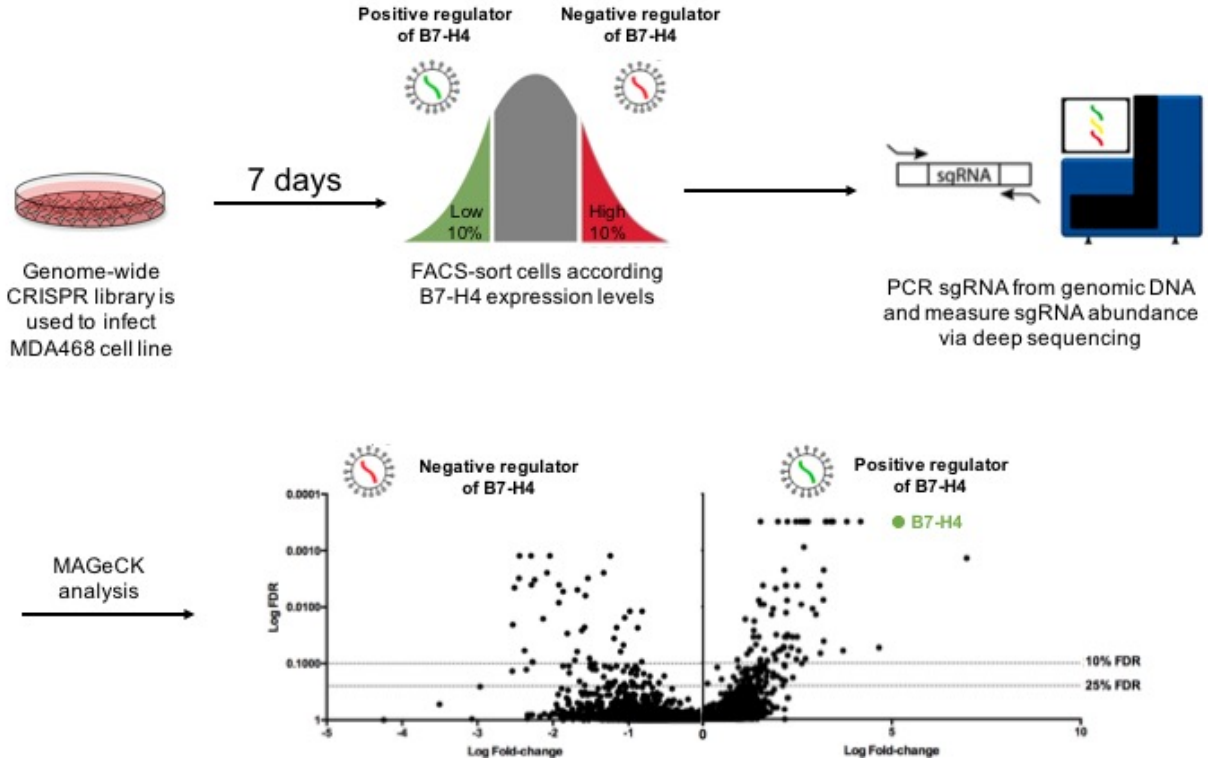

Figure 8: Flow chart illustrating procedure for performing genome-wide CRISPR screen for regulators of B7-H4 cell surface regulators. The B7-H4-expressing, MDA468 cell line was infected with a genome-wide CRISPR library at 0.3 MOI. 7 days after infection, the cells were stained, collected and FACS-sorted into B7-H4^{hi} and B7-H4^{lo} populations. Cellular DNA was extracted, and the library was amplified, followed by deep sequencing. Reads of each gene are then subject to fold-change and MAGeCK analysis.

2.1. Outline of experimental procedure

The genome-wide CRISPR library used was the Brunello library (with four sgRNAs per gene and approximately 76,000 sgRNAs in total), commercially obtained through Addgene (147). I received the viral library directly through Dr. Sidong Huang's

facility/laboratory as a 1-vector system, already in corresponding media and ready to add to cells for lentiviral infection. The MOI of the library was determined by titration and the MDA468 cell line was infected at an MOI of 0.3 and a coverage of 1000X as described in Materials and Methods. Seven days post-infection with the library, cells were stained for B7-H4 cell surface levels (BioLegend PE anti-human B7-H4 antibody) and a viability marker (BD Horizon™ Viability stain 510 or FVS 510) and sorted into the top and bottom 10%-B7-H4-expressing cells using FACS (Figure 9 illustrating gating strategy for one sample).

The isolated cell populations (in two batches; for the first batch of 57M cells, 4.2M were isolated as B7-H4^{hi} and 4.2M B7-H4^{lo}, for the second batch of 71.25M cells,

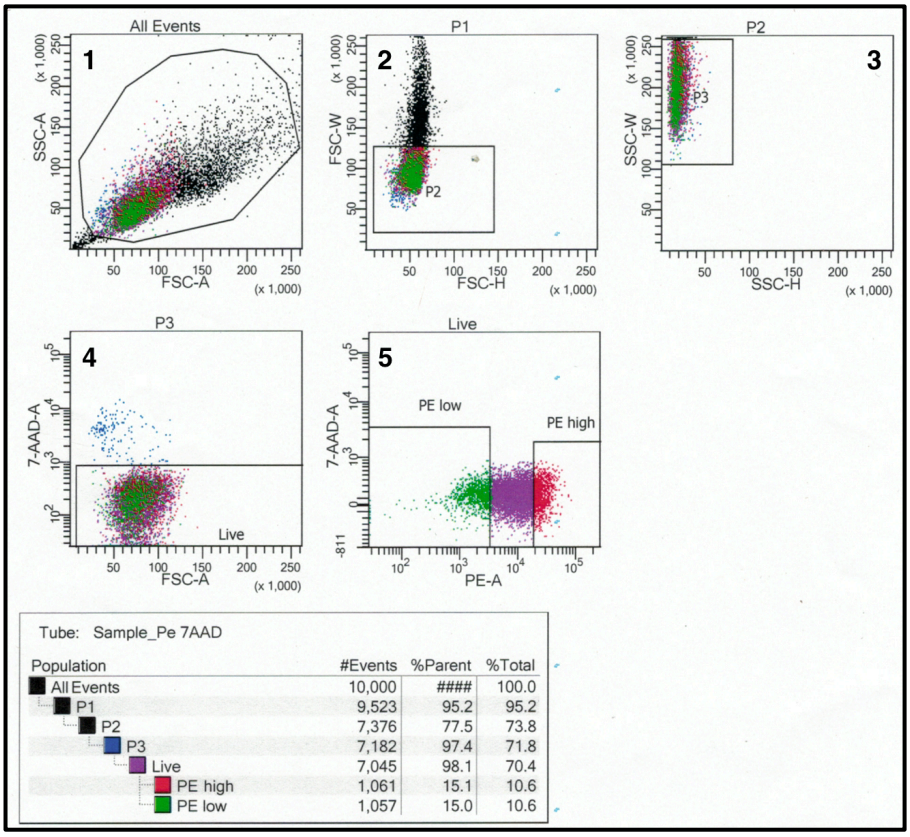

Figure 9: FACS gating strategy during acquisition of MDA468 cells infected with genome-wide CRISPR library. The total cell population was first isolated in 1). In 2), doublets of cells were excluded and re-visualized by side-scatter in 3). In 4), dead cells are excluded by selecting cells negative for 7-AAD, a fluorophore with a strong affinity for DNA. In 5), cells are displayed according to the PE expression, the fluorophore conjugated to the monoclonal B7-H4 antibody used to stain MDA468 cells. Cells are hereby selected for the top and bottom 10% B7-H4-expressing populations, as seen by the statistics view below.

3.69M were isolated as B7-H4^{hi} and 3.82M were isolated as B7-H4^{lo}; requirements of the Brunello library sgRNA content requires at least 4M cells per condition for optimal analysis, these conditions were met) were handed back to Dr. Huang's laboratory where their DNA was harvested and sent for sequencing at the TCAG SickKids Facility.

2.2. MAGeCK analysis performed on sequencing results of sgRNA's isolated from extracted DNA

MAGeCK analysis (145) was run on the sequencing data by Dr. Geneviève Morin in Dr. Huang's laboratory, and presented in a gene-centric format (the data from all four sgRNAs for each gene were pooled together to give a 'score' to each gene). MAGeCK-assigned rankings based on the developed algorithm determined the rank of each gene as a positive or negative regulator of B7-H4. The fold-change identified for each gene represented the fold-change in sgRNA's for a specific gene from the top 10% B7-H4-expressing cells to the bottom 10% B7-H4-expressing cells. For example, sgRNAs targeting B7-H4 were found in a ~5-fold higher number in the bottom 10% B7-H4-expressing cells when compared to the top 10% B7-H4-expressing cells, as these guides are destined to knock-out B7-H4 expression, and therefore accumulate in the population of cells with the lowest B7-H4 expression. Importantly, B7-H4 was identified as the top positive regulator of the screen, signifying that knock-out of B7-H4 itself resulted in the most significant decrease in B7-H4 surface protein levels, providing validation for the screen (Figure 10). As such, positive regulators were defined as genes that increase or support B7-H4 surface expression, and upon their knock-out with CRISPR sgRNAs, surface levels of B7-H4 decrease. On the other hand, negative regulators were defined

as genes that suppress B7-H4 surface expression, and upon their knock-out with CRISPR sgRNAs, surface levels of B7-H4 increase.

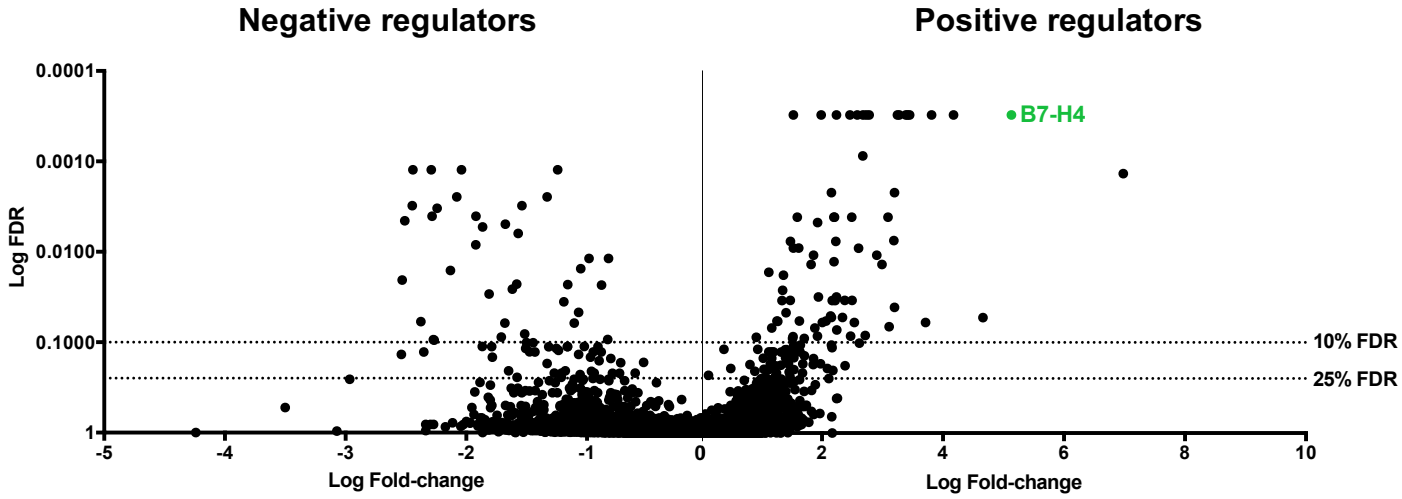

Figure 10: Volcano plot displaying genes targeted in the CRISPR screen, ranked by their log fold-change, from the top 10% to the bottom 10% B7-H4-expressing cells, and log false-discovery rate (FDR). Hits obtained from the CRISPR screen following MAGeCK analysis were mapped on Graph Pad to illustrate the density distribution of results and representation of B7-H4 as the strongest positive regulator relative to other screen hits.

2.3. Selection of significant screen hits by false-discovery rate stringency

As a first step towards identifying regulators of interest, putative positive and negative regulators of B7-H4 were ranked according to their false-discovery rate or FDR values (determined by MAGeCK analysis (145)). Hits were first delineated with an FDR value below 25%, followed by a more stringent selection of hits with an FDR value below 10% (Figure 10). A compounded list of the individual function of both positive and negative regulators with an FDR value below 25% was generated. Each of these significant hits were researched within TNBC literature to identify those with prior relevance within the

cancer and immunotherapy field and could be good initial candidates for further validation tests.

2.4. Pathway analysis of positive and negative regulators

Positive and negative regulators (both under 25% and 10% FDR) were analyzed as a group by pathway analysis software, to group different hits together according to their potential function. I used Gene Set Enrichment Analysis (GSEA) (148). I initially observed that when analyzing positive and negative regulators separately, and using either a 10% or 25% FDR stringency, the 25% FDR stringency did not produce significant results outside of those present within the 10% stringency, therefore I decided to pursue my analyses only with those regulators that had an FDR value of below 10%, as used in other CRISPR screen publications (149). Furthermore, analyzing positive and negative regulators as a combined group failed to reveal a novel pathway that was absent when analyzing both groups separately. The higher number of significant positive regulators compared to negative regulators diluted the significance of the pathways present within negative regulators. Therefore, I proceeded by analyzing each regulator group separately.

2.4.1. Positive regulators

GSEA Pathway analysis of the hits classified as positive regulators of B7-H4 revealed several housekeeping functions, such as protein catabolism and metabolism, transcription, protein modification and cellular organization (Figure 11). Individual analysis of each positive regulator revealed a few potential targets of interest for further validation, including: EP300, SFPQ, SOX9, CUL3, FBXW7, and AMD1, which are detailed in their role in Table 1. However, negative regulators showed the presence of an

important pathway, glycosylation, which, as described in my introduction, was recently shown as crucial for the cell surface integrity of several immune checkpoints (126). Therefore, I chose to focus on those genes with a role in glycosylation as identified in the screen to establish if they regulated B7H4 surface levels.

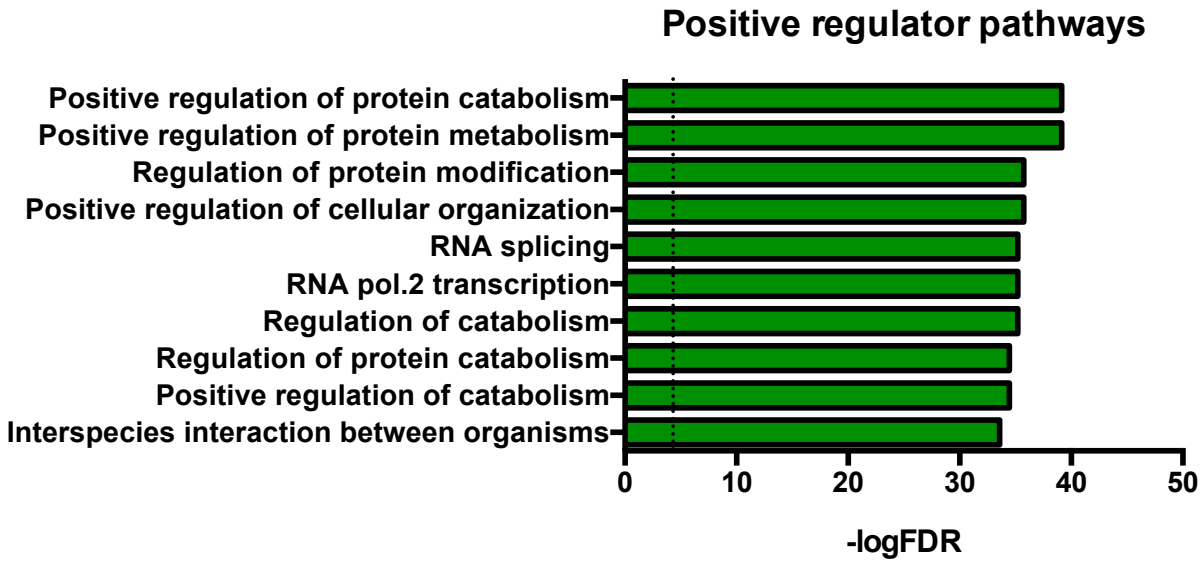

Figure 11: Significance of identified pathways by GSEA within positive regulators of B7-H4. Pathways identified through GSEA were ranked according to their significance with values generated by the software. Higher -logFDR represents higher significance. Line on the X-axis represents a delimitation of 5% FDR significance (within this analysis), all values beyond the line have an FDR Q-value of under 0.05.

2.4.2. Negative regulators

GSEA pathway analysis identified 'glycosylation' as a top pathway among the negative regulators, indicating that several pathway members are likely involved (all regulators with a role in glycosylation identified within the screen are summarized in Table 2). Moreover, glycoprotein metabolism, N-linked glycosylation and glycosyltransferase activity were also identified as prevalent pathways (Figure 12). This proved of interest given the recent highlights on the importance of PD-L1 glycosylation for its interaction with receptor PD-1, (126) and the clinical implications of targeting glycosylated immune checkpoints for

treatment regimens to lower toxicity. I chose to validate several key glycosylation hits as negative regulators in my screen for this reason.

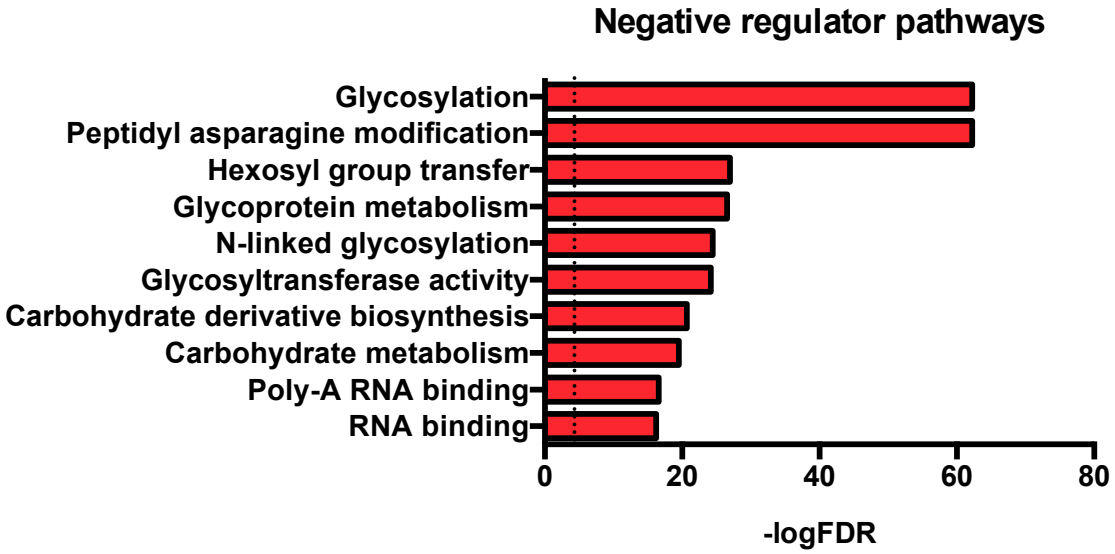

Figure 12: Significance of identified pathways by GSEA within negative regulators of B7-H4. Pathways identified through GSEA were ranked according to their significance with values generated by the software. Higher -logFDR represents higher significance. Line on the x-axis represents a delimitation of 5% FDR significance (within this analysis), all values beyond the line have an FDR Q-value of under 0.05.

3. shRNA-based validation of results from CRISPR screen

I chose initially to test all components of the OST complex, which were present as negative regulators within my screen, including RPN1, RPN2, DDOST, DAD1 and STT3B (see introduction for details on their respective roles, additionally in Table 2). Additional genes chosen for validation included B3GNT2 and MGAT1. The OST complex components were chosen due their presence within the hits (25% of all negative regulators with an FDR value under 0.1), in order to elucidate the different consequences that knock-down of each component could have on B7H4 glycosylation state. B3GNT2, a glycosyltransferase responsible for glycosylation branching in the Golgi (150), was chosen due to the recently documented importance of B3GNT3, a similar

glycosyltransferase, to the immunosuppressive role of PD-L1 (126). MGAT1, a target of interest in the cancer research field (151-152) is also a key enzyme in the first step of glycan branching editing, and therefore represented an intermediate step within the glycosylation process, between the OST complex-mediated transfer of the core oligosaccharide, and the higher-level branching later performed by B3GNT2.

To validate the impact of these genes, I obtained shRNAs (Sigma-Aldrich) specific for RPN1, RPN2, DDOST, DAD1, STT3B, B3GNT2 and MGAT1 from the RNAi Consortium (TRC) collection from the Broad Institute, available and distributed by Dr. Sidong Huang's laboratory. Three shRNAs were ordered for each gene to validate them individually in my candidate cell line, MDA468. Once obtained as a bacterial glycerol stock, plasmid DNA was extracted from bacterial cultures and packaged into lentiviral vectors, which were subsequently used to infect MDA468 cells. Cells were infected in sequential triplicates (n=3 for all the experiments shown below, unless otherwise specified) and assessed by immunoblotting and flow cytometry to quantify variations in B7-H4 cell surface protein levels; RNA isolated from cells was also subjected to RT-PCR to confirm knockdown of the targeted glycosylation pathway gene by the shRNAs. DDOST and STT3B shRNA-targeted cell lines showed poor viability post-infection, and significant cell loss did not yield enough to perform the described procedures. Instead I focused on those genes which did not diminish cell viability, since B7-H4 knock-down alone did not significantly decrease cell viability when tested in parallel and in the past by CRISPR. The results are outlined for each validation experiment for the remainder of the chosen regulators (being RPN1, RPN2, DAD1, B3GNT2 and MGAT1).

3.1. Flow cytometry (Figure 13)

Flow cytometry procedures revealed variations in B7-H4 surface levels and only RPN1, a catalytic subunit of the OST complex and B3GNT2, a glycosyltransferase involved in branching, showed a robust and reproducible increase in B7-H4 surface levels upon their respective knock-down with shRNA.

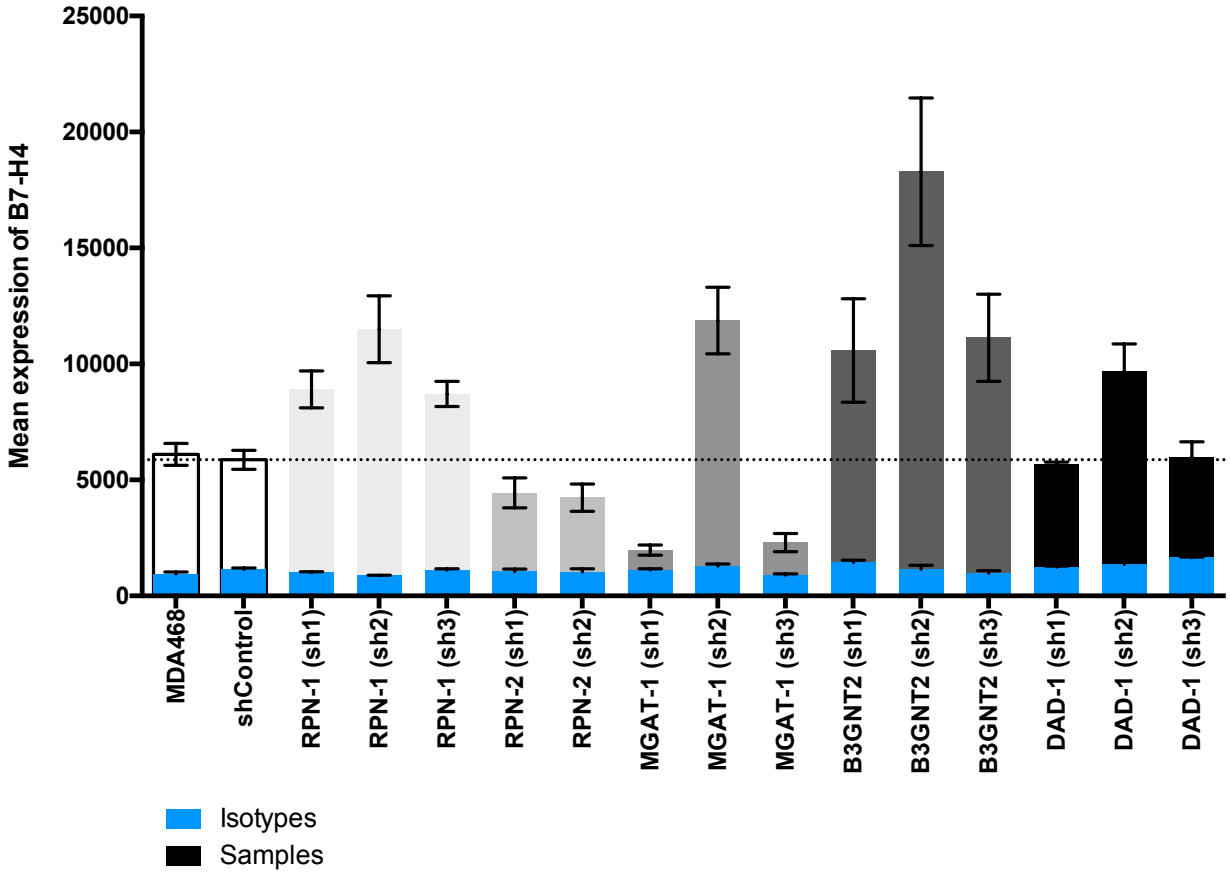

Figure 13: Flow cytometry results for B7-H4 cell surface expression in cells with shRNA knockdown of various glycosylation-related genes obtained from the CRISPR screen (n=3). Knock-down by shRNA was conducted for listed genes with available shRNAs. Cells were isolated and stained or flow cytometry to assess cell surface expression levels of B7-H4 (n=3). Isotype controls are included in blue. Please note, the sh3 sample for RPN2 showed poor viability, and therefore the limited number of cells available were only sufficient for immunoblotting and RT-PCR, as these procedures require lesser cell numbers than flow cytometry.

3.2. Immunoblotting (Figure 14)

Examining total B7-H4 protein levels in MDA468 cells following shRNA knock-down for select glycosylation targets only partly correlated with surface B7-H4 as observed by flow cytometry, where only sh2 against B3GNT2 showed a significant increase in total protein levels of B7-H4. Moreover, the data observed by immunoblotting for B7-H4 following gene knockdown with shRNAs against RPN2 indicated a more significant decrease in B7-H4 levels than shown by flow cytometry. Interestingly, the flow cytometry samples that showed the highest increase in B7-H4 cell surface levels, including sh2 for RPN1, sh2 for B3GNT2 and sh2 for MGAT1, with the exclusion of sh2 for DAD1, showed a corresponding shift in the migration and density distribution of B7-H4, consistent with modification of B7-H4 glycosylation. Please note that all samples for all three replicates were examined by SDS-PAGE, and a representative example is shown in Figure 14.

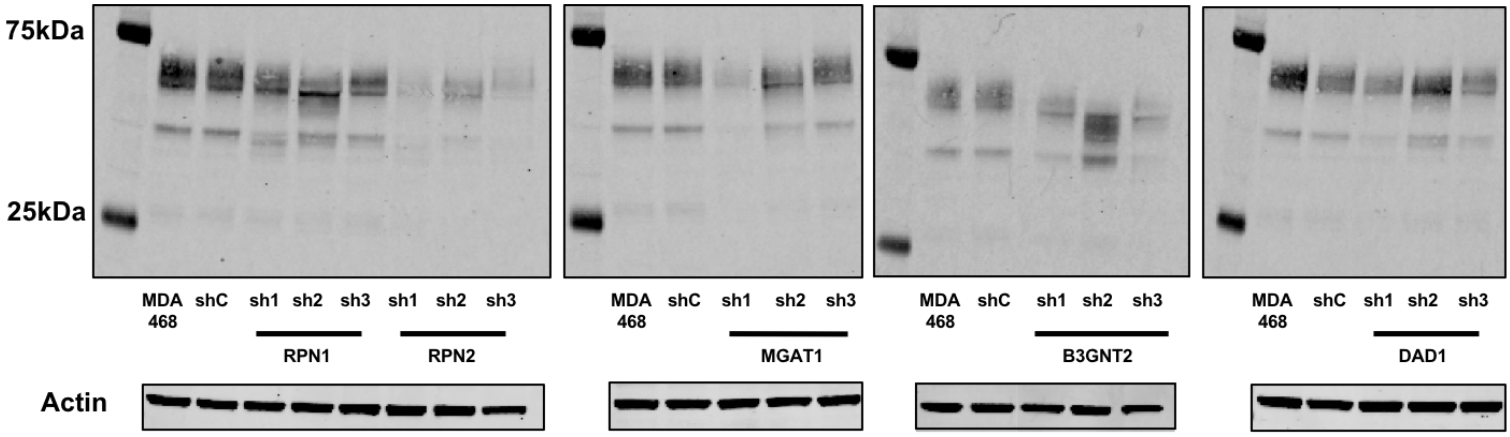

Figure 14: Immunoblotting for B7-H4 expression in cells with shRNA knockdown of various glycosylation-related genes obtained from the CRISPR screen. Knock-down by shRNA was conducted for listed genes with available shRNAs. Cells were lysed and run on an SDS-PAGE gel, subsequently blotted for B7-H4 protein. Representative sample is shown from an n=3.

3.3. RT-PCR (Figure 15)

To confirm whether the shRNAs used were indeed knocking down the expression of the targeted gene, I amplified the cDNA of the target gene by RT-PCR. Apart from B3GNT2, shRNA against RPN1, RPN2, DAD1 and MGAT1 showed robust and consistent knock-down levels of ~50% and below (MGAT1 showed a lesser knockdown compared to RPN1, RPN2 and DAD1) of target mRNAs. B3GNT2 shRNA showed poor knock-down efficiency, with sh3 showing poor reproducibility and only sh2 showing a near 50% decrease in expression. Interestingly, this shRNA also caused the greatest increase in B7-H4 surface expression when observed by flow cytometry, indicating that a small decrease in the expression of B2GNT2 could greatly affect B7-H4 expression. It is important to note that cells infected with the shRNA targeting B3GNT2 also proved difficult to culture, though enough cells could be gathered for each experiment, it is important to keep in mind the bias their health state can incur on the obtained results.

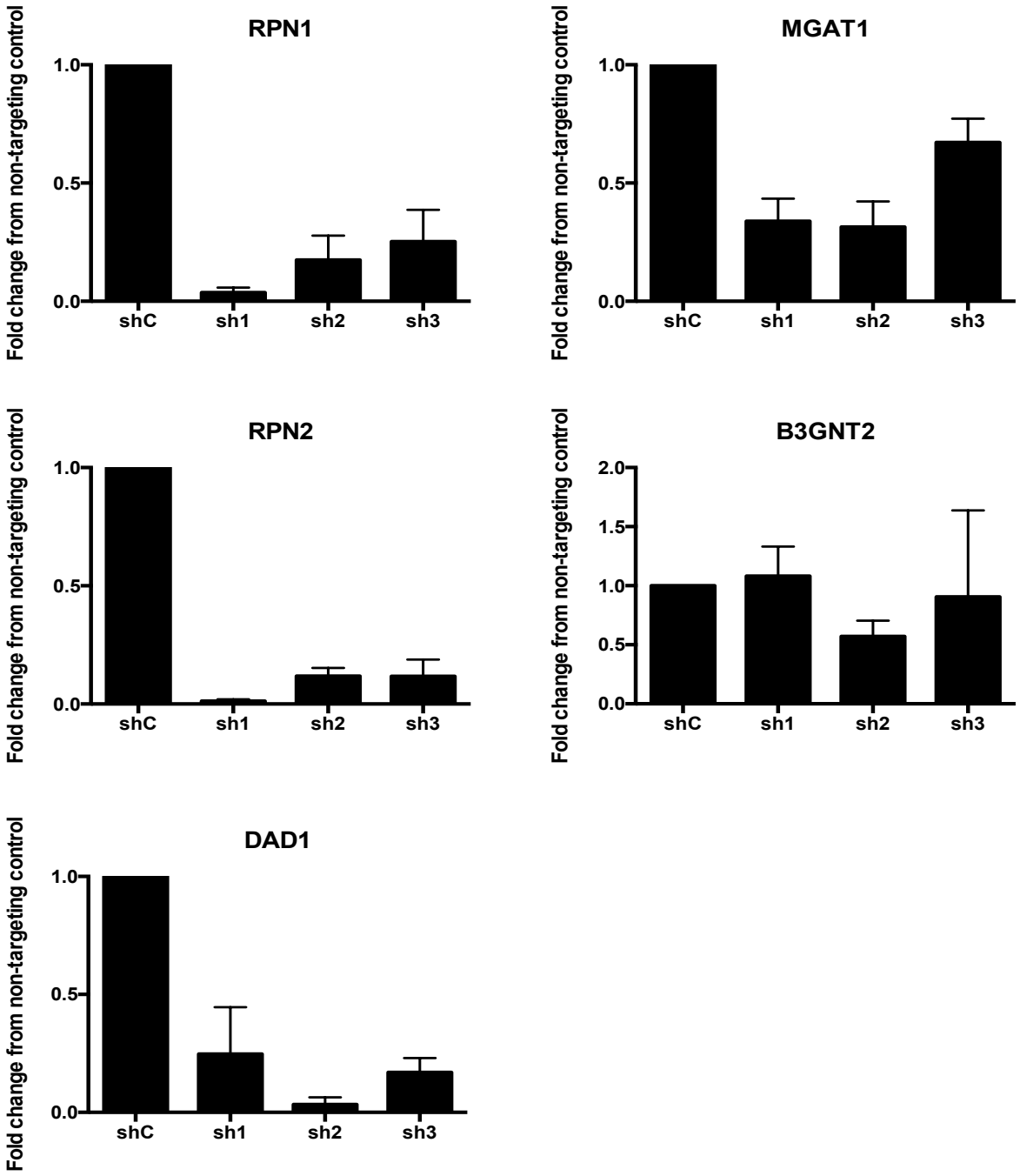

Figure 15: RT-PCR data to assess knock-down efficiency of glycosylation-related genes targeted by shRNA. Knock-down by shRNA was conducted for listed genes with available shRNAs. RNA from cells was isolated and cDNA was amplified for the targeted gene (indicated in titles of each graph) by RT-PCR to confirm knock-down of selected genes (n=3).

4. Summary

Results from the genome-wide CRISPR screen for B7-H4 regulators in the basal breast cancer cell line MDA468 indicated that the glycosylation pathway was a key negative regulator of B7-H4 cell surface expression. However, validation by shRNA of the effect of these glycosylation-related genes, being RPN1, RPN2, DAD1, B3GNT2 and MGAT1, did not fully replicate the phenotype observed using CRISPR technology for genome-editing. Only the genes RPN1 and B3GNT2 consistently showed an increase in B7-H4 cell surface expression upon their knock-down by shRNA, both by total protein levels and surface expression. Knock-down of targeted genes by shRNA was confirmed by amplifying the cDNA of the target gene by RT-PCR.

Discussion

The goal of my B7-H4 CRISPR genome-wide screen was to gain insight into the regulatory mechanisms of B7-H4 in a tumor intrinsic context. As the immune checkpoint is poorly characterized and difficult to study due to its lack of a known receptor, I hoped to uncover pathways contributing to its increased expression in TNBC, as observed in the Park lab's cohort of TNBC samples and demonstrated in our recent publication (74). Curating the data of my screen through pathway analysis software (GSEA) allowed me to identify glycosylation as an important regulator of B7-H4 expression within the context of a TNBC cell line, and the conditions of my screen, though in an opposite fashion to what was expected. The consensus in the literature is that glycosylation helps regulate protein stability, and loss of it would result in removal of the protein from the cell surface (153). In the case of my screen, knock-out of various proteins involved in the protein glycosylation pathway unequivocally showed an increase in B7-H4 levels at the cell surface. With the current developing interest in the cancer field into the tumor 'glyco-code' (127) and the recent finding by Li et al. (126) that PD-L1 glycosylation is crucial to its interaction with PD-1 and could potentially be targeted as a therapeutic strategy. It is possible that glycosylation could have a similar role for other immune checkpoints including B7-H4.

1. Lack of concurrence between results from the CRISPR screen to corresponding validation by shRNA

OST complex components were abundantly present within the CRISPR screen hits, and were chosen as validation candidates, along with B3GNT2 and MGAT1, for reasons

described above. Only RPN1 and B3GNT2 replicated the robust increase in B7-H4 surface levels by FACS that were observed in the CRISPR screen and variable data was obtained by shRNA validation of other CRISPR hits. Several explanations could be given for this fact, for one, I am using two different gene editing methods, and as previously described in the introduction, RNA-based genome editing techniques can often render an incomplete or fleeting silencing effect (137-138). To confirm results from the CRISPR screen I would need to design CRISPR guides targeting the select genes, as previously performed for B7-H4 (Figure 7) and clone them into viral vectors and infect the MDA468 cell line.

An interesting observation from my validation experiments arose from the differences between cell surface expression of B7-H4 as established by flow cytometry and the corresponding immunoblots for total protein levels. Data by flow cytometry appeared skewed to a higher level of surface B7-H4 expression, especially in the case of B3GNT2 samples (Figure 13), than was observed by immunoblot for the same sample (Figure 14). This may be as a result where aberrantly glycosylated B7-H4 may be more stable at the cell surface. In support of this possibility, the highest protein levels of B7-H4 (as detected by FACS) as in the case of sh2 for B3GNT2, corresponded with a shift in the migration and density pattern of the protein by SDS PAGE (Figure 14), indicating a modification in its glycosylation branching. This observation led me to question whether the fluorophore-conjugated antibody utilized for the FACS showed enhanced avidity towards B7-H4 surface proteins with impaired glycosylation.

2. Glycosylation interaction with FACS antibody

The fluorophore-conjugated antibody commercially obtained for FACS did not provide information with respect to the epitope it recognizes, and it was not disclosed where it bound to its target molecule, B7-H4 (BioLegend). Upon contacting the manufacturer, I was informed that epitope mapping was not performed for this antibody (Catalogue #358103). Hence, I could not confirm whether its binding site was located near on one of the 7 N-linked glycosylation sites of B7-H4. This became important consideration for my screen analysis, as the kinetics of antibody binding may play an important role in interpreting my results. To circumvent this issue in my validation strategy, I would assess cell surface levels of B7-H4 after genome manipulation using a biotinylation assay to measure cell surface levels of a select protein (ThermoScientific) (154), thus bypassing antibody bias and providing more robust data. Biotinylation assays harness the high affinity of biotin for avidin. Biotin is used to label all surface proteins on a cell, or a population of cells, which are then isolated by binding biotin to avidin through the use of a column. The isolated cell surface proteins bound to biotin are then lysed and run on an SDS-PAGE gel and stained for the protein of interest. This technique has been used in several other publications for various proteins (154-155). As the B7-H4 immunoblotting antibody I have used for all my previous experiments does not bind to a glycosylation site, i.e it will still recognize B7-H4 protein treated *in vitro* with shRNA against B3GNT2, RPN1 or other glycosylation genes identified in my screen , this would provide a more robust method to assess cell surfaces of B7-H4 and bypass any potential antibody bias that could skew results toward showing higher B7-H4 protein levels than there really are. Moreover, this observation led me to consider the fact that if the process of ‘de-bulking’

an immune checkpoint by inhibiting specific glycosyltransferases that are involved in its branching (such as B3GNT2, potentially for B7-H4, or B3GNT3 as was documented for PD-L1) can make it more readily available to antibody binding, this could prove an important consideration for future therapeutic treatments for antibody-drug conjugates (ADC).

3. Considerations for further experiments

Although I pursued validation of B3GNT2, knock-down of RPN2 also showed correspondence between cell surface levels as detected by flow cytometry and total protein levels by immunoblot. Although RPN2 was identified in the screen as a negative regulator of B7-H4, my downstream validation would indicate the opposite, where knockdown of RPN2 shows a robust and corresponding decrease in B7-H4 levels both at the cell surface and total protein levels. Although I chose glycosylation as the most prevalent pathway towards which to aim my downstream validation strategies, positive regulators play an important role in increasing or supporting B7-H4 expression in epithelial cell lines, which could be highly relevant in patients whose tumors display high B7-H4 expression. Therapy options are aimed at reducing B7-H4 levels to improve prognosis, and as such, the positive regulators I identify here (through the screen or by downstream validation as was performed for RPN2) could directly contribute to identifying potential therapeutic targets. Of course, the apparent lack of correlation of some targets between the CRISPR screen data and shRNA validation will have to be elucidated at the mechanistic level, with the use of CRISPR guides against RPN2 as well as other potential hits.

To identify additional regulators of B7-H4 cell surface levels, in addition to the strategies outlined in sections 1 and 2 of this discussion, I would propose to re-examine the positive regulators of B7-H4 identified in my CRISPR screen. To this end, I have correlated genes up-regulated in low-immune patient samples from the TNBC cohort available in the Park lab to the regulators of B7-H4 that I have identified in my screen. Only one gene was observed as significant through this analysis, AMD1. AMD1 is an essential protein for the biosynthesis of the polyamines: spermidine and spermine. It promotes maintenance and self-renewal of embryonic stem cells, by maintaining spermine levels. Moreover, a paper published in Science in 2018 provided evidence of the central role of polyamines in cell proliferation and cancer growth (156). They proposed the concept that whereas glucose, amino acids, and lipids represent the primary fuel of cancer cells, polyamines serve as the oil for the cancer engine to function at optimal capacity. Moreover, they report that these metabolites are found at higher abundance in various types of cancer and have also been postulated as non-invasive biomarkers through their detection in biofluids. Hence there is increasing interest in the role of AMD1 in cancer, although this has yet to be characterized in TNBC. However, the relevance of this protein in our own patient samples is evidence enough to pursue the validation of this positive regulator of B7-H4 in parallel with the glycosylation-related negative regulators, with all the previously discussed considerations for troubleshooting of my validation procedure included.

Adding to the previous mention of the tumor ‘glyco-code’, an immunotherapy field that focuses on the targeting of glycans as a new therapeutic opportunity (glycosylation can alter how the body perceives the tumor, and in parallel, glycosylation of tumor proteins can generate neo-antigens serving as targets for tumour-specific T-cells) (127). A

literature review indicated relevance for RPN2 and B3GNT2 in the field of cancer and immunotherapy. The role of RPN2 has previously been documented in breast tumor initiation and metastasis, whereby RPN2 knockdown promoted GSK3β-mediated suppression of heat shock proteins essential to the stabilization of a mutant p53 gain-of-function mutation (157). Moreover, Honma et al. showed that drug resistance in a breast cancer cell line was conferred by the expression RPN2, and that silencing of the gene made the cells hypersensitive to docetaxel (158). B3GNT2, additionally to the research previously outlined on a member of its family, B3GNT3, has been itself documented as an altered (at a higher than expected background rate) glycosyltransferases in colorectal cancer, causing increased susceptibility to inherited colorectal cancers (159).

4. Future directions for B7-H4 in TNBC

Much remains to be learned about the role of B7-H4 in TNBC, and how does it correlate to the negative prognosis associated with its expression on tumor epithelium in TNBC patients, and other cancers. More research is required to identify its receptor, which would facilitate the design of experiments, similar to how is currently done for the B7.1/B7.2 and CTLA-4 pair, or PD-1 and PD-L1. The results of my screen have provided some understanding of mechanisms for B7-H4 regulation intrinsically in tumor cells. However, much remains to be elucidated about how these mechanisms precisely affect B7-H4 expression on the tumor cells. The discovery that glycosylation is also an important player in B7-H4 regulation, similarly to PD-L1, provides new strategies to study B7-H4 by drawing parallels to other, better characterized immune checkpoints. Moreover, once it is better characterized and harnessed for use in treatment strategies for TNBC patients,

glycosylation of B7-H4 could prove useful in improving treatment responses, by potentially facilitating B7-H4 binding of antibody-drug-conjugates if it is utilized as a biomarker, or lowering toxicity, as is currently being observed for PD-L1. As it so happens, anti-B7-H4 antibodies and immunoconjugates and methods of using the same have been patented by Genentech, a pharmaceutical company, back in 2014 (160). An ADC has already been created and published by the company (161) The current momentum in immunotherapy will prove useful in harnessing the field's attention to the study of B7-H4, to potentially turn this immune checkpoint into the next successful immunotherapy strategy in clinic.

Conclusion

This project began with the observation that the immune checkpoint B7-H4 showed a high epithelial expression in the tumors of TNBC patients with poor immune infiltration of $CD8^+$ T-cells (74). Little was known about this molecule, therefore I sought out to elucidate its tumor intrinsic role by identifying regulators of cell surface of B7-H4 in a basal cancer cell line. Conducting a genome-wide CRISPR screen allowed me to identify all the most significant genes and pathways involved in the positive and negative regulation of B7-H4 cell surface expression. By doing so, I identified the importance of glycosylation for B7-H4 expression, though this complex process presented with varying phenotypes when validation steps were undertaken. More studies are required to understand how glycosylation alters B7-H4 expression, and whether it is a process that can be harnessed therapeutically to enhance B7-H4 targeting with antibodies. Moreover, the other identified regulators also require advanced analysis to build a map of the B7-H4 regulation path and to uncover genes that could be targeted therapeutically for cancer treatment, such as AMD1, which was also observed to be up-regulated in our TNBC patient cohort. Finally, I believe these findings will contribute to the search for B7-H4's corresponding ligand by providing insight into its regulation and will pave the way for more genome-wide studies of B7-H4 but for protein interactors as well. I believe the data I have generated within this project will contribute to the cancer immunotherapy field by providing insight into immune checkpoints not only as immune-expressed but also tumor-expressed molecules with an intrinsic role in tumor biology, an aspect of immune checkpoint expression that has been overlooked for many years.

Supplementary information

Table 1: Positive regulators of B7-H4 identified through genome-wide CRISPR screen chosen as potential hits to target in early validation

Name	FDR value	Function	References
EP300	0.000309	This gene encodes the adenovirus E1A-associated cellular p300 transcriptional co-activator protein. It functions as a histone acetyltransferase that regulates transcription via chromatin remodeling and is important in the processes of cell proliferation and differentiation. This gene has also been identified as a co-activator of HIF1A (hypoxia-inducible factor 1 alpha), and thus plays a role in the stimulation of hypoxia-induced genes such as VEGF. Moreover, EP300 has been tied to regulatory T-cell biology, with overexpression resulting in increased Foxp3 expression, a transcription factor tied to T_{reg} function.	162-164
SFPQ	0.000309	SFPQ (Splicing Factor Proline And Glutamine Rich) is a Protein Coding gene. Diseases associated with SFPQ up-regulation include Renal Cell Carcinoma, Papillary and Adrenal Neuroblastoma. It is also highly expressed in breast cancer and associated with poor clinicopathological parameters and an aggressive breast cancer phenotype.	162, 165
SOX9	0.000309	SRY (Sex Determining Region Y)-related HMG-box (SOX) genes belong to a super-family of genes, which is characterized by a homologous sequence called the HMG-box residing on the Y-chromosome. Several reports have been documented of its role in breast cancer by promoting proliferation and a metastatic phenotype, with its up-regulation causing relative endocrine resistance.	162, 166-167
CUL3	0.000309	This gene encodes a member of the cullin protein family. The encoded protein plays a critical role in the polyubiquitination and	162, 168

		subsequent degradation of specific protein substrates as the core component and scaffold protein of an E3 ubiquitin ligase complex. Moreover, CUL3 has been shown to interact with PD-L1 and regulate its stability, and that its depletion increased the protein abundance of endogenous PD-L1.	
FBXW7	0.000309	Constitutes one of the four subunits of ubiquitin protein ligase complex, which function in phosphorylation-dependent ubiquitination. Mutations in this gene are detected in ovarian and breast cancer cell lines, implicating the gene's potential role in the pathogenesis of human cancers. Moreover, it has been implicated in cancer-mediated T-cell dysfunction through its involvement with the EZH2 pathway (regulates effector T-cell polyfunctionality and survival).	162, 169-170
AMD1	0.008818	This gene encodes an important intermediate enzyme in polyamine biosynthesis. The polyamines spermine, spermidine, and putrescine are low-molecular-weight aliphatic amines essential for cellular proliferation and tumor promotion. AMD1 has been implicated in polyamine metabolism in prostate cancer with activated mTORC1, but also in oncogenic signaling in a variety of other cancers, with inhibitors available in prostate cancer, leukemia, osteosarcoma and melanoma.	156, 162, 171

Table 2: Negative, glycosylation-related regulators of B7-H4 identified through genome-wide CRISPR screen chosen as potential hits to target in early validation

Name	FDR value	Function	References
COG3	0.001238	This gene encodes a component of the conserved oligomeric Golgi (COG) complex which is composed of eight different subunits and is required for normal Golgi morphology and localization. Defects in the COG complex result in multiple deficiencies in protein glycosylation. The protein encoded by this gene is involved in ER-Golgi transport.	162, 172
RPN1	0.001238	This gene encodes a type I integral membrane protein found only in the rough endoplasmic reticulum. The encoded protein is part of an N-oligosaccharyl transferase complex that links high mannose oligosaccharides to asparagine residues found in the Asn-X-Ser/Thr consensus motif of nascent polypeptide chains.	162, 173-175
STT3B	0.003713	The protein encoded by this gene is a catalytic subunit of a protein complex that transfers oligosaccharides onto asparagine residues.	162, 173-175
DDOST	0.004189	This gene encodes a component of the oligosaccharyltransferase complex which catalyzes the transfer of high-mannose oligosaccharides to asparagine residues on nascent polypeptides in the lumen of the rough endoplasmic reticulum.	162, 173-175
DAD1	0.020509	DAD1, the defender against apoptotic cell death, was initially identified as a negative regulator of programmed cell death in the temperature sensitive tsBN7 cell line. The DAD1 protein disappeared in temperature-sensitive cells following a shift to the non-permissive temperature, suggesting that loss of the DAD1 protein triggered apoptosis. DAD1 is believed to be a tightly associated subunit of oligosaccharyltransferase both in the intact membrane and in the purified enzyme,	162, 173-175

		thus reflecting the essential nature of N-linked glycosylation in eukaryotes.	
B3GNT2	0.058894	This gene encodes a member of the beta-1,3-N-acetylglucosaminyltransferase family. This enzyme is a type II transmembrane protein. It prefers the substrate of lacto-N-neotetraose and is involved in the biosynthesis of poly-N-acetyllactosamine chains.	150, 162, 176
MGAT1	0.060843	There are believed to be over 100 different glycosyltransferases involved in the synthesis of protein-bound and lipid-bound oligosaccharides. UDP-N-acetylglucosamine:alpha-3-D-mannoside beta-1,2-N-acetylglucosaminyltransferase I is a medial-Golgi enzyme essential for the synthesis of hybrid and complex N-glycans..	151-152, 162, 174, 177
ALG5	0.093914	This gene encodes a member of the glycosyltransferase 2 family. The encoded protein participates in glucosylation of the oligomannose core in N-linked glycosylation of proteins. The addition of glucose residues to the oligomannose core is necessary to ensure substrate recognition, and therefore, effectual transfer of the oligomannose core to the nascent glycoproteins.	162, 178
RPN2	0.094059	This gene encodes a type I integral membrane protein found only in the rough endoplasmic reticulum. The encoded protein is part of an N-oligosaccharyl transferase complex that links high mannose oligosaccharides to asparagine residues found in the Asn-X-Ser/Thr consensus motif of nascent polypeptide chains.	162, 173-175

References

1. Murphy, K., Weaver, C., Mowat, A., Berg, L., Chaplin, D., Janeway, C., . . . Walport, M. (2017). *Janeway's immunobiology* (9th edition. ed.). New York, NY: Garland Science, Taylor & Francis Group, LLC.
2. Mary Cavanagh, E. G. F. T-cell activation. Retrieved from https://www.immunology.org/public-information/bitesized-immunology/systems-and-processes/t-cell-activation
3. Sharma, P., Wagner, K., Wolchok, J. D., & Allison, J. P. (2011). Novel cancer immunotherapy agents with survival benefit: recent successes and next steps. *Nat Rev Cancer, 11*(11), 805-812. Retrieved from https://www.ncbi.nlm.nih.gov/pubmed/22020206. doi:10.1038/nrc3153
4. Leung, J. P. T. (2015). *Regulation of anti-tumor T cell immunity by the B7 family member B7-H4.* (Doctor of Philosophy), McGill University, Montréal.
5. Fridman, W. H., Zitvogel, L., Sautes-Fridman, C., & Kroemer, G. (2017). The immune contexture in cancer prognosis and treatment. *Nat Rev Clin Oncol, 14*(12), 717-734. Retrieved from https://www.ncbi.nlm.nih.gov/pubmed/28741618. doi:10.1038/nrclinonc.2017.101
6. Oiseth, S. J., & Aziz, M. S. Cancer immunotherapy: a brief review of the history, possibilities, and challenges ahead.
7. Coulie, P. G., Van den Eynde, B. J., van der Bruggen, P., & Boon, T. (2014). Tumour antigens recognized by T lymphocytes: at the core of cancer immunotherapy. *Nat Rev Cancer, 14*(2), 135-146. Retrieved from https://www.ncbi.nlm.nih.gov/pubmed/24457417. doi:10.1038/nrc3670
8. Abadi, Y. M., Jeon, H., Ohaegbulam, K. C., Scandiuzzi, L., Ghosh, K., Hofmeyer, K. A., . . . Zang, X. (2013). Host b7x promotes pulmonary metastasis of breast cancer. *J Immunol, 190*(7), 3806-3814. Retrieved from https://www.ncbi.nlm.nih.gov/pubmed/23455497. doi:10.4049/jimmunol.1202439
9. Leung, J., & Suh, W. K. (2013). Host B7-H4 regulates antitumor T cell responses through inhibition of myeloid-derived suppressor cells in a 4T1 tumor transplantation model. *J Immunol, 190*(12), 6651-6661. Retrieved from https://www.ncbi.nlm.nih.gov/pubmed/23686485. doi:10.4049/jimmunol.1201242
10. Rahbar, R., Lin, A., Ghazarian, M., Yau, H. L., Paramathas, S., Lang, P. A., . . . Ohashi, P. S. (2015). B7-H4 expression by nonhematopoietic cells in the tumor microenvironment promotes antitumor immunity. *Cancer Immunol Res, 3*(2), 184-195. Retrieved from https://www.ncbi.nlm.nih.gov/pubmed/25527357. doi:10.1158/2326-6066.CIR-14-0113
11. Hewitt, H. B., Blake, E. R., & Walder, A. S. (1976). A critique of the evidence for active host defence against cancer, based on personal studies of 27 murine tumours of spontaneous origin. *Br J Cancer, 33*(3), 241-259. Retrieved from https://www.ncbi.nlm.nih.gov/pubmed/773395.

12. Kreymborg, K., Haak, S., Murali, R., Wei, J., Waitz, R., Gasteiger, G., . . . Allison, J. P. (2015). Ablation of B7-H3 but Not B7-H4 Results in Highly Increased Tumor Burden in a Murine Model of Spontaneous Prostate Cancer. *Cancer Immunol Res, 3*(8), 849-854. Retrieved from https://www.ncbi.nlm.nih.gov/pubmed/26122284. doi:10.1158/2326-6066.CIR-15-0100
13. Drake, C. G., Jaffee, E., & Pardoll, D. M. (2006). Mechanisms of immune evasion by tumors. *Adv Immunol, 90*, 51-81. Retrieved from https://www.ncbi.nlm.nih.gov/pubmed/16730261. doi:10.1016/S0065-2776(06)90002-9
14. Snyder, A., Makarov, V., Merghoub, T., Yuan, J., Zaretsky, J. M., Desrichard, A., . . . Chan, T. A. (2014). Genetic basis for clinical response to CTLA-4 blockade in melanoma. *N Engl J Med, 371*(23), 2189-2199. Retrieved from https://www.ncbi.nlm.nih.gov/pubmed/25409260. doi:10.1056/NEJMoa1406498
15. Sharma, P., & Allison, J. P. (2015). The future of immune checkpoint therapy. *Science, 348*(6230), 56-61. Retrieved from https://www.ncbi.nlm.nih.gov/pubmed/25838373. doi:10.1126/science.aaa8172
16. Walunas, T. L., Lenschow, D. J., Bakker, C. Y., Linsley, P. S., Freeman, G. J., Green, J. M., . . . Bluestone, J. A. (1994). CTLA-4 can function as a negative regulator of T cell activation. *Immunity, 1*(5), 405-413. Retrieved from https://www.ncbi.nlm.nih.gov/pubmed/7882171.
17. Krummel, M. F., & Allison, J. P. (1995). CD28 and CTLA-4 have opposing effects on the response of T cells to stimulation. *J Exp Med, 182*(2), 459-465. Retrieved from https://www.ncbi.nlm.nih.gov/pubmed/7543139.
18. Leach, D. R., Krummel, M. F., & Allison, J. P. (1996). Enhancement of antitumor immunity by CTLA-4 blockade. *Science, 271*(5256), 1734-1736. Retrieved from https://www.ncbi.nlm.nih.gov/pubmed/8596936.
19. Hurwitz, A. A., Yu, T. F., Leach, D. R., & Allison, J. P. (1998). CTLA-4 blockade synergizes with tumor-derived granulocyte-macrophage colony-stimulating factor for treatment of an experimental mammary carcinoma. *Proc Natl Acad Sci U S A, 95*(17), 10067-10071. Retrieved from https://www.ncbi.nlm.nih.gov/pubmed/9707601.
20. van Elsas, A., Hurwitz, A. A., & Allison, J. P. (1999). Combination immunotherapy of B16 melanoma using anti-cytotoxic T lymphocyte-associated antigen 4 (CTLA-4) and granulocyte/macrophage colony-stimulating factor (GM-CSF)-producing vaccines induces rejection of subcutaneous and metastatic tumors accompanied by autoimmune depigmentation. *J Exp Med, 190*(3), 355-366. Retrieved from https://www.ncbi.nlm.nih.gov/pubmed/10430624.

21. Waitz, R., Fasso, M., & Allison, J. P. (2012). CTLA-4 blockade synergizes with cryoablation to mediate tumor rejection. *Oncoimmunology, 1*(4), 544-546. Retrieved from https://www.ncbi.nlm.nih.gov/pubmed/22754781.
22. Zamarin, D., Holmgaard, R. B., Subudhi, S. K., Park, J. S., Mansour, M., Palese, P., . . . Allison, J. P. (2014). Localized oncolytic virotherapy overcomes systemic tumor resistance to immune checkpoint blockade immunotherapy. *Sci Transl Med, 6*(226), 226ra232. Retrieved from https://www.ncbi.nlm.nih.gov/pubmed/24598590. doi:10.1126/scitranslmed.3008095
23. Hodi, F. S., O'Day, S. J., McDermott, D. F., Weber, R. W., Sosman, J. A., Haanen, J. B., . . . Urba, W. J. (2010). Improved survival with ipilimumab in patients with metastatic melanoma. *N Engl J Med, 363*(8), 711-723. Retrieved from https://www.ncbi.nlm.nih.gov/pubmed/20525992. doi:10.1056/NEJMoa1003466
24. Robert, C., Thomas, L., Bondarenko, I., O'Day, S., Weber, J., Garbe, C., . . . Wolchok, J. D. (2011). Ipilimumab plus dacarbazine for previously untreated metastatic melanoma. *N Engl J Med, 364*(26), 2517-2526. Retrieved from https://www.ncbi.nlm.nih.gov/pubmed/21639810. doi:10.1056/NEJMoa1104621
25. Pardoll, D. M. (2012). The blockade of immune checkpoints in cancer immunotherapy. *Nat Rev Cancer, 12*(4), 252-264. Retrieved from https://www.ncbi.nlm.nih.gov/pubmed/22437870. doi:10.1038/nrc3239
26. Freeman, G. J., Long, A. J., Iwai, Y., Bourque, K., Chernova, T., Nishimura, H., . . . Honjo, T. (2000). Engagement of the PD-1 immunoinhibitory receptor by a novel B7 family member leads to negative regulation of lymphocyte activation. *J Exp Med, 192*(7), 1027-1034. Retrieved from https://www.ncbi.nlm.nih.gov/pubmed/11015443.
27. Greenwald, R. J., Freeman, G. J., & Sharpe, A. H. (2005). The B7 family revisited. *Annu Rev Immunol, 23*, 515-548. Retrieved from https://www.ncbi.nlm.nih.gov/pubmed/15771580. doi:10.1146/annurev.immunol.23.021704.115611
28. Dong, H., Strome, S. E., Salomao, D. R., Tamura, H., Hirano, F., Flies, D. B., . . . Chen, L. (2002). Tumor-associated B7-H1 promotes T-cell apoptosis: a potential mechanism of immune evasion. *Nat Med, 8*(8), 793-800. Retrieved from https://www.ncbi.nlm.nih.gov/pubmed/12091876. doi:10.1038/nm730
29. Weber, J. S., O'Day, S., Urba, W., Powderly, J., Nichol, G., Yellin, M., . . . Hersh, E. (2008). Phase I/II study of ipilimumab for patients with metastatic melanoma. *J Clin Oncol, 26*(36), 5950-5956. Retrieved from https://www.ncbi.nlm.nih.gov/pubmed/19018089. doi:10.1200/JCO.2008.16.1927
30. Yang, J. C., Hughes, M., Kammula, U., Royal, R., Sherry, R. M., Topalian, S. L., . . . Rosenberg, S. A. (2007). Ipilimumab (anti-CTLA4 antibody) causes regression

of metastatic renal cell cancer associated with enteritis and hypophysitis. *J Immunother, 30*(8), 825-830. Retrieved from https://www.ncbi.nlm.nih.gov/pubmed/18049334. doi:10.1097/CJI.0b013e318156e47e

31. van den Eertwegh, A. J., Versluis, J., van den Berg, H. P., Santegoets, S. J., van Moorselaar, R. J., van der Sluis, T. M., . . . Gerritsen, W. R. (2012). Combined immunotherapy with granulocyte-macrophage colony-stimulating factor-transduced allogeneic prostate cancer cells and ipilimumab in patients with metastatic castration-resistant prostate cancer: a phase 1 dose-escalation trial. *Lancet Oncol, 13*(5), 509-517. Retrieved from https://www.ncbi.nlm.nih.gov/pubmed/22326922. doi:10.1016/S1470-2045(12)70007-4
32. Carthon, B. C., Wolchok, J. D., Yuan, J., Kamat, A., Ng Tang, D. S., Sun, J., . . . Sharma, P. (2010). Preoperative CTLA-4 blockade: tolerability and immune monitoring in the setting of a presurgical clinical trial. *Clin Cancer Res, 16*(10), 2861-2871. Retrieved from https://www.ncbi.nlm.nih.gov/pubmed/20460488. doi:10.1158/1078-0432.CCR-10-0569
33. Hodi, F. S., Butler, M., Oble, D. A., Seiden, M. V., Haluska, F. G., Kruse, A., . . . Dranoff, G. (2008). Immunologic and clinical effects of antibody blockade of cytotoxic T lymphocyte-associated antigen 4 in previously vaccinated cancer patients. *Proc Natl Acad Sci U S A, 105*(8), 3005-3010. Retrieved from https://www.ncbi.nlm.nih.gov/pubmed/18287062. doi:10.1073/pnas.0712237105
34. Schadendorf, D., Hodi, F. S., Robert, C., Weber, J. S., Margolin, K., Hamid, O., . . . Wolchok, J. D. (2015). Pooled Analysis of Long-Term Survival Data From Phase II and Phase III Trials of Ipilimumab in Unresectable or Metastatic Melanoma. *J Clin Oncol, 33*(17), 1889-1894. Retrieved from https://www.ncbi.nlm.nih.gov/pubmed/25667295. doi:10.1200/JCO.2014.56.2736
35. Brahmer, J. R., Tykodi, S. S., Chow, L. Q., Hwu, W. J., Topalian, S. L., Hwu, P., . . . Wigginton, J. M. (2012). Safety and activity of anti-PD-L1 antibody in patients with advanced cancer. *N Engl J Med, 366*(26), 2455-2465. Retrieved from https://www.ncbi.nlm.nih.gov/pubmed/22658128. doi:10.1056/NEJMoa1200694
36. Powles, T., Eder, J. P., Fine, G. D., Braiteh, F. S., Loriot, Y., Cruz, C., . . . Vogelzang, N. J. (2014). MPDL3280A (anti-PD-L1) treatment leads to clinical activity in metastatic bladder cancer. *Nature, 515*(7528), 558-562. Retrieved from https://www.ncbi.nlm.nih.gov/pubmed/25428503. doi:10.1038/nature13904
37. Hamid, O., Robert, C., Daud, A., Hodi, F. S., Hwu, W. J., Kefford, R., . . . Ribas, A. (2013). Safety and tumor responses with lambrolizumab (anti-PD-1) in melanoma. *N Engl J Med, 369*(2), 134-144. Retrieved from https://www.ncbi.nlm.nih.gov/pubmed/23724846. doi:10.1056/NEJMoa1305133

38. Robert, C., Ribas, A., Wolchok, J. D., Hodi, F. S., Hamid, O., Kefford, R., . . . Daud, A. (2014). Anti-programmed-death-receptor-1 treatment with pembrolizumab in ipilimumab-refractory advanced melanoma: a randomised dose-comparison cohort of a phase 1 trial. *Lancet, 384*(9948), 1109-1117. Retrieved from https://www.ncbi.nlm.nih.gov/pubmed/25034862. doi:10.1016/S0140-6736(14)60958-2
39. Robert, C., Long, G. V., Brady, B., Dutriaux, C., Maio, M., Mortier, L., . . . Ascierto, P. A. (2015). Nivolumab in previously untreated melanoma without BRAF mutation. *N Engl J Med, 372*(4), 320-330. Retrieved from https://www.ncbi.nlm.nih.gov/pubmed/25399552. doi:10.1056/NEJMoa1412082
40. Garcia-Teijido, P., Cabal, M. L., Fernandez, I. P., & Perez, Y. F. (2016). Tumor-Infiltrating Lymphocytes in Triple Negative Breast Cancer: The Future of Immune Targeting. *Clin Med Insights Oncol, 10*(Suppl 1), 31-39. Retrieved from https://www.ncbi.nlm.nih.gov/pubmed/27081325. doi:10.4137/CMO.S34540
41. Dua, I. (2017). Immunotherapy for triple-negative breast cancer: a focus on immune checkpoint inhibitors. *American Journal of Hematology/Oncology®, 13*(5).
42. Savas, P., Salgado, R., Denkert, C., Sotiriou, C., Darcy, P. K., Smyth, M. J., & Loi, S. (2016). Clinical relevance of host immunity in breast cancer: from TILs to the clinic. *Nature reviews Clinical oncology, 13*(4), 228.
43. Society, C. C. (2018). Breast Cancer Statistics.
44. Sung, Y.-C. V. (2018). *Mechanisms of MET-dependent tumour initiation and progression.* (Doctor of Philisophy), McGill University, Montréal.
45. Haybittle, J. L., Blamey, R. W., Elston, C. W., Johnson, J., Doyle, P. J., Campbell, F. C., . . . Griffiths, K. (1982). A prognostic index in primary breast cancer. *Br J Cancer, 45*(3), 361-366. Retrieved from https://www.ncbi.nlm.nih.gov/pubmed/7073932.
46. Elkin, E. B., Hudis, C., Begg, C. B., & Schrag, D. (2005). The effect of changes in tumor size on breast carcinoma survival in the U.S.: 1975-1999. *Cancer, 104*(6), 1149-1157. Retrieved from https://www.ncbi.nlm.nih.gov/pubmed/16088887. doi:10.1002/cncr.21285
47. Woodward, W. A., Strom, E. A., Tucker, S. L., McNeese, M. D., Perkins, G. H., Schechter, N. R., . . . Buchholz, T. A. (2003). Changes in the 2003 American Joint Committee on Cancer staging for breast cancer dramatically affect stage-specific survival. *J Clin Oncol, 21*(17), 3244-3248. Retrieved from https://www.ncbi.nlm.nih.gov/pubmed/12947058. doi:10.1200/JCO.2003.03.052
48. Bloom, H. J., & Richardson, W. W. (1957). Histological grading and prognosis in breast cancer; a study of 1409 cases of which 359 have been followed for 15 years. *Br J Cancer, 11*(3), 359-377. Retrieved from https://www.ncbi.nlm.nih.gov/pubmed/13499785.

49. Onitilo, A. A., Engel, J. M., Greenlee, R. T., & Mukesh, B. N. (2009). Breast cancer subtypes based on ER/PR and Her2 expression: comparison of clinicopathologic features and survival. *Clin Med Res, 7*(1-2), 4-13. Retrieved from https://www.ncbi.nlm.nih.gov/pubmed/19574486. doi:10.3121/cmr.2009.825
50. Slamon, D. J., Clark, G. M., Wong, S. G., Levin, W. J., Ullrich, A., & McGuire, W. L. (1987). Human breast cancer: correlation of relapse and survival with amplification of the HER-2/neu oncogene. *Science, 235*(4785), 177-182. Retrieved from https://www.ncbi.nlm.nih.gov/pubmed/3798106.
51. Piccart-Gebhart, M. J., Procter, M., Leyland-Jones, B., Goldhirsch, A., Untch, M., Smith, I., . . . Herceptin Adjuvant Trial Study, T. (2005). Trastuzumab after adjuvant chemotherapy in HER2-positive breast cancer. *N Engl J Med, 353*(16), 1659-1672. Retrieved from https://www.ncbi.nlm.nih.gov/pubmed/16236737. doi:10.1056/NEJMoa052306
52. Romond, E. H., Perez, E. A., Bryant, J., Suman, V. J., Geyer, C. E., Jr., Davidson, N. E., . . . Wolmark, N. (2005). Trastuzumab plus adjuvant chemotherapy for operable HER2-positive breast cancer. *N Engl J Med, 353*(16), 1673-1684. Retrieved from https://www.ncbi.nlm.nih.gov/pubmed/16236738. doi:10.1056/NEJMoa052122
53. Foulkes, W. D., Smith, I. E., & Reis-Filho, J. S. (2010). Triple-negative breast cancer. *N Engl J Med, 363*(20), 1938-1948. Retrieved from https://www.ncbi.nlm.nih.gov/pubmed/21067385. doi:10.1056/NEJMra1001389
54. Bauer, K. R., Brown, M., Cress, R. D., Parise, C. A., & Caggiano, V. (2007). Descriptive analysis of estrogen receptor (ER)-negative, progesterone receptor (PR)-negative, and HER2-negative invasive breast cancer, the so-called triple-negative phenotype: a population-based study from the California cancer Registry. *Cancer, 109*(9), 1721-1728. Retrieved from https://www.ncbi.nlm.nih.gov/pubmed/17387718. doi:10.1002/cncr.22618
55. Lehmann, B. D., Bauer, J. A., Chen, X., Sanders, M. E., Chakravarthy, A. B., Shyr, Y., & Pietenpol, J. A. (2011). Identification of human triple-negative breast cancer subtypes and preclinical models for selection of targeted therapies. *J Clin Invest, 121*(7), 2750-2767. Retrieved from https://www.ncbi.nlm.nih.gov/pubmed/21633166. doi:10.1172/JCI45014
56. Lehmann, B. D., Jovanovic, B., Chen, X., Estrada, M. V., Johnson, K. N., Shyr, Y., . . . Pietenpol, J. A. (2016). Refinement of Triple-Negative Breast Cancer Molecular Subtypes: Implications for Neoadjuvant Chemotherapy Selection. *PLoS One, 11*(6), e0157368. Retrieved from https://www.ncbi.nlm.nih.gov/pubmed/27310713. doi:10.1371/journal.pone.0157368
57. Perou, C. M., Sorlie, T., Eisen, M. B., van de Rijn, M., Jeffrey, S. S., Rees, C. A., . . . Botstein, D. (2000). Molecular portraits of human breast tumours. *Nature,*

406(6797), 747-752. Retrieved from https://www.ncbi.nlm.nih.gov/pubmed/10963602. doi:10.1038/35021093

58. Herschkowitz, J. I., Zhao, W., Zhang, M., Usary, J., Murrow, G., Edwards, D., . . . Rosen, J. M. (2012). Comparative oncogenomics identifies breast tumors enriched in functional tumor-initiating cells. *Proc Natl Acad Sci U S A, 109*(8), 2778-2783. Retrieved from https://www.ncbi.nlm.nih.gov/pubmed/21633010. doi:10.1073/pnas.1018862108
59. Sorlie, T., Perou, C. M., Tibshirani, R., Aas, T., Geisler, S., Johnsen, H., . . . Borresen-Dale, A. L. (2001). Gene expression patterns of breast carcinomas distinguish tumor subclasses with clinical implications. *Proc Natl Acad Sci U S A, 98*(19), 10869-10874. Retrieved from https://www.ncbi.nlm.nih.gov/pubmed/11553815. doi:10.1073/pnas.191367098
60. Sorlie, T., Tibshirani, R., Parker, J., Hastie, T., Marron, J. S., Nobel, A., . . . Botstein, D. (2003). Repeated observation of breast tumor subtypes in independent gene expression data sets. *Proc Natl Acad Sci U S A, 100*(14), 8418-8423. Retrieved from https://www.ncbi.nlm.nih.gov/pubmed/12829800. doi:10.1073/pnas.0932692100
61. Parker, J. S., Mullins, M., Cheang, M. C., Leung, S., Voduc, D., Vickery, T., . . . Bernard, P. S. (2009). Supervised risk predictor of breast cancer based on intrinsic subtypes. *J Clin Oncol, 27*(8), 1160-1167. Retrieved from https://www.ncbi.nlm.nih.gov/pubmed/19204204. doi:10.1200/JCO.2008.18.1370
62. Prat, A., & Perou, C. M. (2011). Deconstructing the molecular portraits of breast cancer. *Mol Oncol, 5*(1), 5-23. Retrieved from https://www.ncbi.nlm.nih.gov/pubmed/21147047. doi:10.1016/j.molonc.2010.11.003
63. Rakha, E. A., Reis-Filho, J. S., & Ellis, I. O. (2008). Basal-like breast cancer: a critical review. *J Clin Oncol, 26*(15), 2568-2581. Retrieved from https://www.ncbi.nlm.nih.gov/pubmed/18487574. doi:10.1200/JCO.2007.13.1748
64. Prat, A., Parker, J. S., Karginova, O., Fan, C., Livasy, C., Herschkowitz, J. I., . . . Perou, C. M. (2010). Phenotypic and molecular characterization of the claudin-low intrinsic subtype of breast cancer. *Breast Cancer Res, 12*(5), R68. Retrieved from https://www.ncbi.nlm.nih.gov/pubmed/20813035. doi:10.1186/bcr2635
65. Sabatier, R., Finetti, P., Guille, A., Adelaide, J., Chaffanet, M., Viens, P., . . . Bertucci, F. (2014). Claudin-low breast cancers: clinical, pathological, molecular and prognostic characterization. *Mol Cancer, 13*, 228. Retrieved from https://www.ncbi.nlm.nih.gov/pubmed/25277734. doi:10.1186/1476-4598-13-228
66. Ali, H. R., Provenzano, E., Dawson, S. J., Blows, F. M., Liu, B., Shah, M., . . . Caldas, C. (2014). Association between CD8+ T-cell infiltration and breast cancer survival in 12,439 patients. *Ann Oncol, 25*(8), 1536-1543. Retrieved from https://www.ncbi.nlm.nih.gov/pubmed/24915873. doi:10.1093/annonc/mdu191

67. Baker, K., Lachapelle, J., Zlobec, I., Bismar, T. A., Terracciano, L., & Foulkes, W. D. (2011). Prognostic significance of CD8+ T lymphocytes in breast cancer depends upon both oestrogen receptor status and histological grade. *Histopathology, 58*(7), 1107-1116. Retrieved from https://www.ncbi.nlm.nih.gov/pubmed/21707712. doi:10.1111/j.1365-2559.2011.03846.x
68. Liu, S., Lachapelle, J., Leung, S., Gao, D., Foulkes, W. D., & Nielsen, T. O. (2012). CD8+ lymphocyte infiltration is an independent favorable prognostic indicator in basal-like breast cancer. *Breast Cancer Res, 14*(2), R48. Retrieved from https://www.ncbi.nlm.nih.gov/pubmed/22420471. doi:10.1186/bcr3148
69. Stagg, J., & Allard, B. (2013). Immunotherapeutic approaches in triple-negative breast cancer: latest research and clinical prospects. *Ther Adv Med Oncol, 5*(3), 169-181. Retrieved from https://www.ncbi.nlm.nih.gov/pubmed/23634195. doi:10.1177/1758834012475152
70. Bianchini, G., Balko, J. M., Mayer, I. A., Sanders, M. E., & Gianni, L. (2016). Triple-negative breast cancer: challenges and opportunities of a heterogeneous disease. *Nat Rev Clin Oncol, 13*(11), 674-690. Retrieved from https://www.ncbi.nlm.nih.gov/pubmed/27184417. doi:10.1038/nrclinonc.2016.66
71. Emens, L. A., Kok, M., & Ojalvo, L. S. (2016). Targeting the programmed cell death-1 pathway in breast and ovarian cancer. *Curr Opin Obstet Gynecol, 28*(2), 142-147. Retrieved from https://www.ncbi.nlm.nih.gov/pubmed/26881392. doi:10.1097/GCO.0000000000000257
72. Emens, L. A., Braiteh, F. S., Cassier, P., Delord, J.-P., Eder, J. P., Fasso, M., . . . Krop, I. (2015). Abstract 2859: Inhibition of PD-L1 by MPDL3280A leads to clinical activity in patients with metastatic triple-negative breast cancer (TNBC). *Cancer Research, 75*(15 Supplement), 2859-2859. doi:10.1158/1538-7445.Am2015-2859
73. Nanda, R., Chow, L. Q., Dees, E. C., Berger, R., Gupta, S., Geva, R., . . . Buisseret, L. (2016). Pembrolizumab in Patients With Advanced Triple-Negative Breast Cancer: Phase Ib KEYNOTE-012 Study. *J Clin Oncol, 34*(21), 2460-2467. Retrieved from https://www.ncbi.nlm.nih.gov/pubmed/27138582. doi:10.1200/JCO.2015.64.8931
74. Gruosso, T., Gigoux, M., Manem, V. S. K., Bertos, N., Zuo, D., Perlitch, I., . . . Park, M. (2019). Spatially distinct tumor immune microenvironments stratify triple-negative breast cancers. *J Clin Invest, 129*(4), 1785-1800. Retrieved from https://www.ncbi.nlm.nih.gov/pubmed/30753167. doi:10.1172/JCI96313
75. Ceeraz, S., Nowak, E. C., & Noelle, R. J. (2013). B7 family checkpoint regulators in immune regulation and disease. *Trends Immunol, 34*(11), 556-563. Retrieved from https://www.ncbi.nlm.nih.gov/pubmed/23954143. doi:10.1016/j.it.2013.07.003

76. MacGregor, H. L., & Ohashi, P. S. (2017). Molecular Pathways: Evaluating the Potential for B7-H4 as an Immunoregulatory Target. *Clin Cancer Res, 23*(12), 2934-2941. Retrieved from https://www.ncbi.nlm.nih.gov/pubmed/28325750. doi:10.1158/1078-0432.CCR-15-2440
77. Prasad, D. V., Richards, S., Mai, X. M., & Dong, C. (2003). B7S1, a novel B7 family member that negatively regulates T cell activation. *Immunity, 18*(6), 863-873. Retrieved from https://www.ncbi.nlm.nih.gov/pubmed/12818166.
78. Zang, X., Loke, P., Kim, J., Murphy, K., Waitz, R., & Allison, J. P. (2003). B7x: a widely expressed B7 family member that inhibits T cell activation. *Proc Natl Acad Sci U S A, 100*(18), 10388-10392. Retrieved from https://www.ncbi.nlm.nih.gov/pubmed/12920180. doi:10.1073/pnas.1434299100
79. Sica, G. L., Choi, I. H., Zhu, G., Tamada, K., Wang, S. D., Tamura, H., . . . Chen, L. (2003). B7-H4, a molecule of the B7 family, negatively regulates T cell immunity. *Immunity, 18*(6), 849-861. Retrieved from https://www.ncbi.nlm.nih.gov/pubmed/12818165.
80. Watanabe, N., Gavrieli, M., Sedy, J. R., Yang, J., Fallarino, F., Loftin, S. K., . . . Murphy, K. M. (2003). BTLA is a lymphocyte inhibitory receptor with similarities to CTLA-4 and PD-1. *Nat Immunol, 4*(7), 670-679. Retrieved from https://www.ncbi.nlm.nih.gov/pubmed/12796776. doi:10.1038/ni944
81. Sedy, J. R., Gavrieli, M., Potter, K. G., Hurchla, M. A., Lindsley, R. C., Hildner, K., . . . Murphy, K. M. (2005). B and T lymphocyte attenuator regulates T cell activation through interaction with herpesvirus entry mediator. *Nat Immunol, 6*(1), 90-98. Retrieved from https://www.ncbi.nlm.nih.gov/pubmed/15568026. doi:10.1038/ni1144
82. Choi, I. H., Zhu, G., Sica, G. L., Strome, S. E., Cheville, J. C., Lau, J. S., . . . Chen, L. (2003). Genomic organization and expression analysis of B7-H4, an immune inhibitory molecule of the B7 family. *J Immunol, 171*(9), 4650-4654. Retrieved from https://www.ncbi.nlm.nih.gov/pubmed/14568939.
83. Wei, J., Loke, P., Zang, X., & Allison, J. P. (2011). Tissue-specific expression of B7x protects from CD4 T cell-mediated autoimmunity. *J Exp Med, 208*(8), 1683-1694. Retrieved from https://www.ncbi.nlm.nih.gov/pubmed/21727190. doi:10.1084/jem.20100639
84. Salceda, S., Tang, T., Kmet, M., Munteanu, A., Ghosh, M., Macina, R., . . . Papkoff, J. (2005). The immunomodulatory protein B7-H4 is overexpressed in breast and ovarian cancers and promotes epithelial cell transformation. *Exp Cell Res, 306*(1), 128-141. Retrieved from https://www.ncbi.nlm.nih.gov/pubmed/15878339. doi:10.1016/j.yexcr.2005.01.018
85. Tringler, B., Zhuo, S., Pilkington, G., Torkko, K. C., Singh, M., Lucia, M. S., . . . Shroyer, K. R. (2005). B7-h4 is highly expressed in ductal and lobular breast

cancer. *Clin Cancer Res, 11*(5), 1842-1848. Retrieved from https://www.ncbi.nlm.nih.gov/pubmed/15756008. doi:10.1158/1078-0432.CCR-04-1658

86. Wang, X., Hao, J., Metzger, D. L., Mui, A., Ao, Z., Verchere, C. B., . . . Warnock, G. L. (2009). Local expression of B7-H4 by recombinant adenovirus transduction in mouse islets prolongs allograft survival. *Transplantation, 87*(4), 482-490. Retrieved from https://www.ncbi.nlm.nih.gov/pubmed/19307783. doi:10.1097/TP.0b013e318195e5fa
87. Hofmeyer, K. A., Scandiuzzi, L., Ghosh, K., Pirofski, L. A., & Zang, X. (2012). Tissue-expressed B7x affects the immune response to and outcome of lethal pulmonary infection. *J Immunol, 189*(6), 3054-3063. Retrieved from https://www.ncbi.nlm.nih.gov/pubmed/22855708. doi:10.4049/jimmunol.1200701
88. Kryczek, I., Zou, L., Rodriguez, P., Zhu, G., Wei, S., Mottram, P., . . . Zou, W. (2006). B7-H4 expression identifies a novel suppressive macrophage population in human ovarian carcinoma. *J Exp Med, 203*(4), 871-881. Retrieved from https://www.ncbi.nlm.nih.gov/pubmed/16606666. doi:10.1084/jem.20050930
89. Yao, Y., Ye, H., Qi, Z., Mo, L., Yue, Q., Baral, A., . . . Zhou, L. (2016). B7-H4(B7x)-Mediated Cross-talk between Glioma-Initiating Cells and Macrophages via the IL6/JAK/STAT3 Pathway Lead to Poor Prognosis in Glioma Patients. *Clin Cancer Res, 22*(11), 2778-2790. Retrieved from https://www.ncbi.nlm.nih.gov/pubmed/27001312. doi:10.1158/1078-0432.CCR-15-0858
90. Cao, Q., Wang, Y., Zheng, D., Sun, Y., Wang, Y., Lee, V. W., . . . Harris, D. C. (2010). IL-10/TGF-beta-modified macrophages induce regulatory T cells and protect against adriamycin nephrosis. *J Am Soc Nephrol, 21*(6), 933-942. Retrieved from https://www.ncbi.nlm.nih.gov/pubmed/20299353. doi:10.1681/ASN.2009060592
91. Suh, W. K., Wang, S., Duncan, G. S., Miyazaki, Y., Cates, E., Walker, T., . . . Mak, T. W. (2006). Generation and characterization of B7-H4/B7S1/B7x-deficient mice. *Mol Cell Biol, 26*(17), 6403-6411. Retrieved from https://www.ncbi.nlm.nih.gov/pubmed/16914726. doi:10.1128/MCB.00755-06
92. Johansson, M., Denardo, D. G., & Coussens, L. M. (2008). Polarized immune responses differentially regulate cancer development. *Immunol Rev, 222*, 145-154. Retrieved from https://www.ncbi.nlm.nih.gov/pubmed/18363999. doi:10.1111/j.1600-065X.2008.00600.x
93. Dangaj, D., Lanitis, E., Zhao, A., Joshi, S., Cheng, Y., Sandaltzopoulos, R., . . . Scholler, N. (2013). Novel recombinant human b7-h4 antibodies overcome tumoral immune escape to potentiate T-cell antitumor responses. *Cancer Res, 73*(15), 4820-4829. Retrieved from

https://www.ncbi.nlm.nih.gov/pubmed/23722540. doi:10.1158/0008-5472.CAN-12-3457

94. Miyatake, T., Tringler, B., Liu, W., Liu, S. H., Papkoff, J., Enomoto, T., . . . Shroyer, K. R. (2007). B7-H4 (DD-O110) is overexpressed in high risk uterine endometrioid adenocarcinomas and inversely correlated with tumor T-cell infiltration. *Gynecol Oncol, 106*(1), 119-127. Retrieved from https://www.ncbi.nlm.nih.gov/pubmed/17509674. doi:10.1016/j.ygyno.2007.03.039
95. Fan, M., Zhuang, Q., Chen, Y., Ding, T., Yao, H., Chen, L., . . . Xu, X. (2014). B7-H4 expression is correlated with tumor progression and clinical outcome in urothelial cell carcinoma. *Int J Clin Exp Pathol, 7*(10), 6768-6775. Retrieved from https://www.ncbi.nlm.nih.gov/pubmed/25400757.
96. Chen, L. J., Sun, J., Wu, H. Y., Zhou, S. M., Tan, Y., Tan, M., . . . Zhang, X. G. (2011). B7-H4 expression associates with cancer progression and predicts patient's survival in human esophageal squamous cell carcinoma. *Cancer Immunol Immunother, 60*(7), 1047-1055. Retrieved from https://www.ncbi.nlm.nih.gov/pubmed/21519829. doi:10.1007/s00262-011-1017-3
97. Wu, L., Deng, W. W., Yu, G. T., Mao, L., Bu, L. L., Ma, S. R., . . . Sun, Z. J. (2016). B7-H4 expression indicates poor prognosis of oral squamous cell carcinoma. *Cancer Immunol Immunother, 65*(9), 1035-1045. Retrieved from https://www.ncbi.nlm.nih.gov/pubmed/27383830. doi:10.1007/s00262-016-1867-9
98. Chen, Y., Sun, J., Zhao, H., Zhu, D., Zhi, Q., Song, S., . . . Li, D. (2014). The coexpression and clinical significance of costimulatory molecules B7-H1, B7-H3, and B7-H4 in human pancreatic cancer. *Onco Targets Ther, 7*, 1465-1472. Retrieved from https://www.ncbi.nlm.nih.gov/pubmed/25170273. doi:10.2147/OTT.S66809
99. Wang, X., Wang, T., Xu, M., Xiao, L., Luo, Y., Huang, W., . . . Geng, W. (2014). B7-H4 overexpression impairs the immune response of T cells in human cervical carcinomas. *Hum Immunol, 75*(12), 1203-1209. Retrieved from https://www.ncbi.nlm.nih.gov/pubmed/25446402.doi:10.1016/j.humimm.2014.10.002
100. Quandt, D., Fiedler, E., Boettcher, D., Marsch, W., & Seliger, B. (2011). B7-h4 expression in human melanoma: its association with patients' survival and antitumor immune response. *Clin Cancer Res, 17*(10), 3100-3111. Retrieved from https://www.ncbi.nlm.nih.gov/pubmed/21378130. doi:10.1158/1078-0432.CCR-10-2268
101. Zhang, X., Cai, L., Zhang, G., Shen, Y., & Huang, J. (2017). B7-H4 promotes tumor growth and metastatic progression in lung cancer by impacting cell

proliferation and survival. *Oncotarget, 8*(12), 18861-18871. Retrieved from https://www.ncbi.nlm.nih.gov/pubmed/28061481. doi:10.18632/oncotarget.14475

102. Li, Z. Y., Zhang, X. H., Chen, Y., Guo, J. G., Sai, K., Yang, Q. Y., . . . Mou, Y. G. (2013). Clinical significance of B7-H4 expression in matched non-small cell lung cancer brain metastases and primary tumors. *Onco Targets Ther, 6*, 869-875. Retrieved from https://www.ncbi.nlm.nih.gov/pubmed/23874109. doi:10.2147/OTT.S48085
103. Arigami, T., Uenosono, Y., Ishigami, S., Hagihara, T., Haraguchi, N., & Natsugoe, S. (2011). Clinical significance of the B7-H4 coregulatory molecule as a novel prognostic marker in gastric cancer. *World J Surg, 35*(9), 2051-2057. Retrieved from https://www.ncbi.nlm.nih.gov/pubmed/21748517. doi:10.1007/s00268-011-1186-4
104. Geng, Y., Wang, H., Lu, C., Li, Q., Xu, B., Jiang, J., & Wu, C. (2015). Expression of costimulatory molecules B7-H1, B7-H4 and Foxp3+ Tregs in gastric cancer and its clinical significance. *Int J Clin Oncol, 20*(2), 273-281. Retrieved from https://www.ncbi.nlm.nih.gov/pubmed/24804867. doi:10.1007/s10147-014-0701-7
105. Zhang, L., Wu, H., Lu, D., Li, G., Sun, C., Song, H., . . . Zhang, X. (2013). The costimulatory molecule B7-H4 promote tumor progression and cell proliferation through translocating into nucleus. *Oncogene, 32*(46), 5347-5358. Retrieved from https://www.ncbi.nlm.nih.gov/pubmed/23318460. doi:10.1038/onc.2012.600
106. Krambeck, A. E., Thompson, R. H., Dong, H., Lohse, C. M., Park, E. S., Kuntz, S. M., . . . Kwon, E. D. (2006). B7-H4 expression in renal cell carcinoma and tumor vasculature: associations with cancer progression and survival. *Proc Natl Acad Sci U S A, 103*(27), 10391-10396. Retrieved from https://www.ncbi.nlm.nih.gov/pubmed/16798883. doi:10.1073/pnas.0600937103
107. Zhou, X., Mao, Y., Zhu, J., Meng, F., Chen, Q., Tao, L., . . . Zhang, X. (2016). TGF-beta1 promotes colorectal cancer immune escape by elevating B7-H3 and B7-H4 via the miR-155/miR-143 axis. *Oncotarget, 7*(41), 67196-67211. Retrieved from https://www.ncbi.nlm.nih.gov/pubmed/27626488. doi:10.18632/oncotarget.11950
108. Radichev, I. A., Maneva-Radicheva, L. V., Amatya, C., Parker, C., Ellefson, J., Wasserfall, C., . . . Savinov, A. Y. (2014). Nardilysin-dependent proteolysis of cell-associated VTCN1 (B7-H4) marks type 1 diabetes development. *Diabetes, 63*(10), 3470-3482. Retrieved from https://www.ncbi.nlm.nih.gov/pubmed/24848066. doi:10.2337/db14-0213
109. Simon, I., Katsaros, D., Rigault de la Longrais, I., Massobrio, M., Scorilas, A., Kim, N. W., . . . Diamandis, E. P. (2007). B7-H4 is over-expressed in early-stage ovarian cancer and is independent of CA125 expression. *Gynecol Oncol, 106*(2),

334-341. Retrieved from https://www.ncbi.nlm.nih.gov/pubmed/17498784. doi:10.1016/j.ygyno.2007.03.035

110. Chen, X., Wang, L., Wang, W., Zhao, L., & Shan, B. (2016). B7-H4 facilitates proliferation of esophageal squamous cell carcinoma cells through promoting interleukin-6/signal transducer and activator of transcription 3 pathway activation. *Cancer Sci, 107*(7), 944-954. Retrieved from https://www.ncbi.nlm.nih.gov/pubmed/27088889. doi:10.1111/cas.12949
111. Jiang, J., Zhu, Y., Wu, C., Shen, Y., Wei, W., Chen, L., . . . Zhang, X. (2010). Tumor expression of B7-H4 predicts poor survival of patients suffering from gastric cancer. *Cancer Immunol Immunother, 59*(11), 1707-1714. Retrieved from https://www.ncbi.nlm.nih.gov/pubmed/20725832. doi:10.1007/s00262-010-0900-7
112. Simon, I., Zhuo, S., Corral, L., Diamandis, E. P., Sarno, M. J., Wolfert, R. L., & Kim, N. W. (2006). B7-h4 is a novel membrane-bound protein and a candidate serum and tissue biomarker for ovarian cancer. *Cancer Res, 66*(3), 1570-1575. Retrieved from https://www.ncbi.nlm.nih.gov/pubmed/16452214. doi:10.1158/0008-5472.CAN-04-3550
113. Thompson, R. H., Zang, X., Lohse, C. M., Leibovich, B. C., Slovin, S. F., Reuter, V. E., . . . Allison, J. P. (2008). Serum-soluble B7x is elevated in renal cell carcinoma patients and is associated with advanced stage. *Cancer Res, 68*(15), 6054-6058. Retrieved from https://www.ncbi.nlm.nih.gov/pubmed/18676826. doi:10.1158/0008-5472.CAN-08-0869
114. Azuma, T., Zhu, G., Xu, H., Rietz, A. C., Drake, C. G., Matteson, E. L., & Chen, L. (2009). Potential role of decoy B7-H4 in the pathogenesis of rheumatoid arthritis: a mouse model informed by clinical data. *PLoS Med, 6*(10), e1000166. Retrieved from https://www.ncbi.nlm.nih.gov/pubmed/19841745. doi:10.1371/journal.pmed.1000166
115. Smyth, M. J., Ngiow, S. F., Ribas, A., & Teng, M. W. (2016). Combination cancer immunotherapies tailored to the tumour microenvironment. *Nat Rev Clin Oncol, 13*(3), 143-158. Retrieved from https://www.ncbi.nlm.nih.gov/pubmed/26598942. doi:10.1038/nrclinonc.2015.209
116. Jeon, H., Vigdorovich, V., Garrett-Thomson, S. C., Janakiram, M., Ramagopal, U. A., Abadi, Y. M., . . . Zang, X. (2014). Structure and cancer immunotherapy of the B7 family member B7x. *Cell Rep, 9*(3), 1089-1098. Retrieved from https://www.ncbi.nlm.nih.gov/pubmed/25437562. doi:10.1016/j.celrep.2014.09.053
117. Callahan, M. K., Postow, M. A., & Wolchok, J. D. (2016). Targeting T Cell Co-receptors for Cancer Therapy. *Immunity, 44*(5), 1069-1078. Retrieved from

https://www.ncbi.nlm.nih.gov/pubmed/27192570. doi:10.1016/j.immuni.2016.04.023

118. Zhu, G., Augustine, M. M., Azuma, T., Luo, L., Yao, S., Anand, S., . . . Chen, L. (2009). B7-H4-deficient mice display augmented neutrophil-mediated innate immunity. *Blood, 113*(8), 1759-1767. Retrieved from https://www.ncbi.nlm.nih.gov/pubmed/19109567. doi:10.1182/blood-2008-01-133223
119. Tivol, E. A., Borriello, F., Schweitzer, A. N., Lynch, W. P., Bluestone, J. A., & Sharpe, A. H. (1995). Loss of CTLA-4 leads to massive lymphoproliferation and fatal multiorgan tissue destruction, revealing a critical negative regulatory role of CTLA-4. *Immunity, 3*(5), 541-547. Retrieved from https://www.ncbi.nlm.nih.gov/pubmed/7584144.
120. Waterhouse, P., Penninger, J. M., Timms, E., Wakeham, A., Shahinian, A., Lee, K. P., . . . Mak, T. W. (1995). Lymphoproliferative disorders with early lethality in mice deficient in Ctla-4. *Science, 270*(5238), 985-988. Retrieved from https://www.ncbi.nlm.nih.gov/pubmed/7481803.
121. Nishimura, H., Nose, M., Hiai, H., Minato, N., & Honjo, T. (1999). Development of lupus-like autoimmune diseases by disruption of the PD-1 gene encoding an ITIM motif-carrying immunoreceptor. *Immunity, 11*(2), 141-151. Retrieved from https://www.ncbi.nlm.nih.gov/pubmed/10485649.
122. Nishimura, H., Okazaki, T., Tanaka, Y., Nakatani, K., Hara, M., Matsumori, A., . . . Honjo, T. (2001). Autoimmune dilated cardiomyopathy in PD-1 receptor-deficient mice. *Science, 291*(5502), 319-322. Retrieved from https://www.ncbi.nlm.nih.gov/pubmed/11209085. doi:10.1126/science.291.5502.319
123. Lee, J. S., Scandiuzzi, L., Ray, A., Wei, J., Hofmeyer, K. A., Abadi, Y. M., . . . Zang, X. (2012). B7x in the periphery abrogates pancreas-specific damage mediated by self-reactive CD8 T cells. *J Immunol, 189*(8), 4165-4174. Retrieved from https://www.ncbi.nlm.nih.gov/pubmed/22972920. doi:10.4049/jimmunol.1201241
124. Leong, S. R., Liang, W. C., Wu, Y., Crocker, L., Cheng, E., Sampath, D., . . . Polson, A. G. (2015). An anti-B7-H4 antibody-drug conjugate for the treatment of breast cancer. *Mol Pharm, 12*(6), 1717-1729. Retrieved from https://www.ncbi.nlm.nih.gov/pubmed/25853436. doi:10.1021/mp5007745
125. Smith, J. B., Lanitis, E., Dangaj, D., Buza, E., Poussin, M., Stashwick, C., . . . Powell, D. J., Jr. (2016). Tumor Regression and Delayed Onset Toxicity Following B7-H4 CAR T Cell Therapy. *Mol Ther, 24*(11), 1987-1999. Retrieved from https://www.ncbi.nlm.nih.gov/pubmed/27439899. doi:10.1038/mt.2016.149
126. Li, C. W., Lim, S. O., Chung, E. M., Kim, Y. S., Park, A. H., Yao, J., . . . Hung, M. C. (2018). Eradication of Triple-Negative Breast Cancer Cells by Targeting

Glycosylated PD-L1. *Cancer Cell, 33*(2), 187-201 e110. Retrieved from https://www.ncbi.nlm.nih.gov/pubmed/29438695. doi:10.1016/j.ccell.2018.01.009

127. RodrIguez, E., Schetters, S. T. T., & van Kooyk, Y. (2018). The tumour glyco-code as a novel immune checkpoint for immunotherapy. *Nat Rev Immunol, 18*(3), 204-211. Retrieved from https://www.ncbi.nlm.nih.gov/pubmed/29398707. doi:10.1038/nri.2018.3
128. Lodish H, Berk A, Zipursky SL, et al. Molecular Cell Biology. 4th edition. New York: W. H. Freeman; 2000. Section 17.7, Protein Glycosylation in the ER and Golgi Complex. Retrieved from: https://www.ncbi.nlm.nih.gov/books/NBK21744/
129. Schwarz, F., & Aebi, M. (2011). Mechanisms and principles of N-linked protein glycosylation. *Curr Opin Struct Biol, 21*(5), 576-582. Retrieved from https://www.ncbi.nlm.nih.gov/pubmed/21978957. doi:10.1016/j.sbi.2011.08.005
130. Mohorko, E., Glockshuber, R., & Aebi, M. (2011). Oligosaccharyltransferase: the central enzyme of N-linked protein glycosylation. *J Inherit Metab Dis, 34*(4), 869-878. Retrieved from https://www.ncbi.nlm.nih.gov/pubmed/21614585. doi:10.1007/s10545-011-9337-1
131. Sanjay, A., Fu, J., & Kreibich, G. (1998). DAD1 is required for the function and the structural integrity of the oligosaccharyltransferase complex. *Journal of Biological Chemistry, 273*(40), 26094-26099.
132. Pathak, R., Hendrickson, T. L., & Imperiali, B. (1995). Sulfhydryl modification of the yeast Wbp1p inhibits oligosaccharyl transferase activity. *Biochemistry, 34*(13), 4179-4185.
133. Fecci, P. E., Ochiai, H., Mitchell, D. A., Grossi, P. M., Sweeney, A. E., Archer, G. E., . . . Sampson, J. H. (2007). Systemic CTLA-4 blockade ameliorates glioma-induced changes to the CD4+ T cell compartment without affecting regulatory T-cell function. *Clin Cancer Res, 13*(7), 2158-2167. Retrieved from https://www.ncbi.nlm.nih.gov/pubmed/17404100. doi:10.1158/1078-0432.CCR-06-2070
134. Addgene. (2015). CRISPR 101: A Desktop Resource. *CRISPR 101: A Desktop Resource.*
135. Mezzadra, R., Sun, C., Jae, L. T., Gomez-Eerland, R., de Vries, E., Wu, W., . . . Schumacher, T. N. M. (2017). Identification of CMTM6 and CMTM4 as PD-L1 protein regulators. *Nature, 549*(7670), 106-110. Retrieved from https://www.ncbi.nlm.nih.gov/pubmed/28813410. doi:10.1038/nature23669
136. Burr, M. L., Sparbier, C. E., Chan, Y. C., Williamson, J. C., Woods, K., Beavis, P. A., . . . Dawson, M. A. (2017). CMTM6 maintains the expression of PD-L1 and regulates anti-tumour immunity. *Nature, 549*(7670), 101-105. Retrieved from https://www.ncbi.nlm.nih.gov/pubmed/28813417. doi:10.1038/nature23643

137. Aldhafeeri, H. (2018). *CRISPR Screen for Identification of Kinases that Mediate Prostate Cancer Cell Invasion.* (Master of Science), The University of Western Ontario, Ontario.
138. Rao, D. D., Senzer, N., Cleary, M. A., & Nemunaitis, J. (2009). Comparative assessment of siRNA and shRNA off target effects: what is slowing clinical development. *Cancer Gene Ther, 16*(11), 807-809. Retrieved from https://www.ncbi.nlm.nih.gov/pubmed/19713999. doi:10.1038/cgt.2009.53
139. Zuber, J., McJunkin, K., Fellmann, C., Dow, L. E., Taylor, M. J., Hannon, G. J., & Lowe, S. W. (2011). Toolkit for evaluating genes required for proliferation and survival using tetracycline-regulated RNAi. *Nat Biotechnol, 29*(1), 79-83. Retrieved from https://www.ncbi.nlm.nih.gov/pubmed/21131983. doi:10.1038/nbt.1720
140. Wang, T., Wei, J. J., Sabatini, D. M., & Lander, E. S. (2014). Genetic screens in human cells using the CRISPR-Cas9 system. *Science, 343*(6166), 80-84. Retrieved from https://www.ncbi.nlm.nih.gov/pubmed/24336569. doi:10.1126/science.1246981
141. Gaj, T., Gersbach, C. A., & Barbas, C. F., 3rd. (2013). ZFN, TALEN, and CRISPR/Cas-based methods for genome engineering. *Trends Biotechnol, 31*(7), 397-405. Retrieved from https://www.ncbi.nlm.nih.gov/pubmed/23664777. doi:10.1016/j.tibtech.2013.04.004
142. Perkel, J. M. (2013). Genome Editing with CRISPRs, TALENs and ZFNs. *Life Science Articles.*
143. Pennisi, E. (2013). The CRISPR craze. *Science, 341*(6148), 833-836. Retrieved from https://www.ncbi.nlm.nih.gov/pubmed/23970676. doi:10.1126/science.341.6148.833
144. Anders, C., Niewoehner, O., Duerst, A., & Jinek, M. (2014). Structural basis of PAM-dependent target DNA recognition by the Cas9 endonuclease. *Nature, 513*(7519), 569-573. Retrieved from https://www.ncbi.nlm.nih.gov/pubmed/25079318. doi:10.1038/nature13579
145. Li, W., Xu, H., Xiao, T., Cong, L., Love, M. I., Zhang, F., . . . Liu, X. S. (2014). MAGeCK enables robust identification of essential genes from genome-scale CRISPR/Cas9 knockout screens. *Genome Biol, 15*(12), 554. Retrieved from https://www.ncbi.nlm.nih.gov/pubmed/25476604. doi:10.1186/s13059-014-0554-4
146. Dai, X., Cheng, H., Bai, Z., & Li, J. (2017). Breast Cancer Cell Line Classification and Its Relevance with Breast Tumor Subtyping. *J Cancer, 8*(16), 3131-3141. Retrieved from https://www.ncbi.nlm.nih.gov/pubmed/29158785. doi:10.7150/jca.18457
147. Doench, J. G., Fusi, N., Sullender, M., Hegde, M., Vaimberg, E. W., Donovan, K. F., . . . Root, D. E. (2016). Optimized sgRNA design to maximize activity and

minimize off-target effects of CRISPR-Cas9. *Nat Biotechnol, 34*(2), 184-191. Retrieved from https://www.ncbi.nlm.nih.gov/pubmed/26780180. doi:10.1038/nbt.3437

148. Subramanian, A., Tamayo, P., Mootha, V. K., Mukherjee, S., Ebert, B. L., Gillette, M. A., . . . Mesirov, J. P. (2005). Gene set enrichment analysis: A knowledge-based approach for interpreting genome-wide expression profiles. *Proceedings of the National Academy of Sciences, 102*(43), 15545-15550. Retrieved from https://www.pnas.org/content/pnas/102/43/15545.full.pdf. doi:10.1073/pnas.0506580102
149. Pusapati, G. V., Kong, J. H., Patel, B. B., Krishnan, A., Sagner, A., Kinnebrew, M., . . . Rohatgi, R. (2018). CRISPR Screens Uncover Genes that Regulate Target Cell Sensitivity to the Morphogen Sonic Hedgehog. *Dev Cell, 44*(1), 113-129 e118. Retrieved from https://www.ncbi.nlm.nih.gov/pubmed/29290584. doi:10.1016/j.devcel.2017.12.003
150. Potapenko, I. O., Haakensen, V. D., Luders, T., Helland, A., Bukholm, I., Sorlie, T., . . . Borresen-Dale, A. L. (2010). Glycan gene expression signatures in normal and malignant breast tissue; possible role in diagnosis and progression. *Mol Oncol, 4*(2), 98-118. Retrieved from https://www.ncbi.nlm.nih.gov/pubmed/20060370. doi:10.1016/j.molonc.2009.12.001
151. Beheshti Zavareh, R., Sukhai, M. A., Hurren, R., Gronda, M., Wang, X., Simpson, C. D., . . . Dennis, J. W. (2012). Suppression of cancer progression by MGAT1 shRNA knockdown. *PLoS One, 7*(9), e43721. Retrieved from https://www.ncbi.nlm.nih.gov/pubmed/22957033. doi:10.1371/journal.pone.0043721
152. Akiva, I., & Birgül Iyison, N. (2018). MGAT1 is a novel transcriptional target of Wnt/β-catenin signaling pathway. *BMC Cancer, 18*(1), 60. Retrieved from https://doi.org/10.1186/s12885-017-3960-7. doi:10.1186/s12885-017-3960-7
153. Dennis, J. W., Lau, K. S., Demetriou, M., & Nabi, I. R. (2009). Adaptive regulation at the cell surface by N-glycosylation. *Traffic, 10*(11), 1569-1578. Retrieved from https://www.ncbi.nlm.nih.gov/pubmed/19761541. doi:10.1111/j.1600-0854.2009.00981.x
154. Pischedda, F., Szczurkowska, J., Cirnaru, M. D., Giesert, F., Vezzoli, E., Ueffing, M., . . . Piccoli, G. (2014). A cell surface biotinylation assay to reveal membrane-associated neuronal cues: Negr1 regulates dendritic arborization. *Mol Cell Proteomics, 13*(3), 733-748. Retrieved from https://www.ncbi.nlm.nih.gov/pubmed/24382801. doi:10.1074/mcp.M113.031716
155. Barat, B., & Wu, A. M. (2007). Metabolic biotinylation of recombinant antibody by biotin ligase retained in the endoplasmic reticulum. *Biomol Eng, 24*(3), 283-

291. Retrieved from https://www.ncbi.nlm.nih.gov/pubmed/17379573. doi:10.1016/j.bioeng.2007.02.003
156. Arruabarrena-Aristorena, A., Zabala-Letona, A., & Carracedo, A. (2018). Oil for the cancer engine: The cross-talk between oncogenic signaling and polyamine metabolism. *Sci Adv, 4*(1), eaar2606. Retrieved from https://www.ncbi.nlm.nih.gov/pubmed/29376126. doi:10.1126/sciadv.aar2606
157. Takahashi RU, Takeshita F, Honma K, Ono M, Kato K, Ochiya T. Ribophorin II regulates breast tumor initiation and metastasis through the functional suppression of GSK3β. Scientific reports. 2013 Aug 20;3:2474.
158. Honma K, Iwao-Koizumi K, Takeshita F, Yamamoto Y, Yoshida T, Nishio K, Nagahara S, Kato K, Ochiya T. RPN2 gene confers docetaxel resistance in breast cancer. Nature medicine. 2008 Sep;14(9):939.
159. Venkitachalam S, Guda K. Altered glycosyltransferases in colorectal cancer. Author Manuscript, available in PMC 2018 Jan. 1.
160. Leong R. Steven; Polson, A. P., Paul; Wu, Yan; Liang, Wei-Ching; Firestein, Ron. (2014). United States Patent No. United States Patent Application Publication.
161. Leong, S. R., Liang, W. C., Wu, Y., Crocker, L., Cheng, E., Sampath, D., . . . Polson, A. G. (2015). An anti-B7-H4 antibody-drug conjugate for the treatment of breast cancer. *Mol Pharm, 12*(6), 1717-1729. Retrieved from https://www.ncbi.nlm.nih.gov/pubmed/25853436. doi:10.1021/mp5007745
162. Center, C. H. G. (1997). *GeneCards©: The Human Gene Database*.
163. Liu, Y., Wang, L., Predina, J., Han, R., Beier, U. H., Wang, L. C., . . . Hancock, W. W. (2013). Inhibition of p300 impairs Foxp3(+) T regulatory cell function and promotes antitumor immunity. *Nat Med, 19*(9), 1173-1177. Retrieved from https://www.ncbi.nlm.nih.gov/pubmed/23955711. doi:10.1038/nm.3286
164. Ghosh, S., Taylor, A., Chin, M., Huang, H. R., Conery, A. R., Mertz, J. A., . . . Lora, J. M. (2016). Regulatory T Cell Modulation by CBP/EP300 Bromodomain Inhibition. *J Biol Chem, 291*(25), 13014-13027. Retrieved from https://www.ncbi.nlm.nih.gov/pubmed/27056325. doi:10.1074/jbc.M115.708560
165. Binothman, N., Hachim, I. Y., Lebrun, J. J., & Ali, S. (2017). CPSF6 is a Clinically Relevant Breast Cancer Vulnerability Target: Role of CPSF6 in Breast Cancer. *EBioMedicine, 21*, 65-78. Retrieved from https://www.ncbi.nlm.nih.gov/pubmed/28673861. doi:10.1016/j.ebiom.2017.06.023
166. Li, Y., Zheng, M., & Lau, Y. F. (2014). The sex-determining factors SRY and SOX9 regulate similar target genes and promote testis cord formation during testicular differentiation. *Cell Rep, 8*(3), 723-733. Retrieved from https://www.ncbi.nlm.nih.gov/pubmed/25088423. doi:10.1016/j.celrep.2014.06.055

167. Jeselsohn, R., Cornwell, M., Pun, M., Buchwalter, G., Nguyen, M., Bango, C., . . . Brown, M. (2017). Embryonic transcription factor SOX9 drives breast cancer endocrine resistance. *Proc Natl Acad Sci U S A, 114*(22), E4482-E4491. Retrieved from https://www.ncbi.nlm.nih.gov/pubmed/28507152. doi:10.1073/pnas.1620993114
168. Zhang, J., Bu, X., Wang, H., Zhu, Y., Geng, Y., Nihira, N. T., . . . Wei, W. (2018). Cyclin D-CDK4 kinase destabilizes PD-L1 via cullin 3-SPOP to control cancer immune surveillance. *Nature, 553*(7686), 91-95. Retrieved from https://www.ncbi.nlm.nih.gov/pubmed/29160310. doi:10.1038/nature25015
169. Yarbrough, W. G., Panaccione, A., Chang, M. T., & Ivanov, S. V. (2016). Clinical and molecular insights into adenoid cystic carcinoma: Neural crest-like stemness as a target. *Laryngoscope Investig Otolaryngol, 1*(4), 60-77. Retrieved from https://www.ncbi.nlm.nih.gov/pubmed/28894804. doi:10.1002/lio2.22
170. Zhao, E., Maj, T., Kryczek, I., Li, W., Wu, K., Zhao, L., . . . Zou, W. (2016). Cancer mediates effector T cell dysfunction by targeting microRNAs and EZH2 via glycolysis restriction. *Nat Immunol, 17*(1), 95-103. Retrieved from https://www.ncbi.nlm.nih.gov/pubmed/26523864. doi:10.1038/ni.3313
171. Zabala-Letona, A., Arruabarrena-Aristorena, A., Martin-Martin, N., Fernandez-Ruiz, S., Sutherland, J. D., Clasquin, M., . . . Carracedo, A. (2017). mTORC1-dependent AMD1 regulation sustains polyamine metabolism in prostate cancer. *Nature, 547*(7661), 109-113. Retrieved from https://www.ncbi.nlm.nih.gov/pubmed/28658205. doi:10.1038/nature22964
172. Shestakova, A., Zolov, S., & Lupashin, V. (2006). COG complex-mediated recycling of Golgi glycosyltransferases is essential for normal protein glycosylation. *Traffic, 7*(2), 191-204. Retrieved from https://www.ncbi.nlm.nih.gov/pubmed/16420527. doi:10.1111/j.1600-0854.2005.00376.x
173. Pfeffer, S., Dudek, J., Gogala, M., Schorr, S., Linxweiler, J., Lang, S., . . . Förster, F. (2014). Structure of the mammalian oligosaccharyl-transferase complex in the native ER protein translocon. *Nature Communications, 5*, 3072. Retrieved from https://doi.org/10.1038/ncomms4072. doi:10.1038/ncomms4072 https://www.nature.com/articles/ncomms4072#supplementary-information
174. Zurich, U. o. (2016). Oligosaccharyltransferase. *N-linked glycosylation.*
175. Breitling, J., & Aebi, M. (2013). N-linked protein glycosylation in the endoplasmic reticulum. *Cold Spring Harb Perspect Biol, 5*(8), a013359. Retrieved from https://www.ncbi.nlm.nih.gov/pubmed/23751184. doi:10.1101/cshperspect.a013359
176. Qiu, H., Duan, W. M., Shu, J., Cheng, H. X., Wang, W. P., Huang, X. E., & Chen, H. L. (2014). B3GNT2, a polylactosamine synthase, regulates glycosylation of EGFR in H7721 human hepatocellular carcinoma cells. *Asian*

Pac J Cancer Prev, 15(24), 10875-10878. Retrieved from https://www.ncbi.nlm.nih.gov/pubmed/25605193.

177. Biswas, B., Batista, F., Sundaram, S., & Stanley, P. (2018). MGAT1 and Complex N-Glycans Regulate ERK Signaling During Spermatogenesis. *Sci Rep, 8*(1), 2022. Retrieved from https://www.ncbi.nlm.nih.gov/pubmed/29386567. doi:10.1038/s41598-018-20465-3
178. Heesen, S., Lehle, L., Weissmann, A., & Aebi, M. (1994). Isolation of the ALG5 locus encoding the UDP-glucose:dolichyl-phosphate glucosyltransferase from Saccharomyces cerevisiae. *Eur J Biochem, 224*(1), 71-79. Retrieved from https://www.ncbi.nlm.nih.gov/pubmed/8076653.